Universitat Autònoma de Barcelona

Departament de Bioquímica i Biologia Molecular
Facultat de Medicina

INc Institut de Neurociències

AMYLOID-β OLIGOMERS REDUCES GLUTAMATERGIC TRANSMISSION AND INHIBITS SYNAPTIC PLASTICITY WITH UNDERLYING MECHANISMS SUGGESTTING AKAP150 MODULATES DIVERSE SYNAPTIC FUNCTIONS

Wenwen Cheng

TESIS DOCTORAL

Bellaterra, 2014

AMYLOID-β OLIGOMERS REDUCES GLUTAMATERGIC TRANSMISSION AND INHIBITS SYNAPTIC PLASTICITY WITH UNDERLYING MECHANISMS SUGGESTTING AKAP150 MODULATES DIVERSE SYNAPTIC FUNCTIONS

Memoria de tesis doctoral presentada por Wenwen Cheng para optar al grado de Doctora en Bioquímica y Biología Molecular por la Universitat Autònoma de Barcelona.

Este trabajo ha sido realizado bajo la dirección del Doctor José Rodriguez Alvarez en la Facultat de Medicina del Departament de Bioquímica i Biologia Molecular y en el Institut de Neurociències de la Universitat Autònoma de Barcelona.

El director, El doctorando,

Dr. José Rodriguez Alvarez Wenwen Cheng

Bellaterra, 2014

“Al sac i ben lligat”

“Qui no s’arrisca no pisca”

Acknowledgements

First I would like to express my deepest gratitude to my supervisor Dr. José Rodriguez Alvarez for giving me the opportunity to do my PhD studies in his lab. He has created an excellent environment in the lab and has shared his insights as I hurdle all the obstacles in the completion this research work. His professionalism has been invaluable for my development. I want to thank him for his inspiring guidance, continued support and encouragement throughout my PhD and finally, lots of thanks for the critical and proof-reading of this thesis.

To my present and past lab members who in one way or another contributed and extended their assistance in this work. Special thanks to Alfredo Minano-Molina and Rut Fadó Andrés for their collaboration and their huge contribution to my work and for many funny times. Many thanks to the past lab members for making a friendly working atmosphere.

I am indebted to many people who have helped me technically during my PhD, including Nuria Barba at the Microscopy Service and special thanks to Cristina, Suzana for the productive work and pleasant company during the long hours spent in the primary cell culture room.

To every investigator and group leader of our department. In particular, I would like to thank all the members of the research groups. Especial thanks to Guillem Sanchez, Virginia Jimenez, Dolores Siedlecki for their help and many useful recommendations. Especially thanks to Meng Chen and Ping Sun. Thanks to all the former as well as current PhD students of the department for their kindness, understanding and hospitability. Thanks a lot!

I would also like to extend my thanks to the administrative staff of the Institut de Neurociències & Departament de Bioquímica i Biologia Molecular. Thanks for facilitating those administrative tasks which were always ambiguous for me.

During these years I have been supported by the China Scholarship Counsel without which this thesis would not have been possible. Throughout the entire process of my PhD studies in UAB I received a lot of support from many people around me who I cannot mention but I express my sincere gratefulness.

I would also like to thank my thesis committee for their precious time.

Bofei Wei deserves my deepest gratitude for her help and the opportunity which she gave to me at the very beginning of my PhD studies.

Finally, I wish to thank my family for their support and encouragement throughout my study.

Moltes gràcies !

TABLE OF CONTENTS

Table of contents

SUMMARY

Beta amyloid (Aβ), a peptide generated from the amyloid precursor protein (APP) by neurons, is widely believed to underlie the pathophysiology of Alzheimer's disease (AD). Aβ is directly involved in the modulation of synaptic function and pathological levels of Aβ inhibit synaptic plasticity. The soluble forms of Aβ affect negatively the process of synaptic transmission involving the loss of synaptic receptors by mechanisms still unknown. The major ionotropic glutamate receptors involved in excitatory synaptic transmission are alpha-amino-3-hydroxy-5-methyl-4-isoxazolepropionic acid receptors (AMPARs) and N-methyl D-aspartate receptors (NMDARs). AMPARs are best studied for their rapid trafficking into and out of the synapse by cycling between intracellular stores and the cell surface during synaptic potentiation and depression, respectively. There is an increasing body of evidence to show that Aβ molecules, especially soluble Aβ oligomers (Aβo), exert a negative impact on glutamate receptor trafficking in central synapses, leading to synaptic deficits. Our studies shown acute applications of soluble Aβo and NMDA promoted AMPARs endocytosis in mature mouse cortical primary culture.

However, the precise cellular mechanisms underlying Aβ effects on glutamate receptors remain to be elucidated. A-kinase anchoring proteins (AKAPs), which anchor receptors and signaling proteins to physiological substrates, especially as the AMPAR-Scaffold proteins-Cytoskeleton, AKAP150, in particular, plays a critical role in synaptic plasticity and the stabilization of AMPA (AMPARs) and NMDA (NMDARs) receptors at synapses, although the role of regulating AMPAR trafficking is unclear until now. In our current study, exposure of cultured cortical neurons to both Aβo and NMDA reduces AKAP150 protein levels.

It is now recognized that the rate and spatial precision of phosphorylation and dephosphorylation reactions in cells are constrained through the anchoring of kinases and phosphatases near their targets by scaffold proteins. In particular, subcellular targeting by AKAP79/150 of the kinase PKA, phosphatase calcineurin (CaN; also known as PP2B and PPP3), and other enzymes promote highly localized signaling events at the postsynaptic membrane of neuronal dendritic spines (note: AKAP150 is the rodent orthologous of human AKAP79). Importantly, AKAP79/150, PKA, CaN, and CaV1.2 exhibit an enrichment and co-localization in dendritic spines of hippocampal neurons. By using NMDAR, AMPAR, CaN, proteasome inhibitors, we

studied the mechanism by which Aβo and NMDA-induced decreases in AKAP150 levels. Our results indicated the reduction of AKAP150 requires NMDAR, CaN and proteasome activities. Moreover, the reducing effect of Aβo and NMDA on AMPAR levels was mimicked by knockdown of AKAP150 and blocked by overexpression of AKAP150.

Aβ can reduce long-term potentiation (LTP), a form of synaptic plasticity that is closely associated with learning and memory and can facilitate long-term depression (LTD), an opposing form of synaptic plasticity. LTP and LTD involve postsynaptic phosphorylation and glutamate receptor trafficking. The observation that Aβ reduces LTP and facilitates LTD is suggestive of a role for Aβ in regulating trafficking of glutamate receptors and postsynaptic phosphorylation, but this has not been previously examined. In our research, neither the Aβo nor the NMDA-induced reduction of AKAP150 could be rescued by chemical LTP (cLTP).

Aβ has a strong inhibitory effect on the induction of LTP. In addition, we have also shown that Aβo inhibits cLTP induction *in vitro*, extending previous report on inhibition of LTP in CA1 *in vivo*. When solubilized in aqueous buffers, Aβ assembles into a variety of structures, including low N-oligomers, ADDLs, protofibrils, and fibrils. The solutions of synthetic Aβ used in this study contain a mixture of these different assemblies. Moreover, the finding that Aβ inhibits AMPARs exocytosis on overexpression of AKAP150, but not unoverexpressed, could be partially rescued by cLTP in vitro confirms that AKAP150 plays an important role of AMPARs trafficking.

Aβo could be involved in the deficit of dendritic transport of mRNAs and their translation. It has been observed that different experimental models of AD have lower number of neurons with dendrites, indicating that Aβ can regulate synaptic structure and function. The miRNAs are small non-coding RNAs that act as post-transcriptional regulators of gene expression. In early AD, which presents dystrophic neurites and synaptic failure, there is an alteration in the levels of certain miRNAs. Long-term exposure of Aβo demonstrated that miR125a and miR132 were both reduced while long-term exposure of NMDA induced the decrease of miR181a. Experiments with

inhibitors indicated that CaN and Ca^{2+} may be involved in the modulation of mir181a by long-term exposure of NMDA.

ABBREVIATIONS

AD	Alzheimer disease
AMPA	α-amino-3-hydroxy-5-methylisoxazole-4-propionic acid
AMPAR	AMPA receptor
NMDA	N-methyl-D-aspartic acid
NMDAR	NMDA receptor
Aβo	Amyloid β oligomer
ADDL	Amyloid beta derived diffusible ligands
AKAP150	A-kinase anchoring protein 150
LTD	long term depression
LTP	long term potentiation
APP	amyloid precursor protein
ACSF	artificial cerebrospinal fluid
F'R	forskolin plus rolipram
BAPTA tetrakis	2-bis (2-aminophenoxy) ethane-N', N', N', N'- tetraacetic acid
cLTP	chemical LTP
CaMKII	calcium/ calmodulin-dependent protein kinase II
PKA	protein kinase A
PKC	protein kinase C
PP2B	protein phosphatase 2B
PSD	postsynaptic density
EPSCs	excitatory postsynaptic currents

Less frequently used abbreviations are defined upon their first use in the text.

INTRODUCTION

Neurons are fundamental building blocks with a complex morphology that represent an essential functional unit within the nervous system. AD is the most common neurodegenerative disease and the leading cause of dementia in the elderly. Accumulating evidence supports Aβo as the leading candidate for the causative agent in AD and synapses as the primary site of Aβo action. However, the molecular and cellular mechanisms by which Aβo cause synaptic dysfunction and cognitive impairments remain poorly understood. Although the underlying mechanisms are unclearly, some research have shown Aβo reduces glutamatergic transmission and inhibits synaptic plasticity, meanwhile, Aβo induced long-term depression (LTD) removes surface and synaptic glutamate receptors (Beattie et al., 2000; Lee et al., 2002; Luscher et al., 1999). Furthermore, application of synthetic Aβo results in surface removal of NMDA and GluR1 receptors in dissociated cultured neurons (Almeida et al., 2005; Snyder et al., 2005). Helen et al., 2006 shown that Aβo employs signalling pathways of LTD to drive endocytosis of synaptic AMPA receptors (AMPARs). Qinwen et al., 2005 also demonstrated that Aβ-mediated inhibition of LTP arises from activation of mGluR5 and stimulation of three kinases, JNKI, Cdk5, and p38 MAP kinase. Synaptic removal of AMPARs is necessary and sufficient to produce loss of dendritic spines and synaptic NMDA responses. Through association with the synaptic scaffolding MAGUK (membrane-associated guanylate kinase) proteins, AKAP79/150 and its associated enzymes (PKA, protein kinase C, and PP2B) are directed to both NMDA- and AMPA-type glutamate receptors (Colledge et al., 2000). The identification of an interaction between AKAP79/150 and the MAGUK synaptic scaffolding proteins, SAP97 and PSD-95, linked AKAP79/150 to synaptic AMPA receptors and provided a mechanism by which AKAP79/150 may regulate postsynaptic excitatory transmission (Colledge et al., 2000). A series of molecular, biochemical and electrophysiological experiments established that AKAP79/150-anchored PKA phosphorylates Ser-845 on GluR1 resulting in alteration of channel activity (Tavalin et al., 2002) and that the PKA site is selectively dephosphorylated during LTD (Kameyama et al., 1998; Lee et al., 2000). AKAP-directed kinase/phosphatase complexes have been implicated in the regulation of AMPA receptor surface expression, a process thought to contribute to LTP and LTD.

1. GLUTAMATE

Glutamate is the most prominent neurotransmitter in the body, and it is the main excitatory neurotransmitter (Petroff et al., 2002), being present in over 50% of nervous tissue. Glutamate was initially discovered to be a neurotransmitter in insect studies in the early 1960s. Glutamate is also used by the brain to synthesise GABA (γ-Aminobutyric acid), the main inhibitory neurotransmitter of the mammalian central nervous system, which plays a role in regulating neuronal excitability throughout the nervous system and is also directly responsible for the regulation of muscle tone in humans (Watanabe et al., 2002).

1.1. GLUTAMATE RECEPTORS

Mammalian glutamate receptors are classified based on their pharmacology. However, glutamate receptors in other organisms have different pharmacology, and therefore these classifications do not hold. One of the major functions of glutamate receptors appears to be the modulation of synaptic plasticity, a property of the brain thought to be vital for memory and learning. Both metabotropic and ionotropic glutamate receptors have been shown to have an effect on synaptic plasticity (Debanne et al., 2003). An increase or decrease in the number of ionotropic glutamate receptors on a postsynaptic cell may lead to long-term potentiation or long-term depression of that cell, respectively (Pérez et al., 2006; Asztély et al., 1996). Additionally, metabotropic glutamate receptors may modulate synaptic plasticity by regulating postsynaptic protein synthesis through second messenger systems (Weiler et al., 1993). Research shows that glutamate receptors are present in CNS glial cells as well as neurons (Teichberg et al., 1991). These glutamate receptors are suggested to play a role in modulating gene expression in glial cells, both during the proliferation and differentiation of glial precursor cells in brain development and in mature glial cells (Steinhäuser et al., 1996).

1.2. GLUTAMATE RECEPTOR TYPES

Glutamate receptors can be divided into two groups according to the mechanism by which their activation gives rise to a postsynaptic current (Palmada et al.,

1996). Ionotropic glutamate receptors (iGluRs) form the ion channel pore that activates when glutamate binds to the receptor. Metabotropic glutamate receptors (mGluRs) indirectly activate ion channels on the plasma membrane through a signaling cascade that involves G proteins. Ionotropic receptors tend to be quicker in relaying information, but metabotropic ones are associated with a more prolonged stimulus. This is due to the usage of many different messengers to carry out the signal, but since there is a cascade, an activation of a G-protein can lead to multiple activations. Glutamate receptors are usually not specifically geared towards glutamate exclusively as the ligand and sometimes even require another agonist. Of the many specific subtypes of glutamate receptors, it is customary to refer to primary subtypes by a chemical that binds to it more selectively than glutamate. The research, however, is ongoing, as subtypes are identified and chemical affinities measured.

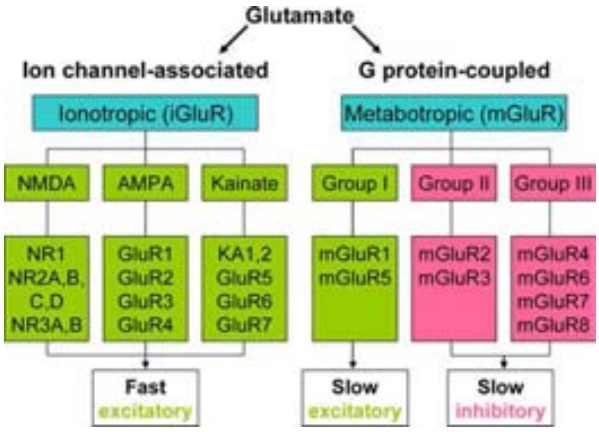

FIGURE 1. Glutamate (Glu) is the major excitatory neurotransmitter in the central nervous system (CNS). It also acts to modulate synaptic transmission both pre- and post-synaptically. These actions are mediated via a large range of ionotropic (iGluR, NMDA, AMPA, and kainate), and metabotropic (mGluR, group I, II, III) receptors. iGluR are directly coupled to cation channels, and their activation evokes fast synaptic events which may lead to longer-term changes in excitability. mGluR exist as eight subtypes of G-protein coupled receptor: Group I (mGluR1 and 5) are excitatory and are believed to act mainly via Gαq/phospholipase C. Group II (mGluR2 and 3), and III (mGluR4, 6, 7, and 8) inhibit adenylate cyclase and alter cation currents via Gαi and Gβγ subunits respectively. Figure is from Blackshaw et al., 2011.

Due to the diversity of glutamate receptors, their subunits are encoded by numerous gene families. Sequence similarities between mammals show a common evolutionary origin for many mGluR and all iGluR genes (Ohashi et al., 2002). Conservation of reading frames and splice sites of GluR genes between chimpanzees and humans are complete, suggesting no gross structural changes after humans diverged from the human-chimpanzee common ancestor. However, there is a possibility that two human-specific "fixed" amino acid substitutions, D71G in GRIN3A and R727H in GRIN3B, are specifically associated with human

brain function (Goto et al., 2009).

1.3. STRUCTURE, MECHANISM AND FUNCTION

Glutamate receptors exist primarily in the central nervous system. These receptors can be found on the dendrites of postsynaptic cells and bind to glutamate released into the synaptic cleft by presynaptic cells. They are also present on both astrocytes and oligodendrocytes (Dingledine et al., 1999). Glutamate binds to the extracellular portion of the receptor and provokes a different response depending on the type of receptors.

1.3.1. IONOTROPIC

Ionotropic glutamate receptors, by definition, are ligand-gated cation channels that allow the flow of K^+, Na^+ and sometimes Ca^{2+} in response to glutamate binding. Upon binding, the agonist will stimulate the receptor, an ion channel, allowing ion flow and causing excitatory postsynaptic current (EPSC). This current is depolarizing and, if enough glutamate receptors are activated, may trigger an action potential in the postsynaptic neuron. All produce excitatory postsynaptic current, but the speed and duration of the current is different for each type. NMDA receptors have an internal binding site for an Mg^{2+} ion, creating a voltage-dependent block, which is removed by outward flow of positive current (Johnson et al., 1990), Since the block must be removed by outward current flow, NMDA receptors rely on the EPSC produced by AMPA receptors to open. NMDA receptors are permeable to Ca^{2+} (Crowder et al., 1987), which is an important cation in the nervous system (Gover et al., 2009) and has been linked to gene regulation (Barbado et al., 2009). The flow of Ca^{2+} through NMDA receptors is thought to cause both LTP (of synapse efficacy) and LTD by transducing signaling cascades and regulating gene expression.

1.3.2. AMPA RECEPTORS

AMPARs are ionotropic glutamate receptors that mediate rapid excitatory transmission in the mammalian brain. They are heterotetrameric cation channels

comprised of a combinatorial assembly of four subunits, GluR1-GluR4 (GluRA-D) (Hollmann et al., 1994). Regulated trafficking of AMPARs has emerged as an important mechanism that underlies the activity-dependent modification of synaptic strength. The GluA2 subunit is uniquely edited at the mRNA level, where a glutamine codon is switched to arginine (Lomeli et al., 1994), which confers channel resistance to calcium. Therefore, AMPAR complexes lacking GluA2 are permeable to sodium and calcium ions resulting in higher conductance. In addition, calcium permeable AMPARs (CP-AMPARs) exhibit inward rectification in current–voltage plots that differs from the linear rectification of predominate AMPARs due to voltage-dependent block by intracellular polyamines (Donevan and Rogawski, 1995). GluA2 lacking AMPARs can be formed through GluA1 homomers or combinations of GluA1, 3, and 4.

Delivery of AMPARs to the postsynaptic membrane leads to LTP, whereas removal of these receptors leads to LTD (Barry et al., 2002; Bredt et al., 2003; Malinow et al., 2002). Both of these forms of synaptic plasticity are influenced by NMDAR activity (Bliss et al., 1993). Regulation of AMPAR synaptic insertion is determined by the receptor subunit composition. While synaptic activity drives GluR1-containing receptors to the synapse, thus enhancing transmission, AMPARs lacking GluR1, such as GluR2/3 heteromers, constitutively cycle in and out of the synapse, in an activity-independent manner, entering and leaving sites initially occupied by GluR1-containing receptors. This distinction in subunit trafficking is determined by the subunit intracellular CTDs (Passafaro et al., 2001).

Changes in synaptic strength are believed to be the basis of learning and memory. These alterations in neuronal communication are controlled in part by the insertion or removal of AMPA receptors (AMPARs) from the postsynaptic membrane of excitatory synapses. Regulation of AMPAR trafficking to and from the plasma membrane can occur through the C-terminal tails of AMPARs, either through interactions with other proteins or changes in phosphorylation (Malinow et al., 2002; Derkach et al., 2007). When surface AMPARs are internalized, subunit-specific interactions with other proteins and changes in their phosphorylation status allow for

their recycling and functional insertion into the plasma membrane (Hirling et al., 2009). Alternatively, AMPARs have been shown to traffic to the lysosome by a distinct pathway, although the mechanisms regulating this process are not well understood (Ehlers et al., 2000; Kessels et al., 2009).

1.3.3. NMDA RECEPTOR

The N-methyl-D-aspartate receptor (also known as the NMDA receptor or NMDAR) is the predominant molecular device for controlling synaptic plasticity and memory function. Activation of NMDRs results in the opening of an ion channel that is nonselective to cations with an equilibrium potential near 0 mV. A property of the NMDA receptor is its voltage-dependent activation, a result of ion channel blocked by extracellular Mg^{2+} & Zn^{2+} ions. This allows the flow of Na^{+} and Ca^{2+} ions into the cell and K^{+} out of the cell to be voltage-dependent (Dingledine et al., 1999; Liu et al., 2000; Cull et al., 2001; Paoletti et al., 2007). The predominant hypothesis for the mechanisms of NMDAR involvement is that the activation of NMDAR elevates intracellular calcium concentrations ($[Ca^{2+}]$) that trigger various intracellular signaling systems. Cytosolic calcium is an important mediator of neuronal signal transduction, participating in diverse biochemical reactions that elicit changes in synaptic function, metabolic rate, and gene transcription. Up-regulation of NMDA receptors or high extracellular glutamate concentration can result in an excessive entry of calcium, triggering a series of cytoplasmic and nuclear processes such as loss of mitochondrial membrane potential, which ultimately results in neuronal cell death. Moreover, calcium flux through NMDARs is thought to be critical in synaptic plasticity, a cellular mechanism for learning and memory. The NMDA receptor is distinct in two ways: first, it is both ligand-gated and voltage-dependent; second, it requires co-activation by two ligands: glutamate and either D-serine or glycine (Kleckner et al., 1988).

The NMDA receptor forms a heterotetramer between two GluN1 and two GluN2 subunits (the subunits were previously denoted as NR1 and NR2), two obligatory NR1 subunits and two regionally localized NR2 subunits. A related gene family of NR3 A and B subunits have an inhibitory effect on receptor activity. Multiple

receptor isoforms with distinct brain distributions and functional properties arise by selective splicing of the NR1 transcripts and differential expression of the NR2 subunits. There are eight variants of the NR1 subunit produced by alternative splicing of GRIN1 (Stephenson et al., 2006): NR1-1a, NR1-1b; NR1-1a is the most abundantly expressed form. NR1-2a, NR1-2b; NR1-3a, NR1-3b; NR1-4a, NR1-4b; GluN2: NR2 subunit in vertebrates and invertebrates. While a single NR2 subunit is found in invertebrate organisms, four distinct isoforms of the NR2 subunit are expressed in vertebrates and are referred to with the nomenclature NR2A through D (coded by GRIN2A, GRIN2B, GRIN2C, GRIN2D). Each NR2 subunit has a different intracellular C-terminal domain that can interact with different sets of signaling molecules (Ryan et al., 2009). Unlike NR1 subunits, NR2 subunits are expressed differentially across various cell types and control the electrophysiological properties of the NMDA receptor. One particular subunit, NR2B, is mainly present in immature neurons and in extrasynaptic locations, and contains the binding-site for the selective inhibitor ifenprodil. Whereas NR2B is predominant in the early postnatal brain, the number of NR2A subunits grows, and eventually NR2A subunits outnumber NR2B. This is called NR2B-NR2A developmental switch, and is notable because of the different kinetics each NR2 subunit lends to the receptor (Liu et al., 2004). For instance, greater ratios of the NR2B subunit leads to NMDA receptors which remain open longer compared to those with more NR2A. This may in part account for greater memory abilities in the immediate postnatal period compared to late in life, which is the principle behind genetically-altered 'doogie mice'. The NR2B and NR2A subunits also have differential roles in mediating excitotoxic neuronal death (Liu et al., 2007). The developmental switch in subunit composition is thought to explain the developmental changes in NMDA neurotoxicity (Zhou et al., 2006). Disruption of the gene for NR2B in mice causes perinatal lethality, whereas the disruption of NR2A gene produces viable mice, although with impaired hippocampal plasticity (Sprengel et al., 1998). One study suggests that Reelin may play a role in the NMDA receptor maturation by increasing the NR2B subunit mobility (Groc et al., 2007).

Each receptor subunit has modular design and each structural module also represents a functional unit: 1) The extracellular domain contains two globular structures: a modulatory domain and a ligand-binding domain. NR1 subunits bind the co-agonist glycine and NR2 subunits bind the neurotransmitter glutamate. 2) The agonist-binding

module links to a membrane domain, which consists of three trans-membrane segments and a re-entrant loop reminiscent of the selectivity filter of potassium channels. The membrane domain contributes residues to the channel pore and is responsible for the receptor's high-unitary conductance, high-calcium permeability, and voltage-dependent magnesium block. Each subunit has an extensive cytoplasmic domain, which contain residues that can be directly modified by a series of protein kinases and protein phosphatases, as well as residues that interact with a large number of structural, adaptor, and scaffolding proteins.

Recently, Lee et al., 2014 presented X-ray crystal structures of the Xenopus laevis GluN1–GluN2B NMDA receptor with the allosteric inhibitor, Ro25-6981, partial agonists and the ion channel blocker, MK-801. Receptor subunits are arranged in a 1-2-1-2 fashion, demonstrating extensive interactions between the amino terminal and ligand-binding domains. The transmembrane domains harbour a closed-blocked ion channel, a pyramidal central vestibule lined by residues implicated in binding ion channel blockers and magnesium, and a twofold symmetric arrangement of ion channel pore loops. These structures provide new insights into the architecture, allosteric coupling and ion channel function of NMDA receptors. The glycine-binding modules of the NR1 and NR3 subunits and the glutamate-binding module of the NR2A subunit have been expressed as soluble proteins, and their three-dimensional structure has been solved at atomic resolution by x-ray crystallography. This has revealed a common fold with amino acid-binding bacterial proteins and with the glutamate-binding module of AMPA-receptors and kainate-receptors.

1.3.4. METABOTROPIC

Metabotropic glutamate receptors, which belong to subfamily C of G protein-coupled receptors are divided into three groups, with a total of eight subtypes (in mammals; this is not necessarily the case for most organisms). The mGluRs are composed of three distinct regions: the extracellular region, the transmembrane region, and the intracellular region (Muto et al., 2007). The extracellular region is composed of a venus flytrap (VFT) module that binds glutamate (Pin et al., 2002), and a cysteine-

rich domain that is thought to play a role in transmitting the conformational change induced by ligand binding from in the VFT module to the transmembrane region. The transmembrane region consists of seven transmembrane domains and connects the extracellular region to the intracellular region where G protein coupling occurs. Glutamate binding to the extracellular region of an mGluR causes G proteins bound to the intracellular region to be phosphorylated, affecting multiple biochemical pathways and ion channels in the cell (Platt et al., 2007). Because of this, mGluRs can both increase or decrease the exitability of the postsynaptic cell, thereby causing a wide range of physiological effects.

2. SYNAPTIC PLASTICITY AND RECEPTOR TRAFFICKING

2. 1. SYNAPTIC PLASTICITY

The most remarkable property of synapses is not that they convey information from one neuron to another, but that they can readily alter the efficiency with which they do this. This property, known as synaptic plasticity, is the basis of information storage in the brain. It enables us to store and use vast amounts of information in the form of learnt behaviors and conscious memories. During the past 40 years, one form of synaptic plasticity, known as LTP has consolidated its status as the pre-eminent synaptic model for investigating the molecular basis of memory (Bliss et al., 1993). LTP has been most extensively studied in the hippocampus, although it is also seen at many synapses throughout the CNS. It is characterized by a long-lasting increase in synaptic strength that is caused by a brief period of coordinated neuronal activity. Although LTP is persistent, the increase in synaptic strength can be reversed by different patterns of neuronal activity by a process known as depotentiation. These same patterns of neuronal activity can, under certain circumstances, lead to LTD of synaptic transmission from the basal (non-potentiated) state, and this *de novo* LTD can be reversed by a process of de-depression. Bi-directional and reversible alterations in synaptic efficiency make possible the dynamic storage of vast amounts of neurally encoded information. GluRs and GABA (-aminobutyric acid) receptors (GABARs) mediate most synaptic transmission in the vertebrate CNS and are pivotal

in the induction, expression and/or modulation of synaptic plasticity. NMDA receptors (NMDARs) are the main triggers for the induction of LTP and LTD, and their activation is tightly regulated by the activation of GABAA and GABAB receptors. Both kainate receptors and mGluRs can trigger the induction of NMDAR independent forms of LTP and LTD. AMPARs mediate the synaptic response that is most commonly studied during LTP and LTD experiments, and are believed to be an important target of modulation during synaptic plasticity. In recent years, glutamate and GABA receptors have been shown to move rapidly around the neuron so as to alter the number and composition of receptors that are available to respond to released neurotransmitters. Receptor trafficking involves the intracellular movement of receptors from sites of synthesis to the plasma membrane, where they function, and then to sites of degradation. The receptors are inserted into and removed from the plasma membrane by exocytosis and endocytosis respectively, and diffuse laterally within the plasma membrane.

2.2. AMPARs TRAFFICKING

It is generally agreed that postsynaptic changes in AMPAR function make an important contribution to the expression of LTP. Broadly speaking, LTP could involve the modulation of AMPARs that are already expressed at the synapse and/or the rapid recruitment of new AMPARs to the synapse to alter the number present (Benke et al., 1998). In the latter mechanism, the new receptors could have either the same properties as the existing population or different ones (Liu et al., 2000; Palmer et al., 2004). Whatever mechanism is employed for LTP, LTD could be its mirror image, or might evoke mechanistically distinct processes to reduce synaptic strength. Studies of AMPAR trafficking in synaptic plasticity have focused on the idea that an alteration in AMPAR number is one of the expression mechanisms for LTP and LTD. Early evidence for this was provided when it was shown that LTP involves the rapid 'unsilencing' of 'silent' synapses (Malinow et al., 2002) - synapses that show NMDAR- but not AMPAR-mediated responses. Further work showed that LTD could involve the 're-silencing' of synapses (Luthi et al., 1999). The mechanistic explanation for silent synapses and the locus of their unsilencing have been hotly debated, but one idea involves the rapid recruitment of AMPARs to the plasma membrane of synapses that previously lacked AMPARs. Consistent with this idea,

antibodies that bind AMPARs on living neurons have revealed that spines with AMPARs on their surface can be found adjacent to spines in which AMPARs can only be detected intracellularly (Richmond et al., 1996). Over the past few years, much information has been obtained concerning the trafficking of AMPARs, from their synthesis and dendritic trafficking to their membrane insertion and removal (Bredt et al., 2003). In this study, we focus on the rapid movement of AMPARs that might be associated with LTD induced by either Aβo or NMDA stimulations. Recently, two broad approaches have been using to visualize AMPARs in living neurons to investigate how their movement relates to synaptic plasticity. One approach uses recombinant AMPAR subunits that contain a fluorescent reporter, such as green fluorescent protein (GFP). LTP was found to be associated with the delivery of GFP–GluR1 to spines in organotypic slice cultures (Shi et al., 1999). As the use of imaging techniques could not determine whether these constructs were inserted into the plasma membrane during LTP, mutated receptors were used that had a distinct electrophysiological signature. Alterations in the rectification properties of the synaptic currents showed that recombinant AMPARs were delivered to the synapse (Hayashi et al., 2000). The development of pH-sensitive GFP-AMPAR constructs means that researchers can now directly observe the insertion and removal of recombinant receptors into and from the membrane, because the pH of the lumen of intracellular vesicles differs from that of the extracellular environment (Ashby et al., 2004). This new approach is likely to facilitate greater understanding of many aspects of AMPAR trafficking in synaptic plasticity. In the second method, antibodies that recognize extracellular epitopes of native AMPAR subunits were used in conjunction with protocols that induce NMDAR dependent LTP and LTD in dissociated cultured neurons; the alteration in native AMPAR distributions was determined using fluorescently conjugated secondary antibodies. This approach has been used to show that AMPARs are internalized during NMDAR-dependent LTD (Beattie et al, 2000; Carroll et al, 2001) and inserted into the membrane during NMDAR dependent LTP (Lu et al., 2001; Pickard et al., 2001). LTD induced by activation of mGluRs might also involve the internalization of AMPARs (Snyder et al., 2001; Xiao et al., 2001).The use of antibodies is a less dynamic and flexible approach than the imaging of recombinant receptors but provides essential information about how native receptors behave during synaptic plasticity.

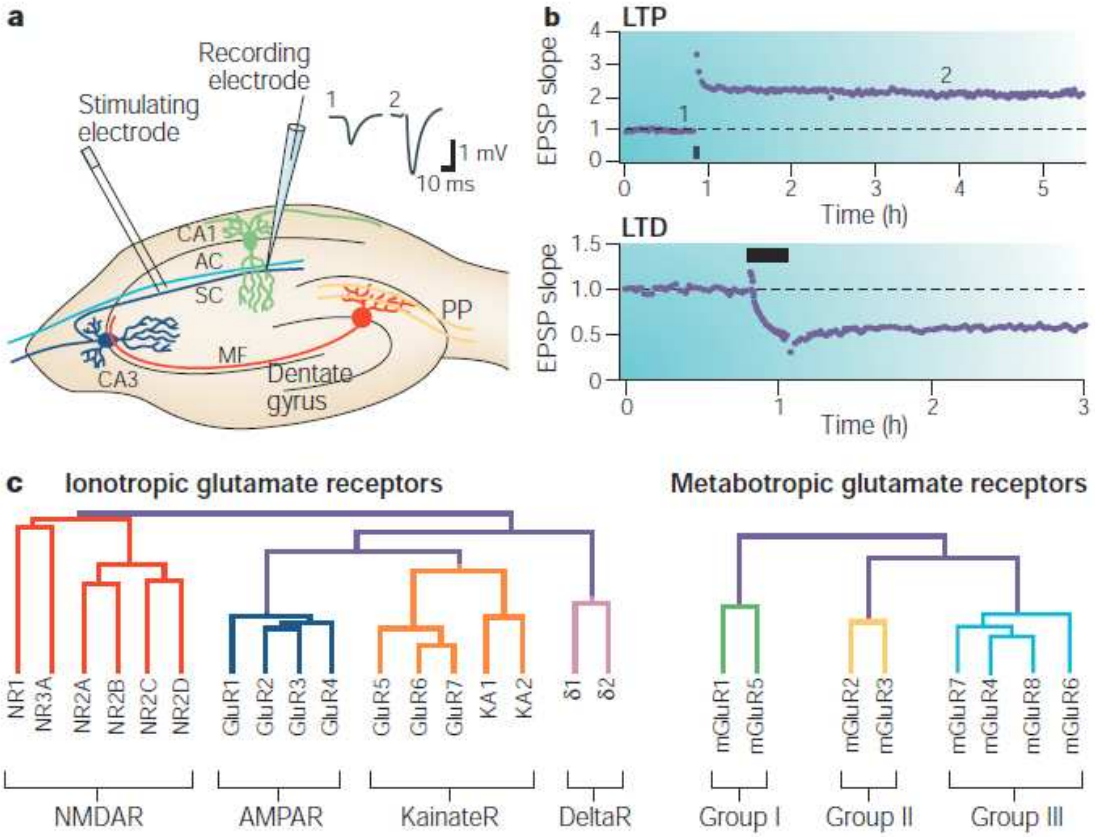

FIGURE 2. Synaptic plasticity in the hippocampus and glutamate receptor subtypes. a. schematic diagram of the rodent hippocampal slice preparation, showing the main excitatory pathways (AC, associational/commissural; MF, mossy fibre; PP, perforant path; SC, Schaffer collateral). Typical electrode placements for studying synaptic plasticity at Schaffer collateral–commissural synapses are indicated. The traces are field excitatory postsynaptic potentials (EPSPs) recorded before (1) and during (2) LTP (long-term potentiation). **b**. Timecourse plots showing alterations in field EPSP (rising slope normalized to baseline) against time, during LTP (100-Hz stimulation, 1 s, baseline intensity) or after the induction of de novo LTD (long-term depression) (1-Hz stimulation, 15 min, baseline intensity). The black bar represents the time of the stimulus and the numbers (1 and 2) indicate the time points illustrated in (a). **c**. KA, kainate receptor subunit. Figure is from Richmond, et al., 1996.

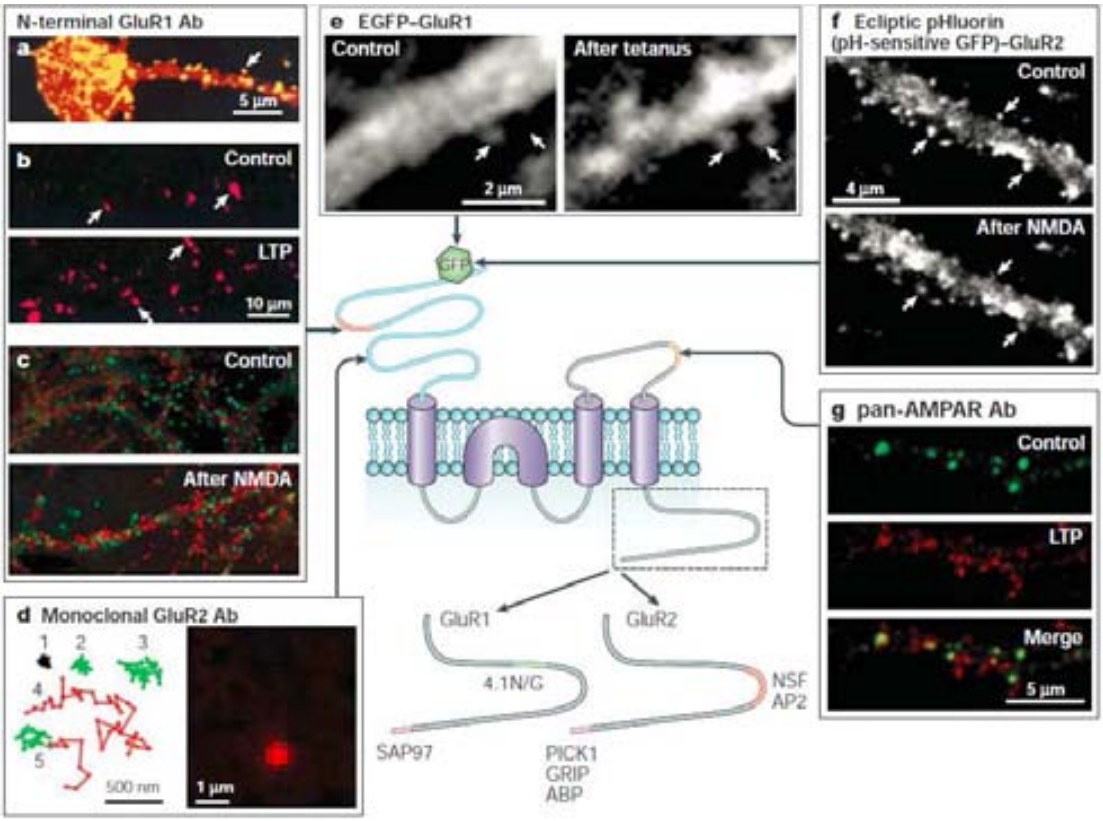

FIGURE 3. Rapid trafficking of AMPARs during synaptic plasticity. Centre: schematic diagram of an AMPA (-amino-3-hydroxy-5-methyl-4-isoxazole-propionic acid) receptor (AMPAR) subunit showing the domain structure, protein–protein interaction sites, GFP (green fluorescent protein) insertion sites and sites of epitopes for various antibodies used for imaging AMPAR trafficking. **a**. Superimposed image showing the localization of surface GluR1 (glutamate receptor 1) subunits using an N-terminal antibody (Ab) on a living hippocampal neuron (yellow) and the localization of total GluR1 using a C-terminal antibody after permeabilization (red). **b**. Induction of LTP (long-term potentiation) using glycine increases surface GluR1 in cultured hippocampal neurons. Surface GluR1 labelled using an N-terminal GluR1 antibody under nonpermeabilizing conditions in control (upper) and glycine-treated (lower) cultures. **c**. NMDA (N-methyl-D-aspartate)-induced internalization of AMPARs in cultured hippocampal neurons. Internalized GluR1 labelled with an N-terminal GluR1 antibody using an acid-stripping protocol (red) and co-localized with transferrin (green) in control (upper) and NMDA-treated (lower) cultures. **d**. AMPARs are mobile in the plasma membrane and in spines. Single-molecule tracking traces for individual GluR2 subunits (left), and an example of the signal from a single molecule (right). e. Redistribution of GFP-tagged GluR1 to spines after LTP induction. Arrows indicate individual spine locations. f. pH-sensitive GFP tagged GluR2 shows the removal of AMPARs from spines after NMDA treatment. **g**. Sequential labelling of surface AMPARs using pan-AMPAR antibodies shows an increase in surface AMPAR puncta (red) after LTP induction. ABP, AMPAR binding protein; AP2, adaptor complex; GRIP, glutamate receptor-interacting protein; NSF, N-ethylmaleimide-sensitive factor; PICK1, protein interacting with C-kinase; SAP97, synapse-associated protein 97; 4.1N/G, BANDS 4.1N AND 4.1G. Figure is from Ashby et al., 2004.

More precise measurements using single molecule fluorescence microscopy have revealed that both immobile receptors and mobile AMPARs are contained in spines

(Tardin et al., 2003). Stimulation with L-glutamate increases the rate of diffusion of synaptic AMPARs, decreases the proportion of immobile receptors and increases the proportion of receptors in the area around synapses. This indicates that lateral movement of AMPARs in the plasma membrane might be a mechanism for the regulation of AMPAR number during synaptic plasticity. In support of this, there is evidence that, after exocytosis, AMPARs are diffusely distributed along dendrites before accumulating at synaptic sites (Passafaro et al., 2001). The lateral diffusion model also predicts that a component of LTD is due to the rapid lateral diffusion of AMPARs from synaptic to extrasynaptic sites where they are then internalized. In agreement with this, endocytic zones close to the postsynaptic density have been identified. Moreover, AMPARs tagged with pH-sensitive GFP have been used to show that NMDAR activation leads to the rapid internalization of AMPARs from extrasynaptic sites, which precedes the loss of AMPARs from synapses (Ashby et al., 2004).

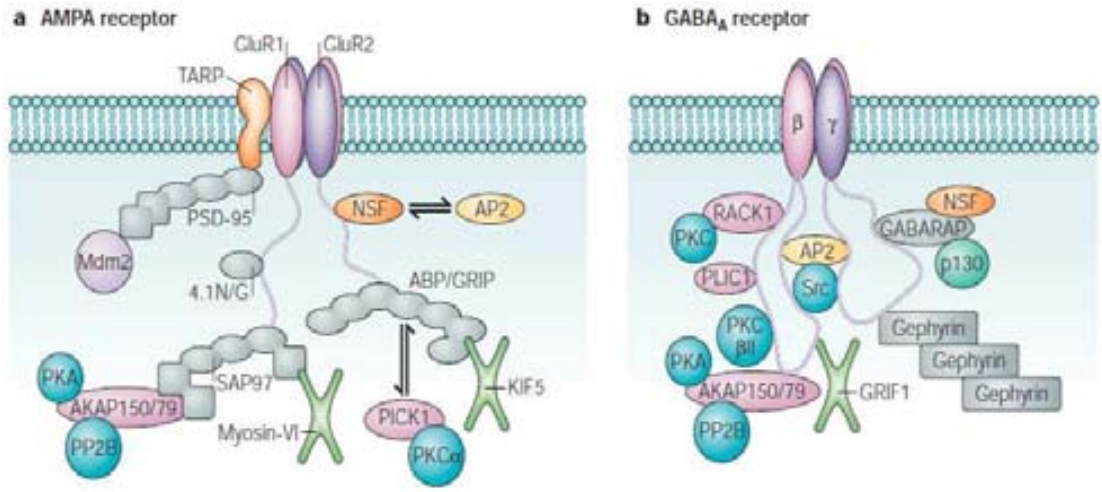

FIGURE 4. Proteins that associate with the C termini of AMPAR (-amino-3-hydroxy-5-methyl-4-isoxazole-propionic acid receptor) (a) or GABAAR (type A -aminobutyric acid receptor) (b) subunits. Multi-domain scaffolding proteins: the multi-PDZ DOMAIN-containing proteins SAP97 (synapse-associated protein 97) for GluR1 (glutamate receptor 1) and GRIP (glutamate receptorinteracting protein)/ABP (AMPAR binding protein) for GluR2 and 3 (a), and the trimeric scaffolding protein gephyrin for -subunits of GABAARs (b). NSF (N-ethylmaleimide-sensitive factor): direct interaction with GluR2 and 3 (a), and association with -subunits through its interaction with GABARAP (GABAR associated protein) (b). AP2 (adaptor complex): interaction with GluR2 and 3 subunits (a), and with the - and -subunits (b). AKAPs (A-kinase-anchoring proteins): AKAP150 (AKAP79) associates with the GluR1 subunit through an interaction with SAP97 (a), and AKAP150 directly interacts with the -subunit (b). Proteins that interact with PKC (protein kinase C) (PKC chaperones): PICK1 (protein interacting with C-kinase) binds directly to GluR2 and 3 (a), and RACK1 (receptor for activated C-kinase) binds to -subunits (b). Cytoskeleton-interacting proteins: bands 4.1N

and 4.1G interact with GluR1 (a), GABARAP interacts with - subunits, and PLIC1 (protein that links IAP to the cytoskeleton) interacts with -subunits (b). Motor proteins: KIF5 (kinesin family member 5) associates with GluR2 and 3 through its interaction with GRIP, myosin-VI associates with GluR1 through its interaction with SAP97 (a), and GRIF1, a hypothesized motor protein, interacts directly with -subunits (b). UBIQUITINATION pathway proteins: the E3 ligase Mdm2 interacts with PSD-95 (postsynaptic density protein 95), which associates with AMPARs through its interaction with TARPs (transmembrane AMPAR regulatory proteins) (a), and PLIC1, which regulates ubiquitination, interacts directly with -subunits (b). PKA, protein kinase A; PP2B, protein phosphatase 2B. Figure is from Collingridge G. et, al., 2004.

So, a general model is emerging in which synaptic plasticity involves both regulated exocytosis and endocytosis of AMPARs at extrasynaptic sites and their regulated lateral diffusion into and out of the synapse, perhaps involving a pool of juxtasynaptic AMPARs that are available for rapid recruitment. What mechanisms drive AMPARs into and out of synapses during LTP and LTD through exocytosis, endocytosis and lateral diffusion? Various protein kinases have been implicated in the induction of NMDAR-dependent LTP; these include protein kinase C (PKC), calcium/ calmodulin-dependent protein kinase II (CaMKII), protein kinase A (PKA), p42/44 mitogen-activated protein kinase (MAPK) and phosphatidylinositol 3-kinase (PI3K).Conversely, protein phosphatases, in particular protein phosphatase 1 (PP1) and protein phosphatase 2B (PP2B), have been implicated in NMDAR-dependent LTD. It is likely that the insertion and removal of AMPARs involves many kinases and phosphatases and that some of these are involved in aspects of LTP and LTD other than AMPAR trafficking. Our discussion of the role of kinases is therefore limited to those studies that directly address the trafficking of AMPARs during synaptic plasticity. There is evidence that CaMKII PKA and PI3K (Man et al., 2003; Esteban et al., 2003) are involved in LTP, and that protein phosphatases and PKC are involved in different forms of LTD.

3. LONG TERM DEPRESSION

Although genetic and pharmacological studies have suggested that NMDAR-LTD of AMPAR-mediated synaptic transmission involves the activation of specific NMDAR subtypes (Collingridge et al., 2004), there is considerable flexibility - for example, GluN2B-containing NMDARs are required for LTD, but only under certain circumstances (Wong et al., 2007; Morishita et al., 2007). It is therefore likely that various NMDAR subtypes can trigger LTD and that the actual subtype(s) that are

involved depend on various factors, such as the induction protocol that is employed, expression levels (which vary according to brain region and developmental stage (Yashiro et al., 2008) and environmental conditions (for example, access to a running wheel) (Vasuta et al., 2007). In addition, in young adult animals proBDNF (the precursor of brain-derived neurotrophic factor (BDNF)), acting via neurotrophin receptor P75 (p75NTR), increases GluN2B expression and so enables a GluN2B-sensitive form of NMDAR-LTD to occur (Woo et al., 2005). Furthermore, hippocampal NMDAR-LTD that is induced in adult animals by blocking l-glutamate uptake may also be dependent on GluN2B activation. De novo NMDAR-LTD in CA1 is pronounced early in development, but is more difficult to induce in brain slices from adult animals (Yang et al., 2005) or in intact rodent hippocampi in vivo (Staubli et al., 1997). However, hippocampal LTD can be induced using certain protocols (Staubli et al., 1997) and is facilitated by exposing an animal to novelty or mild stress (Kemp et al., 2007). The effects of stress can be mimicked by blocking l-glutamate uptake (Yang et al., 2005). As the CNS develops, glutamate transporter mechanisms may limit activation of the NMDARs that would otherwise trigger LTD. Some studies have also shown strain differences, with LTD being more easily induced in Wistar and Sprague - Dawley strains than in hooded rat strains (Manahan et al, 2000a; Manahan et al, 2000b). However, there is also evidence that NMDAR-LTD is important for certain forms of learning and memory in the adult animal in the absence of stress. NMDAR-LTD (A). In NMDAR-LTD (A), Ca2+ that enters through NMDARs binds to calmodulin to activate PP2B (also known as calcineurin), which dephosphorylates inhibitor-1 and this leads to the activation of protein phosphatase 1 (PP1) (Mulkey et al., 1993). PP1 then dephosphorylates its substrate(s), including ser845 on the AMPAR subunit GluA1 and this leads to LTD. In addition, Ca^{2+} entry triggers Ca^{2+} release from intracellular stores (Nishiyama et al., 2000) and this may serve to activate Ca^{2+} sensitive enzymes that are located further away from the postsynaptic density (PSD), where endocytosis may occur. The first clue to the molecular mechanism that drives the endocytosis of AMPARs during NMDAR-LTD was the observation that disruption of an interaction between GluA2 and N-ethylmaleimide-sensitive factor (NSF; an ATPase involved in membrane fusion events) causes AMPAR internalisation, mimicking NMDAR-LTD. Later, it was shown that clathrin-mediated endocytosis was involved in this process and that the clathrin adaptor protein AP2 also binds to the NSF site on the GluA2 subunit. This

suggests that AMPARs are stabilised on the membrane by NSF and that AP2 replaces NSF to initiate AMPAR endocytosis during NMDAR-LTD. A potential mechanism for the triggering of this exchange involves hippocalcin, a member of the neuronal calcium sensor (NCS) family. On sensing small rises in Ca^{2+} hippocalcin translocates to the plasma membrane, where it forms a complex with AP2 and GluA2 that may initiate clathrin-mediated AMPAR endocytosis (Palmer et al., 2005). In addition, the small GTPase Rab5 has been implicated in LTD (Brown et al., 2005). Other steps in clathrin-mediated endocytosis that underlies NMDAR-LTD are also beginning to be determined - for example, calcyon, a protein that regulates clathrin assembly is involved in NMDAR-LTD in the hippocampus (Davidson et al., 2009). Protein interacting with C kinase 1 (PICK1) is another protein that binds directly to GluA2 and has been implicated in NMDAR-LTD. PICK1 is a low-affinity Ca^{2+} sensor that can also bind protein kinase Cα (PKCα) and that can sense, and perhaps induce, membrane curvature. PICK1 competes with the scaffolding proteins AMPAR binding protein (ABP) and glutamate receptor interacting protein (GRIP) for binding to the carboxy-terminal (C-terminal) region of GluA2 and it also promotes internalization of GluA2-containing AMPARs. It was originally proposed that during NMDAR-LTD PICK1 may promote the synaptic removal of AMPARs by inducing the PKCα-mediated phosphorylation of ser880 of GluA2 to dissociate AMPARs from ABP–GRIP. However, most of the experimental data do not support this hypothesis. NMDA-induced internalization of AMPARs is not dependent on the phosphorylation status of ser880 or on PICK1 (Lin et al., 2007) and PKC inhibitors do not affect NMDAR-LTD (Peineau et al., 2009; Oliet et al., 1997). Experiments that use inhibitors of the GluA2–PICK1 interaction have yielded conflicting results. One study acutely applied an interfering peptide and reported no effect on NMDAR LTD, whereas a subsequent report described a partial inhibition. A small-molecule inhibitor of the GluA2–PICK1 interaction was also found to partially inhibit NMDAR-LTD (Thorsen et al., 2010). These partial effects are in contrast with the abolition of NMDAR-LTD that results from chronic manipulation of PICK1 (Terashima et al., 2008). Thus, the presence of PICK1 may be necessary for NMDAR-LTD in the long-term but it probably plays only a minor part, if any, in the release of AMPARs from their synaptic tethers. A more important role of ABP–GRIP may be to anchor AMPARs at non-synaptic sites (intracellular or extra-synaptic sites on the plasma membrane), as recently confirmed by paired-cell recording experiments (Emond et

al., 2010). NMDAR-LTD becomes unstable if the ability of AMPARs to bind ABP-GRIP is impaired. This implies that by retaining AMPARs at non-synaptic sites this scaffolding molecule is crucial for the expression of this form of LTD. PICK1 may enable the disassociation of AMPARs from ABP–GRIP at these non-synaptic sites, thereby enabling de-depression (re-potentiation) of synaptic transmission. Another key function of PICK1 in NMDAR-LTD may be to enable actin depolymerization through an interaction with F-actin and the actin-related protein 2/3 (Arp2/3 complex), and through this process to modify neuronal architecture (Rocca et al., 2008). NMDAR-LTD (A) is classically assumed to require the activation of phosphatases. However, studies using kinase inhibitors have implicated various serine/ threonine (Ser/Thr) protein kinases in this process as well. These include PKA (Brandon et al., 1995), cyclin-dependent kinase 5 (Ohshima et al., 2005), P38 mitogen-activated protein kinase (p38MAPK) (Zhu et al., 2005) and glycogen synthase kinase-3 (GSK3) (Peineau et al., 2007). As with all inhibitor studies, potential off-target effects should be taken into account and this is particularly important for protein kinases because the mammalian genome encodes over 500 protein kinases. A role for GSK3 in NMDAR-LTD is supported by the effects of six different GSK3 inhibitors including lithium, which may exert some of its therapeutic actions via this mechanism. A direct link between the protein phosphatase cascade and GSK3 was observed during NMDAR-LTD; PP1 dephosphorylates GSK3β and its upstream inhibitor Akt and these actions result in activation of GSK3β (Peineau et al, 2007). An additional mechanism of GSK3 activation may occur via caspase-3 (Li et al, 2010). This protease is activated during NMDAR-LTD through a cascade involving cytochrome c and caspase-9 and is able to cleave Akt, thus removing its tonic inhibition of GSK3. The finding that both caspases and GSK3β, an enzyme that is deregulated in patients with Alzheimer's disease, are involved in NMDAR-LTD raises the possibility that the neurodegeneration that underlies Alzheimer's disease and related dementias may be caused at least in part by pathological activation of this form of LTD. NMDAR-LTD is associated with tyrosine phosphorylation of GluA2 and this suggests that protein tyrosine kinases (PTKs) are also involved. PTKs of the sarcoma (Src) family phosphorylate GluA2 at a tyrosine residue in a tyrosine-rich region of the C-terminal tail of GluA2 and this is thought to be required for AMPAR endocytosis. Consistent with this idea, a peptide that mimics this tyrosine-rich region has been found to block NMDAR-LTD (Ahmadian et al., 2004). What are the targets

of enzymes that are activated during NMDAR-LTD and underlie an alteration in the synaptic expression of AMPARs? A major target seems to be PSD95, which positions calcineurin near the mouth of the NMDAR channel through an interaction with A-kinase anchor protein (AKAP)-150 (Bhattacharyya et al., 2009) and which is dephosphorylated on ser295 during LTD to enable the removal of PSD95 from the synapse and thereby permit AMPAR endocytosis (Kim et al., 2007). These mechanisms occur rapidly after NMDAR LTD is triggered. However, protein synthesis is required for LTD to be sustained as inhibitors of translation cause a recovery of synaptic transmission in a few hours. How these newly synthesized proteins sustain LTD for longer periods of time is not known but regulators of gene transcription that may be involved in NMDAR-LTD are starting to be investigated (Wu et al., 2010).

4. SOLUBLE PROTEIN OLIGOMERS IN NEURODEGENERATION: FROM THE ALZHEIMER'S AMYLOID β-PEPTIDE

4.1 THE DISCOVERY OF THE FIRST AD CAUSATIVE GENE

The AD causative gene encodes -amyloid precursor protein (APP), which is a single-transmembrane, receptor-like protein that is expressed ubiquitously in neural and non-neural cells. After the Bavarian psychiatrist Alois Alzheimer presented his first clinic-pathological case in Tübingen on November 3, 1906 (Alzheimer A 1907), it became clear that amyloid plaques in the cerebral cortex (were invariably associated with the disease that now bears his name. In the 1980s, biochemists focused on the isolation of the amyloid to identify its principal component. Glenner and Wong purified microvascular amyloid deposits from the meninges of AD brains and provided a partial sequence of an ~4-kDa subunit protein that they named amyloid -protein. Shortly thereafter, Masters, Beyreuther and co-workers identified the same protein as the subunit of amyloid plaque cores that were isolated from post-mortem AD cortices (Masters et al., 1985). Around the same time, the microtubule-associated protein tau was identified as the main constituent of the hallmark neurofibrillary tangles that accumulate inside many neurons and their processes in brains (Grundke et al., 1986; Kosik et al., 1986). Tau is a highly soluble cytoplasmic protein that binds to tubulin

during its polymerization into microtubules in neurons and thereby stabilizes these important cytoskeletal organelles. Glenner also showed that the amyloid deposits that occur in the brain vessels of young adults with Down syndrome were composed of AD. Since 1969, it had been known that middle-aged patients with Down syndrome develop the amyloid plaques and neurofibrillary tangles that are typical of AD (Olson et al., 1969). On this basis, Glenner assumed that the gene ultimately found to encode might be causative of AD cases. The subsequent cloning of *APP*, which encodes a large, type 1 membrane glycoprotein, by Beyreuther and co-workers in 1987, and its localization to the long arm of chromosome, was consistent with this hypothesis (Kang et al., 1987). These biochemical findings pointed strongly to the *APP* gene as a site which geneticists should search for AD-causing mutations. The first such mutation was discovered in a family with hereditary cerebrovascular amyloidosis with multiple haemorrhages (Levy et al., 1990). Shortly thereafter, a distinct APP missense mutation was found in a family with early-onset AD (Goate et al., 1991), and then additional mutations in other families were detected (Chartier et al., 1991). These and other findings led to the formal proposal of a hypothesis of disease in which excessive accumulation and deposition could trigger a complex downstream cascade that resulted in the symptoms of AD (Hardy et al., 1992). In its most recent iteration (Hardy et al., 2002), the amyloid (or Aβ) hypothesis states that the gradual accumulation and aggregation of this small hydrophobic peptide initiates a slow but deadly cascade that leads to synaptic alterations, microglial and astrocytic activation, the modification of the normally soluble tau protein into oligomers and then into insoluble paired helical filaments, and progressive neuronal loss associated with multiple neurotransmitter deficiencies and cognitive failure.

4.2 THE REGULATED INTRAMEMBRANE PROTEOLYSIS OF APP

Initially, the mechanism by which the partially intra-membrane region could be liberated as a free peptide from its precursor was enigmatic and was considered to require some pre-existing membrane injury. It was assumed that the hydrophobic interior of the membrane bilayer would need to be damaged to allow access of a protease and water to effect cleavage. But this concept was disproven when was unexpectedly discovered to be produced normally by the intramembranous proteolysis of APP throughout life and APP was found to circulate in extracellular fluids,

including cerebrospinal fluid (CSF) and plasma (Busciglio et al., 1993). This discovery opened up the dynamic study of A, which heretofore had only been obtained through painstaking isolation from post-mortem human brain. As predicted by the amyloid hypothesis, all AD-causing APP mutations that have been identified so far occur either within or flanking the region of this large polypeptide. Accordingly, the mutations that flank the region increase the production of the highly amyloidogenic Aβ 42 isoform, whereas the mutations within the region enhance the oligomerization of the peptide (Haass et al., 2004).

4.3. PROCESSING OF AMYLOID PRECURSOR PROTEIN

Cleavage by α-secretase interior to the β-amyloid peptide (Aβ) sequence initiates nonamyloidogenic processing. A large amyloid precursor protein (sAPPα) ectodomain is released, leaving behind an 83-residue carboxy-terminal fragment. C83 is then digested by γ-secretase, liberating extracellular p3 and the amyloid intracellular domain (AICD). A myloidogenic processing is initiated by β-secretase beta-site amyloid precursor protein–cleaving enzyme 1 (BACE-1), releasing a shortened sAPPα. The retained C99 is also a γ-secretase substrate, generating Aβ and AICD. γ-Secretase cleavage occurs within the cell membrane in a unique process termed “regulated intramembranous proteolysis.” sAPPα and sAPPβ are secreted APP fragments after α-secretase and β-secretase cleavages, respectively. AICD is a short tail (approximately 50 amino acids) that is released into the cytoplasm after progressive ε-to-γ cleavages by γ-secretase. AICD is targeted to the nucleus, signaling transcription activation. Lipid rafts are tightly packed membrane micro-environments enriched in sphingomylelin, cholesterol, and glycophosphatidylinositol (GPI)–anchored proteins. Soluble Aβ is prone to aggregation. Activation of NMDAR led to rapid internalization of cell surface (Querfurth and LaFerla, 2010).

4.4. OLIGOMERS INDUCE SYNAPTIC DYSFUNCTION

Research on AD seeks to answer a central question: what causes the onset of a subtle, intermittent impairment of hippocampal neuronal function and, therefore, episodic memory? However, perhaps the most persistent argument against the amyloid hypothesis as summarized earlier is that many apparently healthy older humans have

substantial amounts of amyloid in their limbic and association cortices upon post-mortem examination. These deposits are overwhelmingly of the diffuse type - they are not composed of amyloid fibrils and they have little or none of the surrounding neuritic and glial cytopathology found in mature neuritic plaques (Dickson et al., 1997). Furthermore, reports of weak quantitative correlations between manual microscopic counts of amyloid plaques in post-mortem brain sections and the extent of cognitive symptoms measured pre-mortem are fraught with methodological challenges. Counting spherical plaques in two-dimensional cross sections provides an imprecise measure of amounts and misses small and heterogeneous Aβ-assembly forms. Last, the cognitive testing done before the patient's death has often been done with simple, insensitive mental status screens. The advent of specific enzyme-linked-immunosorbent assays (ELISAs) coupled with western blotting and mass spectrometry has now enabled a more precise and comprehensive assessment of quality and quantity. Such studies indicate that biochemically measured levels of soluble Aβ, including soluble oligomers, correlate much better with the presence and degreeof cognitive deficits than do simple plaque counts (McLean et al., 1999). This evidence, coupled with the fact that large (~20-120-m diameter) fibrillar plaques present much less surface area to neuronal membranes than do a multitude of small oligomers that can diffuse into synaptic clefts, indicates that such soluble assembly forms are better candidates for inducing neuronal and/or synaptic dysfunction than plaques, *per se*. Importantly, the idea that large aggregates of a disease causing protein can actually be inert or even protective to neurons has been supported by work on other protein folding disorders. For example, in cell-culture studies of HD, less cell death has been observed when large aggregates of polyglutamine-rich huntingtin protein are present in the cells than when only soluble huntingtin is present without these inclusions (Schaffar et al., 2004). Analogous findings have been reported in a mouse model of spinocerebellar ataxia in which the polyglutamine-rich forms of the ataxin-1 protein are expressed (Cummings et al., 1999). However, it must also be pointed out that large plaques of fibrillar in AD brains typically show surrounding dystrophic neurites, indicating that insoluble aggregates might contribute to neuronal injury. Indeed, fibrillar deposits have been associated with local synaptic abnormalities and even with the breakage of neuronal processes (Tsai et al., 2004). The problem is that large, insoluble protein aggregates are likely to be intimately surrounded by a number of smaller, more diffusible, assemblies (for example,

oligomers). So, it becomes difficult to ascertain whether the large aggregates are directly inducing local neuronal injury and dysfunction. At the current stage of research, one should not conclude that either large, insoluble deposits or small, soluble oligomers represent the sole neurotoxic entity; indeed, a continuous dynamic exchange between these forms might well be detrimental. Nevertheless, we hypothesize that diffusible oligomers have the principal role, particularly during the earliest, even pre-symptomatic, stages of the AD process.

4.5. ADDLS INDUCE MEMORY LOSS

An intensively studied electrophysiological correlate of learning and memory is LTP. Repetitive, high frequency electrical stimulation of certain synaptic circuits, for example the CA3-Schaefer collateral-CA1 pathway in the mammalian hippocampus, can induce a prolonged potentiation of synapse firing (LTP) that is referred to as inducing synaptic plasticity. There is now considerable evidence that ADDLs of synthetic human and soluble, low-number (low-n) oligomers of naturally secreted human ADDLs can all inhibit the maintenance of hippocampal LTP. In the case of the cell-derived oligomers, this inhibition occurs at low- to sub-nanomolar concentrations that are similar to those that can be found in human CSF. This effect has been shown by both *in vivo* micro injection in living rats and by treatment of hippocampal slices (Walsh et al., 2002). The effects of the natural oligomers on LTP are specifically neutralized by anti-antibodies *in vivo*, either through active vaccination or passive infusion (Klyubin et al., 2005). The same oligomers have been shown to interfere rapidly and reversibly with the memory of a learned behaviour in wake, behaving rats (Cleary et al., 2005). Taken together, these various results provide compelling evidence that decreased hippocampal LTP and altered memory function can be directly attributed to an isolated, biochemically defined, assembly form of human A (with low-n soluble oligomers probably ranging from dimers to dodecamers), in the absence of amyloid fibrils or PFs.

4.6. OLIGOMERIC ASSEMBLY CHARACTERISTICS

The biochemical mechanism by which soluble oligomers bind to synaptic plasma membranes and interfere with the complex system of receptor and/or channel proteins

and signaling pathways that are required for synaptic plasticity is under intensive study. Intriguingly, Kamenetz and colleagues (Kamenetz et al., 2003) showed that neuronal electrical activity stimulated BACE and therefore increased generation, and the resulting increased levels of then depressed synaptic transmission. Moreover, Cirrito and colleagues used *in vivo* microdialysis probes to demonstrate that interstitial fluid concentrations correlate with the synaptic activity in APP transgenic mice (Cirrito et al., 2005). It is possible that soluble oligomers interfere with signalling pathways downstream of certain NMDA or AMPA receptors at synaptic plasma membranes in a manner that allows an initial LTP response but not its persistence. In this regard, it is interesting to note that the application of Aβ to cortical slices has been reported to promote the endocytosis of some NMDA receptors through a mechanism that involves initial binding of the Aβ to nicotinic receptors (Snyder and Nong et al., 2005). Consistent with this model, treatment lowered NMDA-evoked currents. It has also been shown that oligomeric can interfere indirectly with LTP through an inhibition of an ubiquitin C-terminal hydrolase (UCH). This enzyme enhances recycling of ubiquitin, which is required to label unfolded proteins destined for proteasome degradation. Treatment inhibited UCH, which in turn blocked LTP. However, it is currently unclear how the extracellular can reach and affect the cytoplasmic ubiquitin system. Again, selective receptors might be involved.

5. A- KINASE-ANCHORING PROTEINS

To ensure specificity of intracellular events, signaling complexes at specific subcellular locations are formed by scaffold proteins, such as AKAPs, which anchor receptors and signaling proteins to physiological substrates. AKAP79/150 is a member of this family, with three orthologs, human AKAP79, rodent AKAP150, and bovine AKAP75. AKAP79/150 recruits protein kinase A (PKA), protein kinase C (PKC), calmodulin (CaM), and calcineurin (CaN) to ion channels, such as glutamate receptors. AKAP79/150-anchored PKA and CaN are thought to be important for regulating AMPA receptor currents and membrane trafficking to control synaptic plasticity in hippocampal neurons (Weisenhaus et al., 2010). It is now recognized that the rate and spatial precision of phosphorylation and dephosphorylation reactions in cells are constrained through the anchoring of kinases and phosphatases near their targets by scaffold proteins (Wong and Scott, 2004). In particular, subcellular

targeting by AKAP79/150 of the kinase PKA, phosphatase, and other enzymes promotes highly localized signaling events at the postsynaptic membrane of neuronal dendritic spines Processing of APP (Murphy et al., 2014). A-kinase anchoring proteins (AKAPs) ensure enzymes are appropriately targeted to optimally facilitate signal transduction. A unifying feature of this group of proteins is their ability to anchor the regulatory (R) subunits of protein kinase A (PKA) in proximity to substrates. However, each anchoring protein associates with a unique subset of signaling effectors comprising protein kinases, phosphoprotein phosphatases, small GTPases, phosphodiesterases, transmembrane receptors, and ion channels (Dodge et al., 2005).

Arguably the most extensively characterized anchoring protein, AKAP79/150, organizes a veritable mecca of signaling proteins. These include the beta adrenergic receptor (bAR), adenylyl cyclase (AC), L-type voltage-gated Ca2+ channels (Cav1.2, Cav1.3), protein kinases A and C (PKA, PKC), and protein phosphatases among others (Scott et al., 2013;). The exquisite control AKAP79/150 exerts on its many partner molecules in a variety of cellular contexts makes this anchoring protein a prototypic example of local signaling specificity (Tunquist et al., 2008). Modulation of signaling molecules through dephosphorylation is a key mechanism of signal transduction (Mochida et al., 2012). A recently defined example is anchoring of the calcium- calmodulin-dependent serine-threonine protein PP2B to neuronal AKAP79/150 (Figure 5). This enzyme is the target of immunosuppres-sant drugs cyclosporine A and FK506. A primary down-stream effector of PP2B is the transcription factor, nuclear factor activated in T cells (NFAT). Work with NFAT has identified a PP2B recognition site intrinsic to many PP2B effector proteins, commonly referred to as PIxIxIT sequence (Li et al., 2011). Although the region of AKAP79/150 required for binding to PP2B was originally mapped more than 10 years ago, recent work has identified a specific sequence within this region, which bears striking resem-blance to the PIxIxIT motif in NFAT (Li et al., 2012). The authors showed that this region was responsible for the AKAP79/ 150-mediated activation of NFAT by PP2B. In rat hippocampal neurons NFAT signaling is initiated via AKAP79/150-anchored Cav1.2-mediated increases in in-tracellular Ca^{2+}, PP2B activation, and NFAT dephosphor-ylation, allowing NFAT translocation to the nucleus where it regulates gene transcription. Additionally, AKAP150- dependent

nuclear translocation of NFAT regulates gene expression of KCNQ2 and KCNQ3 potassium channels and is abolished in AKAP150 null mice (Zhang et al., 2012). Activation of AKAP-anchored PP2B involves local Ca^{2+} influx through the L-type voltage-gated Ca^{2+}channel, Cav1.2. However, negative feedback regulation of the channel also appears to be modulated by PP2B as deletion of the

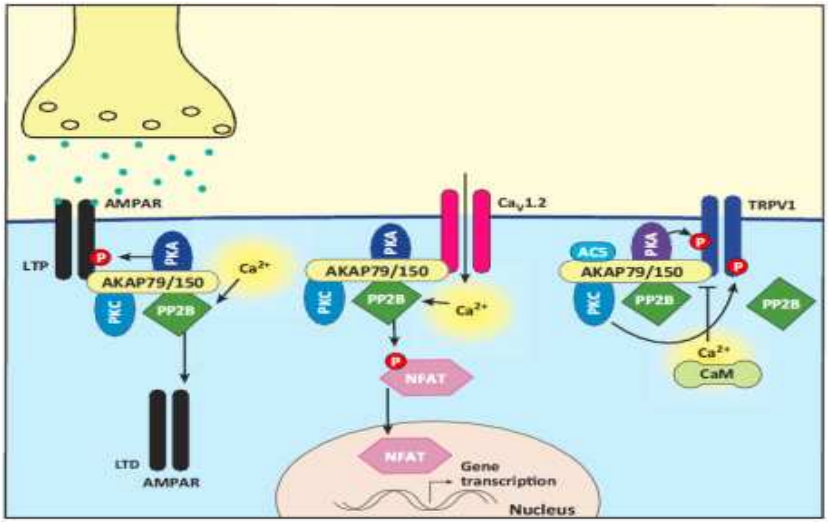

FIGURE 5. AKAP79/150 modulates diverse synaptic functions through anchored PP2B. Diagram depicting PKA-mediated phosphorylation of AMPAR GluA1 subunit primes the receptor for insertion in the postsynaptic membrane during LTP, whereas dephosphorylation by PP2B removes the receptor from the synaptic space during LTD. AKAP79/150-anchored Cav1.2 increases intracellular Ca^{2+}, triggering PP2B activation and NFAT dephosphorylation, allowing NFAT translocation to the nucleus where it regulates gene transcription. AKAP79/150-associated PP2B dephosphorylates the channel in a negative feedback loop. AKAP150-anchored PKA and PKC phosphorylate the TRPV1 channel, increasing channel sensitivity. This process is facilitated by AC5 and blocked by Ca^{2+}/ CaM. PP2B dephosphorylates the receptor independently of AKAP anchoring. Figure adapted from Li et al., 2011.

PP2B-binding motif on AKAP79/150 (DPIX), the use of interfering peptides, or pharmacological PP2B inhibition prevents feedback channel inhibition (Oliveria et al., 2012). LTP and LTD are systemic processes underlying learning and memory. LTP and LTD are Ca^{2+}-dependent processes mediated through AMPA- and NMDA-type glutamate receptor ion channels (Bliss et al., 1993). PKA-mediated phosphorylation of AMPA receptor GluA1 subunit primes the receptor for insertion in the postsynaptic membrane during LTP, whereas subunit de-phosphorylation by PP2B removes the receptor from the synaptic space during LTD. Genetic removal of AKAP79/ 150 in rat CA1 pyramidal neurons increases AMPA receptor-mediated excitatory postsynaptic currents (EPSCs) as well as NMDA receptor LTD. Interestingly, this is reversed upon reintroduction of wild type AKAP79/150 as well

as AKAP mutants lacking the PKA- or PKC-binding sites, but not with a mutant lacking the PP2B-binding domain (Jurado et al., 2010). DPIX transgenic mice exhibit greater AMPA receptor phosphorylation than wild type animals and dis-play simultaneous decreased LTP and enhanced LTD at hippocampal CA1 synapses (Sanderson et al., 2012). Finally, a novel mechanism of GABAergic LTD through dopamine D2L receptor depends on IP3 receptor activation and AKAP79/150-an-chored PP2B activity (Dacher et al., 2013). These selected examples illustrate the diversity of synaptic functions modulated byAKAP-anchored PP2B.

6. MICRORNAS AT THE SYNAPSE

In the mammalian brain, nerve cells are interconnected by trillions of specialized junctions, known as synapses. The proper formation and function of synapses is crucial for cognition, and several neurological disorders are characterized by synaptic dysfunction. Synapse development follows a stereotypic, multi-stage process (McAllister et al., 2007). Importantly, during postnatal development and in the adult, neural circuits are shaped by sensory experience. This process of experience-dependent plasticity, which occurs at the level of dendrites and synapses, underlies the brain's ability to adapt to changes in the environment and store information (Kandel et al., 2001). At the molecular level, plasticity is orchestrated by sophisticated gene expression programs that ensure that environmental stimuli are converted into long-lasting alterations in synapse structure and function (Flavell et al., 2008). Among these mechanisms, the local control of mRNA translation in neuronal dendrites can account for the tight spatial regulation of plasticity at the level of individual dendrites or spines (Sutton et al., 2006). MicroRNAs (miRNAs) are a recently discovered, extensive class of small non-coding RNAs that act as post-transcriptional regulators of gene expression (Figure. 6). Several recent reviews provide detailed descriptions of miRNA biogenesis and mode of action (Filipowicz et al., 2008). miRNAs have been described as important developmental switches that help to establish a differentiated cell type by targeting crucial master regulatory genes (Reinhart et al., 2000). Therefore, most research into neuronal miRNAs initially centered around neuronal differentiation (Kosik et al., 2006). miRNA functions in postnatal neurons are just beginning to emerge.

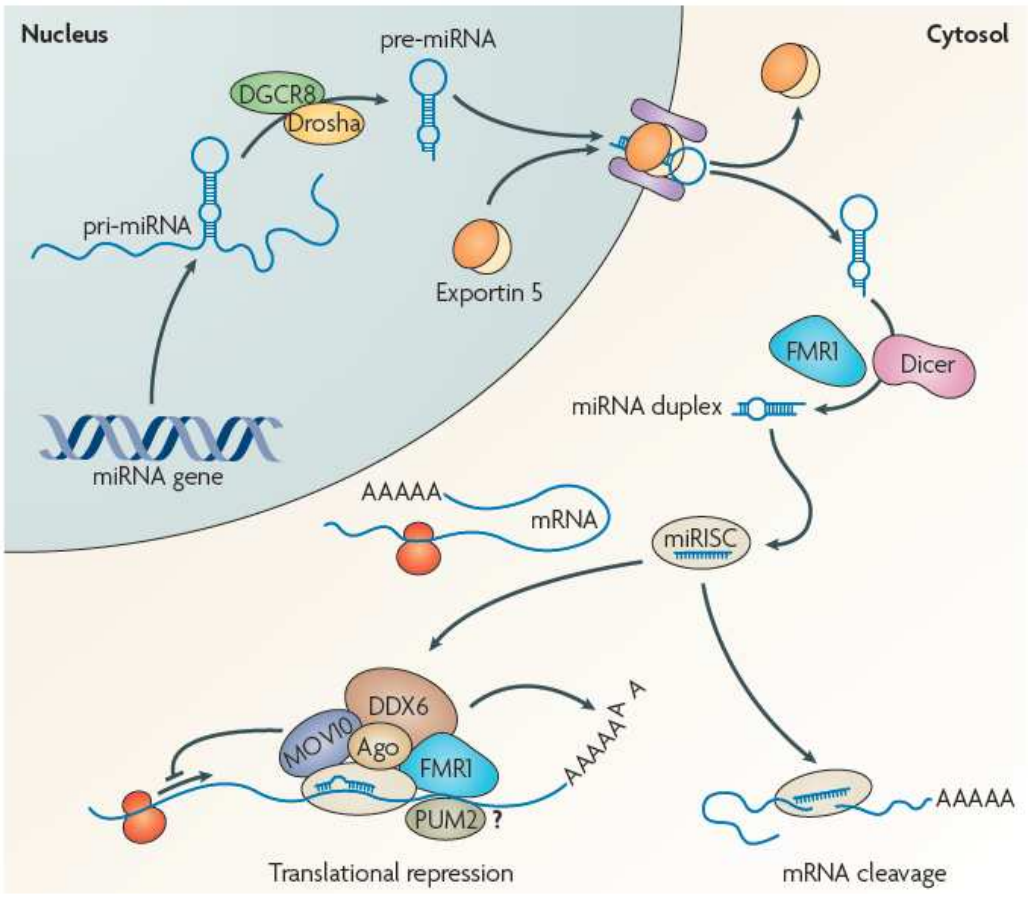

FIGURE 6. RNA biogenesis and mode of action. Transcription of microRNA (miRNA) genes by RNA polymerase II (Pol II) leads to the generation of primary miRNA transcripts (pri-miRNAs), which are cleaved in the nucleus by the microprocessor complex (which includes the proteins Drosha and DGCR8). The cleavage product is a precursor miRNA hairpin (pre-miRNA) that is exported to the cytoplasm by an exportin 5-dependent pathway. There, the pre-miRNA is further processed by the RNase Dicer (the activity of which can be modulated by accessory proteins, for example FMR1) to an intermediate miRNA duplex. Depending on the thermodynamic characteristics of the miRNA duplex, one strand (the leading strand) is loaded into a multi-protein complex (miRNA-induced silencing complex (miRISC)), whereas the other strand (the passenger strand) is usually degraded. The resulting miRNA-associated miRISC is guided to target mRNAs owing to extensive but imperfect pairing of the miRNA to target sequences that are preferentially located within the 3′ untranslated regions of the mRNA. This interaction leads to translational repression and/or degradation of the target mRNA, by a mechanism that is still controversial. Important components of miRISC with regard to synaptic function include Argonaute (Ago) and the helicases MOV10 (Armitage in Drosophila melanogaster) and DDX6 (also known as RCK and p54). In addition, accessory RNA-binding proteins (FMR1 and PUM2) are thought to modulate the activity of miRISC in neurons. Please note that only the pathway components that have been shown to have a role in miRNA regulation in postmitotic neurons have been shown for simplicity. Figure is adapted from Gerhard, et al., 2011.

But what features make miRNAs especially well suited to regulate important aspects of synapse development and plasticity? First, a large pool of different miRNA sequences is expressed in post-mitotic neurons at times of synapse development, and

many of these miRNAs are associated with translation regulatory complexes (Kim et al., 2004). This enormous complexity offers miRNA-regulated pathways the capacity to control the expression of several synapse-relevant proteins simultaneously. In addition, recent estimates indicate that each individual miRNA usually has up to a few hundred different target mRNAs (Bartel et al., 2009), although not every interaction is necessarily of physiological relevance. Another feature of interest is that many miRNAs do not act as on-off switches, but rather fine-tune gene expression profiles (Karres et al., 2007; Bartel et al., 2004). miRNA-mediated fine-tuning usually occurs in the absence of mRNA degradation, a scenario that fits well with the local regulation of dendritic mRNAs during storage and/or activation at the synapse. Related to this, miRNA-directed suppression of mRNA translation has been shown to be reversible in several cases (Vasudevan et al., 2007). This is important, because if miRNAs are to play a part in activity-dependent synapse development and plasticity, the dynamic regulation of miRNA function in response to synaptic stimuli is a prerequisite. Similarly, recent bioinformatics studies revealed that co-expression of neural miRNAs with their target mRNAs is a common feature, giving rise to the hypothesis that they might participate in feedback mechanisms that connect global transcriptional activation with the control of local dendritic protein synthesis (Tsang et al., 2007).

6.1. REGULATION OF MIRNA BY NEURONAL ACTIVITY

The regulation of gene expression programs by neural activity allows neurons to adapt their connectivity to changes in the environment. Many important synaptic regulators are influenced by neuronal activity, and miRNAs are no exception. A first layer of activity control occurs at the level of miRNA gene transcription. Several promoters of neural miRNAs are occupied by classical activity-regulated transcription factors, such as CREB and MEF2, which couple Ca^{2+}-regulated signaling cascades to the transcriptional machinery (Fiore et al., 2009). Furthermore, several post-transcriptional mechanisms can influence the expression and activity of mature miRNAs (Thomson et al., 2006). In synaptosomes, activity-dependent calpain cleavage stimulates Dicer activity, which could result in enhanced miRNA production at activated synapses (Lugli et al., 2005). The relevance of these mechanisms in the nervous system deserves more attention. Finally, the regulation of miRNA-associated

proteins has a significant impact on the ability of miRNAs to regulate target gene expression. For example, synaptic stimulation can lead to the inactivation or complete destruction of the miRNA-induced silencing complex (miRISC) component Armitage, offering the possibility of dynamically regulate target gene expression at individual synapses (Ashraf et al., 2006). These studies indicate that miRNAs and their associated protein complexes are a convergence point of intricate activity-regulated signaling networks, which enables them to control adaptive processes such as dendritic or synaptic plasticity.

6.2. MIRNAS IN NEUROLOGICAL DISORDERS

miRNAs, small non-coding RNAs that regulate gene expression have recently been implicated in Alzheimer's Disease in that their dysregulation leads to the proteomic changes that result in AD. They play a role in the disease onset and their abundance in body fluids such as the blood and the cerebrospinal fluid (CSF) make them potential biomarkers for early detection of the disease using everyday laboratory techniques such as northern blot and RT-PCR (Ciesla et al., 2011). miRNAs act through the RNA interference pathway which can be used to silence gene expression. This technique can be used as a potential treatment for AD by targeting the aberrantly expressed proteins to alleviate some symptoms of the disease during its early phases (Lee et al., 2012). miRNAs have certain advantages over other potential biomarkers for neurodegenerative diseases. They are relatively stable and highly specific for diseases such as AD. miRNAs participate early on in the post-transcriptional stages of gene expression. Changes in miRNA levels would precede any effects they might cause, making them perfect candidates for detecting diseases early on during their asymptomatic stage. Early detection allows for health-care providers to intervene during a stage where the best treatments and chances of modifying the disease could be provided (Ciesla et al., 2011).

In 2007, Walter J. Lukiw used small-scale profiling studies to provide the first clues into miRNA changes in AD (Lukiw, 2007). Since then, several groups, including the Lukiw laboratory, have performed large-scale genome-wide studies demonstrating that miRNA expression patterns are altered not only in the AD brain but also in blood and cerebrospinal fluid (CSF) (Nunez-Iglesias et al., 2010). Zhang et al (2013)

proposes a mechanism linking the onset of cognitive impairment, a condition often linked to AD, to a dysregulation in miR-106a. The JAK2/STAT3 pathway is a transcription activator that plays an important role in in the development of the central nervous system. It has often been linked to memory impairment and AD as its inhibition can be achieved through either age-dependent factors or high levels of β-Amyloid in hippocampal neurons, one the main brain areas for memory formation. Nevertheless, it remains difficult to predict whether these changes are a cause or a consequence of the neurodegenerative process and dementia. As discussed in detail elsewhere (Hébert and De Strooper, 2009), further validation is required; however, these observations open the door to novel diagnostic and possibly therapeutic tools for AD.

Most informative in this regard have been genetic mouse models that show certain characteristics of neuropsychiatric diseases. In humans, microdeletions at 22q11, for example, dramatically increase the risk of developing schizophrenia. A mouse model of this has been generated, and these mice have impaired expression of mature miRNAs, including miR-134 (Stark et al., 2008). Impaired miRNA biogenesis could be attributed to the loss of the Dgcr8 gene, encoding a component of the microprocessor complex. The behavioural defects in these mice coincide with abnormal dendrite and spine morphogenesis, further supporting a role for miRNAs in the regulation of neural connectivity. One of the hallmarks of schizophrenia is NMDAR hypofunction in the prefrontal cortex. One study implicated miR-219 in the control of NMDAR signaling by targeting the downstream component CAMKIIγ (Kocerha et al., 2009). The authors speculated that the observed downregulation of miR-219 in patients with schizophrenia could be part of a compensatory mechanism to restore NMDA signaling. In addition to these animal studies, cellular assays have uncovered both miRNA regulatory proteins and miRNA targets that are mutated in neuropsychiatric diseases, including FMR1 (Fragile-X-syndrome), LIMK1 (Willliams syndrome; targeted by miR-134) (Hoogenraad et al., 2004) and MECP2 (Rett syndrome; targeted by miR-132) (Klein et al., 2007). Neurons have evolved mechanisms to keep their firing rates constant in the face of perturbation, a concept known as neuronal homeostasis (Turrigiano et al, 2007). It was recently put forward that failure in neuronal homeostasis could underlie the common phenotypes (that is, mental retardation and autistic behaviour) in neuropsychiatric diseases (Ramocki et

al., 2008). miRNA-dependent fine-tuning of key disease-associated genes could be an important mechanism to maintain neuronal homeostasis and allow neural circuits to adequately respond to environmental insults whether miRNA regulation is directly involved in typical homeostatic adaptations of neural circuits, such as synaptic scaling, the inhibitory/excitatory synapse ratio or overall excitability is a topic for future research. Fewer than 5 years of work have provided compelling evidence for a crucial function of miRNAs at all stages of synapse development. Moreover, it is emerging that miRNAs themselves are subject to regulation by neuronal activity, putting them in a unique position to control experience-dependent remodelling of neural circuits, with obvious implications for information storage and neuropsychiatric disorders. The local control of protein synthesis seems to be a preferred site of action of neural miRNAs, although a definitive proof that miRNAs function in a localized manner in the neurons of any organism in vivo is still lacking. Examples of miRNAs operating at the whole-neuron level are beginning to be revealed. Elucidating how local and global control of gene expression exerted by miRNAs is coordinated within neurons is likely to enrich our mechanistic understanding of synaptic plasticity, neuronal homeostasis and synaptic tagging. These studies will greatly benefit from tools that have recently been developed to monitor stimulus-evoked translation at the level of individual synapses (Wang et al., 2009). With the ability of miRNAs to simultaneously fine-tune the expression of hundreds of target genes in response to extracellular cues, it is easy to foresee a great potential for miRNA-based therapeutics for the treatment of neurological disorders of complex genetic origin, such as mood disorders and autism-spectrum diseases. Here, the challenge will be to control potential nonspecific, off-target effects, a phenomenon that is well known from the RNA interference field. The discovery of miRNAs as an extra layer of post-transcriptional control has revolutionized our perception of gene regulation. Nevertheless, as deep-sequencing technologies reveal that the vast majority of the vertebrate genome is transcribed, miRNAs are only a tiny piece in the puzzle of non-coding RNAs, the completion of which will keep researchers busy for decades to come.

AIM

AIM 1.-To analyze the role of AKAP150 in AMPARs trafficking induced by cLTD (NMDA) and Aβo in primary cultures of cortical neurons

1.1- To analyze the trafficking of AMPARs and level changes of AKAP150 induced by NMDA and Aβo in the primary cultures of cortical neurons

1.2- To investigate whether altered function of AKAP150 contributes to alterations of synaptic plasticity by the treatments of NMDA and Aβo in the primary cortical neurons

AIM 2.-To investigate changes in miRNAs induced by the long term exposure of NMDA and Aβo in the primary cultures of cortical neurons

METHODS

1. EXPERIMENTAL ANIMAL MODEL

To obtain embryonic primary cultures, experimental mattings were set in which the day of pregnancy was determined after the appearance of the vaginal plug. At the appropriate day, pregnant mice were euthanized by cervical dislocation and embryos dissected out from the uterus. All animal-related procedures were performed in compliance with the 214/1997 Act for the care and use of laboratory animals, and approved by the Universitat Autònoma de Barcelona ethical committee of animal care under a Generalitat de Catalunya project license.

2. PRIMARY CELL CULTURES

Neurons were cultured from E14.5–15.5 C57BL/6 wild-type mouse embryo forebrains. Cells were enzymatically and mechanically disrupted in the presence of trypsin and DNase I before plating in poly-D-lysine (50 μg/ml)-coated 24-well plates, 35- to 60-mm dishes, or on coverslips. Cells were seeded at a density of 5×10^4 cells/cm2 in Dulbecco's modified Eagle's medium (DMEM) supplemented with 10% fetal bovine serum (FBS, heat inactivated), 50 units/ml penicillin, 50 μg/ml streptomycin, 2mM glutamine, and 30mM glucose. Four hours after seeding, medium was replaced with serum-free Neurobasal medium supplemented with 2% B27 (Invitrogen), 50 units/ml penicillin, 50 μg/ml streptomycin, 2 mM glutamine, 30 mM glucose, which yielded nearly pure neuronal cultures. Culture medium was partially replaced every 3-4 days with fresh Neurobasal supplemented with B27. Cell cultures were kept at 37 °C in a humidified incubator with 5% CO2 / 95% air, and neurons were used for experiments after 12–14 days in vitro. Briefly, Cerebral cortical were dissected and the cells were enzymatically dissociated for 10 min at 37ºC in Solution 2 that consist on Krebs Ringer Buffer (120 mM NaCl, 4.8 mM KCl, 1.2 mM KH_2PO_4, 25 mM $NaHCO_3$, 14.3 mM glucose) containing 0.3% BSA, 0.03% $MgS0_4$ and 0.25 mg/ml of trypsin. The enzymatic digestion was stopped by adding solution 4 (see Table 1).

SOLUTION	REAGENTS	QUANTITY
PBS (1X)	H_2O	430 ml
	PBS 10X	50 ml
	Glucose 30%	10 ml
	Penicillin 10000U/ml-Streptomycin 10mg/ml	12.5 ml
Krebs-Ringer Buffer (KRB) 10X	NaCl	70.70 g
	KCl	3.60 g
	KH_2PO_4	1.66 g
	$NaHCO_3$	21.40 g
	Glucose	25.70 g
	H_2O	till 1000 ml
Magnesium Stock 3.8%	$MgSO_4 \cdot 7H_2O$	19 g
	H_2O	to 50 ml
Calcium Stock 1.2%	$CaCl_2 \cdot 2H_2O$	0.12 g
	H_2O	to 10ml
CELL CULTURE SOLUTIONS, FRESHLY PREPARED		
Solution 1	KRB 1X	50 ml
	BSA Fraction V	0.15 g
	Magnesium Stock 3.8%	0.4 ml
Solution 2	Solution 1	10 ml
	Trypsin	2.5 mg
Solution 3	Solution 1	10 ml
	DNase	0.8 mg
	Trypsin Inhibitor	5.2 mg
	Magnesium Stock 3.8%	0.1 ml
Solution 4	Solution 1	8.4 ml
	Solution 3	1.6 ml
Solution 5	Solution 1	5 ml
	Magnesium Stock 3.8%	40 µl
	Calcium Stock 1.2%	6 µl

TABLE 1. Solutions and media used for primary culture preparation and maintenance. A list of recipes for the preparation of solutions and mediums used in the primary cultures is provided.

The disaggregated tissue was then pelleted by centrifugation for 0.5 min at 1500 rpm, the supernatant was discarded and the pellets were mechanically dissociated in Solution 3 consisting on Krebs Ringer Buffer containing 0.3% BSA, 0.03% $MgS0_4$, 0.08 mg/ml DNase and 0.52 mg/ml trypsin inhibitor by gentle pipetting using a fire-polished Pasteur pipette to produce a single cell suspension. Cells were collected and added to solution 5 consisting on Krebs Ringer Buffer containing 0.3% BSA, 0.03% $MgS0_4$ and 0.0014% $CaCl_2$. Cells were then centrifuged for 5 min at 1000 rpm and resuspended, then counted with the Scepter^{TM} 2.0 Handheld Automated Cell Counter

(Millipore) and finally diluted in DMEM (Dulbecco´s Modified Eagle Medium, Sigma Aldrich #D5796) complemented with 30 mM glucose, 2 mM L-Glutamine, 250 U/ml penicillin-0.25 mg/ml streptomycin and 10% FBS (Fetal Bovine Serum, GIBCO #10270). The cortical cells were plated onto poly-D-Lysine (50 µg/ml) coated 24-well plates for cell viability studies, or 6-well plates for Western blot analysis, at a density of 15 x 10^4 cells/ml, whereas hippocampal cells were plated onto poly-D-Lysine (150 µg/ml) coated 12-mm diameter glass cover slips in 24-well plates at a density of 5 x 10^4 cells/ml. The cells were allowed to attach to the plate for two hours and then the medium replaced by Neurobasal™ medium (GIBCO #21103) complemented with 30 mM glucose, 2 mM L-Glutamine, 250 U/ml penicillin-0.25 mg/ml streptomycin and 2% B27 Supplement (GIBCO #17504). Cells were maintained at 37°C in a humidified incubator containing 5% CO2 in normoxia conditions. Cerebellar granule cell cultures were prepared from dissociated cerebella of 8-day old mice by mechanically chopping up the cerebellum followed by trypsin digestion and trituration as described in the previous paragraph. Cells were plated in BME (Basal Medium Eagle, Sigma Aldrich #B1522) supplemented with 25 mM KCl, 10% FBS, 250 U/ml penicillin-0.25 mg/ml streptomycin. Cells were plated onto 30 mm diameter culture plates coated with 50 µg/ml Poly-D-Lysine at a density of 1.5 × 10^5 cells/ml.

3. Aβ OLIGOMER PREPARATION

Synthetic Aβ 1–42 (Bachem, United Kingdom) was dissolved in hexafluor-2-propanol and kept at –80 °C after evaporation of hexafluor-2-propanol. Aβ oligomers (Aβos) were prepared freshly by dissolving the peptide film with DMSO and cold F-12 medium without phenol red to yield a 100 µM stock as previously described (Klein, 2002). Samples were incubated at 4 °C for 24 h and centrifuged at 14,000 g for 10 min at 4 °C. The supernatant containing a mixture of Aβo was biochemically analyzed by SDS-PAGE.

4. CELL STIMULATION AND LYSATE PREPARATION

Cultures were first incubated in ACSF for 30 min at room temperature (in mM): 125 NaCl, 2.5 KCl, 1 MgCl2, 2 CaCl2, 33 D-glucose, and 25 HEPES (pH 7.3), followed by stimulation with 50 μM NMDA in ACSF (no MgCl2). After 10 min of stimulation, neurons were replaced in regular ACSF and then subjected to different procedures at indicated time points. For total lysate preparation, Cultures were then washed once with ice-cold PBS and scraped in cold 1% Nonidet P-40 homogenization buffer (in mM: 20 Tris, pH 7.5, 150 NaCl, 5 EDTA, 1 PMSF, 1 Na_2VO_4, 1 × Sigma protease inhibitor and phosphatase inhibitor cocktails) to obtain cell lysates. Lysates were centrifuged at 12,000 × g for 10 min at 4 °C, and the protein in the supernatant was quantified by the Bradford method (Bio-Rad Laboratories, Inc.).

5. SURFACE BIOTINAYLATION

After NMDA or Aβ stimulations, cultured neurons were transferred to ice-cold PBS-Ca^{2+} - Mg^{2+} buffer (pH 7.4, 1 mM $CaCl_2$, 0.1 mM $MgCl_2$), followed by biotinylation in 1 mg/ml biotin (EZ-Link Sulfo-NHS-SS-Biotin, Pierce) for 30 min with slow agitation. Free biotin was quenched by 3× wash in cold PBS-Ca^{2+} -Mg^{2+} glycine (0.1 M). Cell cultures were immediately scraped in cold 1% Triton X-100 homogenization buffer (in mM: 50 NaCl, 10 EDTA, 10 EGTA, 1 Na_3VO_4, 50 NaF, 25 NaPPi, 1×-glycerophosphate, 1 PMSF, 1 × protease inhibitor mixture, 1×phosphatase inhibitor mixture, and 50 HEPES, pH 7.5). 1% Triton X-100 was performing to avoid solubilization of postsynaptic densities and is, therefore, selective for extrasynaptic AMPARs. Homogenates from cultures were centrifuged at 10,000 × g for 20 min to pellet insoluble fraction. 75 μl of the supernatant was mixed and heated with 25 μl of 4× SDS sample buffer to determine total fraction of GluA1 (surface plus internal). Biotinylated surface proteins in the remaining supernatant (~225 μl) were pulled down with 40 μl of 50% avidin-agarose beads (ImmunoPureImmobilized Avidin, Pierce) overnight at 4 °C. The beads were pelleted, and 75 μl of the supernatant (internal fraction) was mixed and heated with 25 μl of 4× SDS sample buffer. The beads were then rinsed three times with 1% Triton X-100 homogenization buffer and heated in 100 μl of 2× SDS sample buffer (surface fraction). Equal volumes of the total, internal, and biotinylated fractions were subjected to 10% SDS-PAGE, probed for total GluA1, and normalized to GAPDH.

6. REVERSE TRANSCRIPT PCR

6.1. RNA extraction

For RNA extraction, cells were seeded in 60 mm diameter plates, after different treatments, cells were washed by PBS and 1ml of Trizol Reagent (Invitrogen) was added, then cells were collected into 2 ml RNA-free tubes and homogenized. Consequently, 0.2 ml chloroform was added into samples and shake vigorously for 15 seconds, afterwards, samples were left in the room temperature for 5 min and centrifuged at 12000 g for 15 min at 4 ºC. To precipitate RNA dissolved in the aqueous phase, supernatant was taken to another new tube, 0.5ml of isopropanol were added, stirred gently and maintained for 10 minutes at room temperature, then, samples were centrifuged at 12000g for 10 min at 4 ºC, supernatant was discarded, adding 0.5ml 75% ethanol and centrifuging at 7.500 g for 5 min at 4 ° C. Supernatant was removed and left to dry no more than 20 minutes. Finally, the sample was diluted in 50µl of water treated with DEPC (Invitrogen) and RNA was solubilized by heating to 50-60 ° C for 10 minutes.

6.2. RNA concentration determination

The concentration of RNA was determined by measuring the absorption of an aqueous solution at a wavelength of 260 nm using a spectrophotometer (Eppendorf). The absorption spectrum was measured at the range of 240 to 320 nm after having calibrated the photometer with pure water. The concentration of the original solution was calculated by the formula: RNA c = 40 x A_{260nm} x dilution factor [µg/mL].

6.3. RNA quality assessment

To assess the quality, 2µl of sample RNA were diluted in loading buffer and were run on a 2% agarose gel with SYBR marked DNA gel stain (Molecular Probes).The state of degradation of RNA referred to the18s and 28s ribosomal.

6.4. Reverse transcription

In order to obtain complementary DNA (cDNA), RNA samples were taken from 1 to 5µg 1µl 10mM dNTP, 1µl of oligodT (primers queue Poly 3 'characteristic of most mRNA) and 12µl EDCP treated water, samples then maintained 5 minutes at 65 ° C in a thermal cycler PTC-100 Peltier Thermal Cycler (MJ Research). Then, 4µl 5X First-Strand Buffer, 1µl of DTT and 1µl of 0.1M RNAse OUT were added and incubated at 42 ° C for 2 minutes. Afterwards, 2µl of the SuperScriptTM II Reverse transcriptase (Invitrogen) was added and incubated 50 minutes at 42 °C, finally, samples were incubated for15 minutes at 70 ° C. The cDNA was kept at - 20 °C.

6.5. Semiquantitative PCR

The polymerase chain reaction (PCR) was performed with primers, previously designed with the FIRST program, from nucleotide sequence of *Mus musculus* GluA1, GluA2, AKAP150, GAPDH and 18S. The existence of sequence homology with other messenger RNAs was also verified with FASTA (http://www.ebi.ac.uk/Tools/fasta33/index.html). The expression of GAPDH or 18S was used as a control for the amount of cDNA. PCR was performed in a reaction mixture consisting of 2µl cDNA of each samples, 1X PCR buffer without Mg^{2+}, dNTP 0.2mM, 1.5mM of $MgCl_2$, 2 units Platinum ® Taq DNA polymerase (Invitrogen), an appropriate concentration of primers and EDCP treated water to a final volume of 50µl. Then the tubes were introduced with the reaction mixture and thermal cycler using the following program for the amplification of cDNAs: 2 minutes 94 ° C for complete denaturation of the double chains and activation enzyme, 30 cycles of 30 seconds at 94 ° C, 30 seconds at 60 ° C (hybridization temperature) and 1 minute for proper extension, and 5 minutes to 72 ° C.

Name	Forward sequences	Reward sequences
GluA1	TAAGAAGCCACAGAAGTCCA	TCTTCTCAAACACAGCGATT
GluA2	CGTGAGAGAAGAGGTGATTG	GTCAGGAAGGCAGCTAAGTT
AKAP150	AGAAAGCAAACGAATGGAGC	CGATAGCATTCTTGACGAGAG
GAPDH	AATTCAACGGCACAGTCAAGGC	TAGTCAGCACCGGCCTCACC
18s	TCAAGAACGAAAGTCGGAGG	GGACATCTAAGGGCATCACA
shAKAP150	AGATCTCCCGGAAAGTGCTTTCATTCAAAG TTCAAGAGACTTTGAATGAAAGCACTTTCC TTTTTA	AAGCTTAAAAAGGAAAGTGCTTTCATTCAAAG TCTCTTGAATTTGAATGAAAGCACTTTCCGGGG

TABLE 2. Primers for RTPCR or sequences for small hairpin RNA

Finally, the results for amplification were run on a agarose gel, reverse transcription PCR

primers are shown in table 2, and the sequences for shAKAP150 also showing.

7. REAL-TIME POLYMERASE CHAIN REACTION (RT-PCR)

7.1. RNA isolation and first strand synthesis

Total RNA isolation, including DNase treatment, was performed using mirVana™ miRNA Isolation Kit (Ambion), followed by the instructions in the manual, the integrity of the total RNA was checked by Servei de Genòmica Bioinformàtica, UAB. The first strand cDNA was synthesized from 1μg of total RNA using the TaqMan® MicroRNA Reverse Transcription Kit. Primers were supplied by Life technologies, and used according to the manufacturer's instructions (Table 3).

Component	Master mix volume per 15-μL reaction*
100mM dNTPs (with dTTP)	0.15 μL
MultiScribe™ Reverse Transcriptase, 50 U/μL	1.00 μL
10× Reverse Transcription Buffer	1.50 μL
RNase Inhibitor, 20 U/μL	0.19 μL
Nuclease-free water	4.16 μL
Total volume	7.00 μL

TABLE 3. Master mix for RT. * Each 15-μL RT reaction consists of 7 μL master mix, 3 μL of 5X RT primer, and 5 μL RNA sample.

7.2. Real-time PCR Protocol

All the samples to be compared were processed in parallel and 3 or 4 independent experiments were performed. Real-time PCR is performed with the Applied Biosystems (ABI) 7500 Fast Real-Time PCR System (Applied Biosystems) and TaqMan One Step RT-PCR Master Mix Kit (Applied Biosystems). A template is created for calculating the quantities of each master mix ingredient per sample being tested; For each sample to be assayed, a master mixture is made as shown in Table 4. These ingredients are combined in a SafeLock 1.5 microfuge tube (Eppendorf), vortexed, and briefly pulsed to remove any drops from the lid.

Component	Volume per 20-μL Reaction (Single reaction)
TaqMan® Small RNA Assay (20×)	1.00 μL
Product from RT reaction	1.33 μL
TaqMan® Universal PCR Master Mix II (2×), no UNG	10.00 μL
Nuclease-free water	7.67 μL
Total volume	20.00 μL

TABLE 4. qPCR reaction mix

Samples are tested on a MicroAmp Fast Optical 96 well reaction plate (Applied Biosystems) along with positive and negative controls. Each plate is loaded with 18.67μL of master mix per well. A volume of 1.33 μL cDNA from RT reaction is added to the appropriate well creating a total reaction volume of 20μL. The mixture is mixed by pipetting up and down carefully so as to not create bubbles or aerosols. An optical adhesive cover (Applied Biosystems) is placed on the plate to seal the wells. The sample plate is loaded in the ABI 7500. The detectors, FAM and TAMRA, are selected and applied to the entire plate. The optimum cycling times are programmed. These include an initial denaturing step of 95ºC for 10 minutes and an amplification step of 50 cycles of 95ºC for 30 seconds followed by 60ºC for 1 minute. The sample volume is set to 20 μL and a run mode of 9600 emulation with detection occurring at the 60ºC stage. The run takes approximately 2 hours to complete.

7.3. TaqMan Analysis

Once the run is completed, the manual Ct and manual baseline settings are selected. Start and end cycles are set to 13 and 25 respectively, based on experimental results. The data is analyzed and cycle threshold (Ct) values are displayed following the instrument instructions. Data analysis was performed by the comparative Ct method using the Ct values and the average value of PCR efficiencies obtained from LinRegPCR software. Gene expression in mouse samples was normalized to mir 92 or U6, or the geometric mean of two of the most stable following genes determined in each experiment.

8. WESTERN BLOT ANALYSIS

8.1. GENERATION OF PROTEIN EXTRACTS FROM CELLS

Primary cortical neurons were cultured for twelve days, stimulated with NMDA or AβO, and the indicated agonists as described in the figure legends. The neurons were rapidly lysed in ice cold Lysis Buffer as shown in Table. 5, 50 mM Tris-HCl pH 7.5, 1 mM EGTA, 1 mM EDTA, 1 mM sodium orthovanadate, 50 mM sodium fluoride, 5 mM sodium pyrophosphate, 10 mM sodium beta glicerophosphate, 0.27 M sucrose, 1% (by mass) Triton-X 100, 0.1% (v/v) 2-mercaptoethanol, 1:100 Protease Inhibitor Cocktail) using the scraper for cell harvesting. The collected lysates were left on ice for 30 min and then centrifuged at 4^{o}C for 10 min at 13000 rpm. The supernatants were collected into fresh eppendorf tubes, frozen quickly in liquid nitrogen and finally kept at -20ºC.

LYSIS BUFFER	REFERENCE	M.W.	grams/L	VOLUME FROM STOCK
50 mM Tris-HCl, pH 7.5	Amresco 0497	121.14		50 ml Tris-HCl 1M pH 7.5
1 mM EGTA	Sigma E0396	380.35		4 ml EGTA 250 mM pH 7.5
1 mM EDTA	Sigma 443885	372.24		2 ml EDTA 500 mM pH 8.0
1 mM Na-orthovanadate	Sigma S6508	183.91		10 ml Na-OTV 100 mM
50 mM Na-fluoride	Sigma 7920	41.99	2.100	
5 mM Na-pyrophosphate	Sigma 221369	446.06	2.230	
10 mM Na-B-glycerol-P	Sigma G6501	216.11	2.161	
0.27 M sucrose	Sigma S9378	342.30	92.421	
1% (by mass) Triton X-100	Sigma X100	n.a	n.a	0.1 ml Triton X-100/10 ml buffer
0.1% 2-mercaptoethanol	Sigma M7154	n.a	n.a	0.01 ml 2-mercapto/10 ml buffer
Proteinase inhibitor	Sigma P8340	n.a	n.a	0.1 ml Prot. Inhibit/10 ml buffer

STOCK	M.W.	PREPARATION
Tris-HCl 1M, pH 7.5	121.14	60.7 g TRIS in 500 ml water, pH to 7.5 with HCl
EGTA 250 mM, pH 7.5	380.35	19.02 g EGTA in 200 ml water, pH to 7.5 with HCl
EDTA 500 mM, pH 8.0	372.24	93.06 g EDTA in 500 ml water, pH to 8.0 with HCl
Na-OTV 100 mM	183.91	3.68 g Na-OTV in 200 ml water, pH to 7.0 with HCl and microwaves to achieve yellow colour

TABLE 5. Lysis Buffer. The composition and procedure to prepare lysis buffer are provided.Protein concentrations were determined by the Bradford method (Coomassie protein assay reagent, Pierce #23200) using bovine serum albumin (BSA) as a standard.

8.2. SODIUM DODECYL SULFATE-POLYACRYLAMIDE GEL ELECTROPHORESIS

8.2.1. SDS-PAGE gel preparation

Polyacrylamide gels were prepared in BIO-RAD mini PAGE (polyacrylamide gel electrophoresis) system (10 well, thickness 1 mm) using solutions listed in table 6.

8.2.2. Running a SDS-PAGE gel

5X Laemmli sample buffer was added to normalized lysate samples, which were then boiled for 5 min at 95ºC before loaded on the SDS-PAGE gel alongside prestained protein markers (250-10kDa) from Bio-Rad (#161-0373). Gels were run on 1X Tris-Glycine Buffer 0.1% (w/v) SDS (see Table 7) at 160 V for 60-100 min depending on the nature of the gel and the protein of interest.

SOLUTIONS (ml)	**RUNNING GEL**						**STACKING GEL**	
PERCENTAGE (%)	**5%**	**6%**	**7.5%**	**10%**	**12%**	**15%**	**3.6%**	**5%**
dH_2O	11.6	10.4	10	8.3	7	5	5.8	3.8
30% acryl 0.8 bis	3.4	4	5	6.7	8	10	1.3	0.85
1.5M Tris pH 8.8	5	5	5	5	5	5	-	-
0.5M Tris pH 6.8	-	-	-	-	-	-	2.5	0.325
20 % SDS	0.25	0.25	0.25	0.25	0.25	0.25	0.05	0.025
10 % APS	0.15	0.15	0.15	0.15	0.15	0.15	0.15	0.05
TEMED	0.03	0.03	0.03	0.03	0.03	0.03	0.03	0.005

TABLE 6. Table of solutions used in the preparation of SDS-PAGE running and stacking BIO-RAD gels. SDS: sodium dodecyl sulphate; TEMED: N, N, N', N'-tetramethylethylenediamine; APS: ammonium persulfate.

8.3. TRANSFER OF PROTEINS TO NITROCELLULOSE MEMBRANES

After SDS-PAGE, proteins were transferred to nitrocellulose membrane (Whatman®GmbH) using the wet transfer system (Bio-Rad). The paper/gel/membrane "sandwich" consisted, from the bottom to the front, on: three (Whatman™ #3030917) 3MM papers soaked in transfer buffer, membrane, gel and another three 3MM papers. Air bubbles were removed after each layer of the "sandwich" was added. The transfer was then performed at 100 V for 90 min. Following the transfer, membranes were

blocked in 10% skimmed milk/1X TBST for 45 min at room temperature. Primary antibodies were diluted in 5% milk/1X TBST (total protein antibodies) or in 0.5% BSA/1X TBST (phospho-protein antibodies) as indicated in Table 9 and incubated for

LAEMMLI-SDS SAMPLE BUFFER

CONCENTRATION	5X	1X	For 100 ml of 5X
Tris-HCl pH 6.8	125 mM	25 mM	25 ml Tris-HCl 0.5 M 6.8
Glycerol	50 %	10 %	50 ml
SDS	10 %	2 %	10 g
Bromophenol Blue	0.01 %	0.0025 %	12.5 mg
β-Mercaptoethanol		1 %	Freshly added

TRIS-GLYCINE SDS ELECTROPHORESIS BUFFER (10X)

CONCENTRATION	1X	10X	For 1 litter of 10X
Tris base	25 mM	250 mM	30.3 g
Glycine	192 mM	1.92 M	144.1 g
SDS	0.1 % (w/v)	1 % (w/v)	10 g

TRIS-GLYCINE TRANSFER BUFFER (10X)

CONCENTRATION	1X	10X	For 1 litter of 10X
Tris base	25 mM	250 mM	30.3 g
Glycine	192 mM	1.92 M	144.1 g

TBS BUFFER (10X)

CONCENTRATION	1X	10X	For 1 litter of 10X
NaCl	150 mM	1.5 M	87.6 g
Tris base	25 mM	250 mM	30.3 g

TABLE 7. Western Blot Buffers. Recipes of western blot buffers are provided as well as the concentrations of their components.

SOLUTION	REAGENTS	FOR 50 ml
ECL1	Tris-HCl 1M pH 8.5	5 ml
	Luminol 0.5M in DMSO	0.25 ml

	P-Coumaric Acid 79.2 mM in DMSO	0.25 ml
ECL2	Tris-HCl 1M pH 8.5	5 ml
	Hydrogen Peroxide 8.8M	0.32 ml

TABLE 8. Recipe of enhanced chemiluminescence (ECL) regents

16 h at 4º C. Dilution factors of the primary antibodies were according to manufacturer's instructions. After 16 h incubation, the membrane was washed three times for 5 min in 1X TBST and then incubated with the appropriate secondary antibodies coupled to horseradish peroxidase diluted 1:5000 in 5% milk/1X TBST for 45 min at room temperature. The membrane was then washed three times for 10 min with 1X TBST. Detection of proteins was performed by the enhanced chemiluminescence (ECL) system (Table 8). Membranes were treated with the ECL reagent mixture for 1 min before exposed to Super RX Fujifilm (MTB) in the dark room. The film was developed to produce the images shown in the figures.

8.3.1. Antibody detection

The primary and secondary antibodies used for western blot (W) and immunofluorescence (I) analysis were of commercial origin and are listed below (Table 9).

PRIMARY ANTIBODY	HOST	SUPPLIER	REFERENCE	DILUTION
GluA1	Mouse	Millipore	MAB2263	1:1000 (W) 1:200 (I)
GluA1	Rabbit	Millipore	AB1504	1:200 (I)
GluA2	Mouse	Millipore	MAB397	1:5000 (W)
Ser 845 of GluA1	Rabbit	Santa Cruz	SC16314	1:1000 (W)
AKAP150	Mouse	Millipore		1:200 (I)
AKAP150	Goat	Santa Cruz	SC/20	1:1000 (W)
PSD95	Mouse	Millipore	MAB1596	1:1000 (W)
PSD95	Mouse	Abcam	ab18258	1:200 (I)
SAP97	Mouse	Neurolab	73-030	1:1000 (W)

SECONDARY ANTIBODY	HOST	SUPPLIER	REFERENCE	DILUTION
Anti-Rabbit HRP-conjugated		BD		1:5000
Anti-Mouse HRP-conjugated		BD		1:5000
Anti-Sheep HRP-conjugated		BD		1:5000
Anti-Rabbit Alexa Fluor 488	Goat	Invitrogen		1:500
Anti-Mouse Alexa Fluor 594	Goat	Invitrogen		1:500
Anti-Mouse Alexa Fluor 568	Goat	Invitrogen		1:500
Anti-Chicken Alexa Fluor 568	Goat	Invitrogen		1:1000

TABLE 9. Primary and secondary antibodies for western blot and immunofluorescence analysis. A list of primary and secondary antibodies is provided, as well as their source and the dilution that was used for western blot and immunofluorescence analysis. SCB, Santa Cruz Biotechnology. BD, Becton, Dickinson and Company

9. LENTIVIRUS AND CONSTRUCT PREPARATION

To generate lentiviruses, the expression vector pWPI-AKAP150, psPAX2 (encoding HIV-1 Gag, Pol, Tat and Rev proteins), and the pMD2G (encoding the VSV G envelope protein) vector were cotransfected into HEK293 cells using calcium phosphate transfection method. The expression vector that we used in this study is called WPI and it is a dual promoter lentiviral vector in which the human H1 promoter drove expression of AKAP150 and an ubiquitin promoter simultaneously drove expression of GFP 48 hr after transfection, supernatants of culture media were collected. AKAP150 cDNA was further amplified using Pfx-DNA polymerase (Invitrogen) and cloned into the PmeI site of the WPI vector.

10. IMMUNOCYTOCHEMISTRY AND IMAGE ANALYSIS

10.1 Immunofluorescence staining for AKAP150 and PSD 95

Transfected and/or NMDA or Aβo-treated untransfected neurons were fixed with 4% paraformaldehyde for 15 min on ice and then permeabilized with 0.1% Triton X-100 for 30 min at room temperature. Anti-rabbit Alexa 488-, anti-mouse Alexa 568-conjugated secondary antibodies (Invitrogen) were used to visualize AKAP150 and PSD 95 respectively. All primary and subsequently secondary antibodies were incubated with cells at 4ºC for overnight and 37ºC for 1 hour, respectively, with multiple PBS washes. For image acquisition, coverslips were mounted on glass slides in Fluoromount-G (Southern Biotech) and were observed imaged with a 42x objective Nikon Eclipse 90i microscope (USA) or obtained with a 63x objective Zeiss LSM700 laser scanning microscope.

10.2. Immunofluorescence staining for AMPARs

After washout of the medium, cells were pre-treated (10 μM MK-801, 10 μM FK-506, 20 μM BAPTA-AM, MG-132, forskolin/rolipram (F'R; 50 μM/0.1 μM) for NMDA or Aβo applications; all drugs from Sigma). Subsequently, NMDA (50 μM) or Aβo (5 μM) were applied for 60 min in the presence of indicated chemicals. All

experiments were allowed to incubate for a total of 30 min at room temperature after initial agonist application. Cells were then fixed in 4% PFA on ice, permeabilized (for total AMPRAs staining) or not (surface AMPARs staining) in 0.1% Triton X-100 for 30 min at room temperature and stained with primary antibody GluA1 and goat anti rabbit Alexa-568 secondary antibody. In order to measure surface AMPARs after agonist application, surface receptors were labeled with the rabbit polyclonal antibody directed against the N-terminus of the GluR1 subunit in live cells and agonists were applied in the presence of the appropriate antagonists as just described. After the 15 min incubation period, cells were fixed in 4% PFA for 15 min on ice without permeabilization and surface receptors were visualized by using saturating amount of goat-anti rabbit Alexa 568 conjugated secondary antibody. All analyses were done blind using raw images. Untreated and treated cells from the same culture preparation were always compared with one another. Images from each experiment were thresholded using identical values for different experimental conditions and the total thresholded area of fluorescently labeled surface and total receptors was measured using Image J software (NIH). To measure the surface receptors in all our assays, surface fluorescence was divided by cell area, which was determined by measuring background fluorescence using a low threshold level. These values were then normalized to the average surface fluorescence of untreated control cells. Each experimental treatment and analysis was performed on a minimum of two coverslips with most experiments using on average six to eight coverslips. For presentation, images were processed using Image J by adjusting brightness and contrast levels to the same degree for all conditions illustrated in each experiment. Cells were incubated with goat-anti mouse Alexa-488 secondary antibody for AKAP150 puncta visualization, thus colocalized to GluA1 puncta visualization. To determine the efficiency of sh95 in reducing endogenous GluA1 levels, cells were infected with the sh95-containing lentivirus for 12 days after infection, consequently fixed with 4% PFA, permeabilized using 0.1% Triton X-100 and stained for GluA1 with a monoclonal anti-GluA1 antibody and goat-anti mouse Alexa-568 secondary antibody. To study the effect of NMDA and AβO application on the synaptic localization of PSD-95 and AKAP150, cells were infected with various AKAP150 constructs. 12 days after infection cells were treated with NMDA and AβO using identical protocols as described above. Cells were then fixed in 4% paraformaldehyde and permeabilized using 0.1% Triton X-100 as described earlier. Subsequently, endogenous PSD-95 was

stained with monoclonal anti-PSD-95 antibody and goat-anti mouse Alexa-488 secondary antibody. Similarly, for endogenous AKAP150 we used polyclonal antibody against AKAP150 and goat-anti rabbit Alexa-488. For visualization of other PSD-95 and AKAP150 constructs anti-GFP polyclonal antibody and goat-anti rabbit Alexa 488-conjugated secondary antibody were used. All primary antibodies were applied overnight at 4ºC and all secondary antibodies were incubated for 1 hour at 37 ºC.

11. PRODUCTION OF HIGH-TITER HIV-1-BASED VECTOR STOCKS BY TRANSIENT TRANSFECTION OF HEK 293T CELLS

11.1. Prepare 293T cells for transfection

293T/17 cells maintained in DMEM-10 medium, in 15-cm tissue culture flasks. A ratio of 1/10 of cell split using trypsin/EDTA twice a week. Cells can be seed Friday for Monday, which means 3 days before the transfection, by plating $1,7\times10^6$ cells / 10cm dish. This allows using only few amounts of cells and results in tightly adherent cells. Alternatively seed 11×10^6 293T cells per dish the day before the transfection. Ideally cells should be ~80% confluent on the day of transfection.

11.2. Co-transfect plasmids encoding vector components

One-two hours before transfection, the medium was replaced with 5 ml of fresh DMEM-10 medium preheated at 37°C. DNA concentration of all plasmids was adjusted to 1 mg/ml in TE buffer, pH 8.0, which including pMD2G, pLVTHM-H1-shRNAi for knock-down of AKAP150 or pWPI for overexpression of AKAP150, psPAX2. For a 10-cm plate to be transfected, I prepared the following transfection mix: 20 µg transfer vector plasmid for either knock-down or overexpression of AKAP150, and 7µg pMD2G, 13µg psPAX2, water was added to be a final volum of 500 µl /plate, 50µl CaCl2 2,5M / plate was added and mixed well by pipetting. 62,5µl of these mix was added to 500µl of 2× HBS dropwise under agitation by vortexing during 2-3 seconds (1/8 of the total volume every time), vigorous vortexing will ensure the formation of a fine precipitate optimal for transfection. The precipitate was left at room temperature at least for 15-20 min but did not exceed 30 min. Drop-wise

1 ml/dish of precipitate was added to the cell. It was mixed by gentle swirling until the medium has recovered a uniformly red color. Cells were incubated with the mix overnight, which was around 12 hours, the medium was aspirated, and 5 ml of fresh DMEM-10, pre-warmed to 37°C was slowly added. Cells were further incubated for 12 hours. Medium replacement is necessary because 293T cells have a high tendency to detach. So I checked for transfection efficiency under microscope if fluorescent reporter was encoded in the vector plasmid.

11.3. Harvest and concentrate vector stocks

The culture medium was harvested from each plate to a 50-ml centrifuge tube. 5 ml of fresh 37°C DMEM-10 was added to the cell monolayer and incubated for 8-12 hours. Supernatant was collected for the first time in the morning, around 8 hours after medium replacement. The second harvest can take place early in the evening around 12 hours later. Supernatant can be harvested 2 or 3 times, every 8-12 hours. Supernatants were kept at 4°C over the collecting period. The cleared supernatants can be kept at 4°C for 5-7 days. Supernatants can be used directly, stored at -80°C as aliquots, or concentrated if needed. Freeze/thaw cycles strongly reduce the titter. Pooled supernatant was filtered the using a 0.45-μm filter unit. Supernatant was slowly pipetted into 38.5-ml Beckman ultra-clear tubes (put at least 26 ml/tube but not more than 28ml). Supernatants were ultra-centrifuged for 120 min at 25,000 × g at 16°C and gently discarded by inversion, afterwards. The tube was dried by inverted. Final volume for 1 plate harvested 3 times was around 20 mL which allowed for using 1 ultra-clear tube. After centrifugation, do not let the pellet dry too much, around 2-3 min is sufficient, remaining medium is removed on the tube with a paper. Pellet was re-suspended (not always visible) with PBS, by pipetting first 10-15 times all around pellet, and then up and down 15 times, or by 175 rpm agitation overnight at 4ºC. The vector pellet of one tube can be re-suspended in a minimal volume of 50 μL. Finally, aliquot supernatant was stored at 80°C.

11.4 REAGENTS AND SOLUTIONS

CaCl2, 2.5 M :

9.18 g CaCl2•2H2O (mol. wt., 147), 25 ml H2O

Filter sterilized through 0.22-µm nitrocellulose filter and stored at +4°C.

HEPES-buffered saline (HBS), 2×

Dissolve the following reagents in 800 ml H2O:

16.36 g NaCl (mol. wt., 58.44; 0.28 M final)

11.9 g HEPES (mol. wt., 238.3; 0.05 M final)

0.213 g anhydrous Na2HPO4 (mol. wt., 142; 1.5 mM final)

Adjust pH to 7.00 with 5 M NaOH (proper pH is critical)

Add H2O to 1000 ml and make final pH adjustment to pH 7.00

Filter sterilize through a 0.22-µm nitrocellulose filter

Store up to 2 years at –70°C in 50-ml aliquots

Once thawed, the HeBS solution can be kept at 4°C for several weeks without significant change in the transfection efficiency.

It is critical that the pH be adjusted accurately; below 6.95, the precipitate will not form; above 7.05, the precipitate will be coarse and the transfection efficiency will be low.

TNE buffer:

50 mM Tris pH 7.5

130 mM NaCl

1 mM EDTA

11.5. TITRATION OF LENTIVIRAL VECTORS

The detail of the procedure is as following:

Day 1 **(9-12am):** Plate 30.000 293t per well on 24 well plate in 0.5 ml medium/well. I usually need 8 wells / lentivirus + 2 wells to count the number of cells at Day 2 + 2 wells used as negative control (no virus will be added).

Day 2 (4-6pm): Count cells on 2 wells, perform the media (should have 40-60.000/well), reduce the volum of the well by half (250µl total volume), transduce the cells with 8-fold serial dilutions: 2 µl, 1 µl, 0.5 µl, 0.25 µl, 0.125 µl, 0.0625 µl, 0.03125 µl and 0.015625 µl as below:

Well 1:2 µl in the first well,

Well 2: 1 µl in the second well,

Well 3: 1 µl of the first dilution 0.5 (4 µl of stock viruses + 4 µl of medium),

Well 4: 1 µl of the second dilution 0.25 (4 µl of first dilution + 4 µl of medium),

Well 5: 1 µl of the third dilution 0.125 (4 µl of second dilution + 4 µl of medium),
Well 6: 1 µl of the fourth dilution 0.0625 (4 µl of third dilution + 4 µl of medium),
Well 7: 1 µl of the fifth dilution 0.03125 (4 µl of fourth dilution + 4 µl of medium) and
Well 8: 1 µl of the sixth dilution 0.015625 (4 µl of fifth dilution + 4 µl of medium).

Day 3 (9-12am): Add 1ml of medium

Day 5 : The medium were removed and plates were washed twice with PBS 1X, added 200 µl of tripsin-EDTA / well, incubated at 37ºC during 2 minutes, added 600 µl of medium with serum / well, collected the cells in a 1.5ml eppendorf, centrifugated 10 seconds at 1000rpm, washed with 500 µl PBS 1X centrifugated 10 seconds at 1000rpm, washed with 500 µl PBS 1X, centrifugated 10 seconds at 1000rpm, added 500 µl PBS 1X, analyzed fluorescence by FACS (Cytomics FC 500; Beckman Coulter) and read percentage from linear values (usually 5-10%). Titer is a number (percentage) of cells transduced by a given volume and counted on D2, for example, 1µl gives us 10% of positive cells and I had 50.000 cells on D2, so I have 5.000TU/µl, it means $5x10^6$ TU/ml.

12. STATISTICAL ANALYSIS

Unless specified otherwise, all data are expressed as the mean ± standard deviation from at least three independent experiments. Both western blot data and Reverse transcript PCR were analyzed using Graphpad 5.0 software. One-way analysis of variance was used to verify the equality of several measures when the number of quantitative variables compared was greater than two, verifying in each case whether the variances were homogeneous. Student's t test was used to determine the statistical significance of differences. $p<0.05$ was considered significant. For multiple comparisons, ANOVA was performed followed by Bonferroni's post-test.

RESULTS

1. THE ENDOCYTOSIS OF AMPARS AND THE CHANGES IN THE LEVELS OF AKAP150 INDUCED BY NMDA AND AβO

LTP and LTD triggered by the activation of NMDARs are extensively studied models for such synaptic modifications and compelling evidence suggests that they result, at least in part, from activity-dependent regulated trafficking of AMPARs to and away from synapses. The detailed molecular mechanisms underlying such AMPAR trafficking, however, are incompletely understood. We first evaluated the effects of NMDA and Aβo on critical AMPAR subunits. Primary neuronal cultures were treated with 50 mM NMDA (cLTD) and 5 μM AβO and levels of GluA1 and GluA2 were analyzed by immunoblotting. As shown in Figure 7C and Figure 7D, we found that NMDA significantly reduced GluA1 after 60 min ($P< 0.05$) stimulations but not 30 min. GluA2 levels were both reduced in a time-dependent manner for 30 min ($P< 0.05$) and 60 min ($P< 0.01$). On the other hand, as shown in Figure 8C and Figure 8D, both surface GluA1 and GluA2 levels were decreased by Aβo for either 30 or 60 min. The endocytosis of AMPARs induced by NMDA was also confirmed by immunocytochemistry as shown in Figure 7G.

AMPARs are heteromeric complexes that are composed of combinations of four subunits termed GluR1–4 (also known as GluRA-D). These complexes are thought to be clustered in the postsynaptic density (PSD) of synapses via the binding of closely associated accessory proteins known as TARPS (transmembrane AMPAR regulatory proteins) to members of the MAGUK family of PDZ domain–containing scaffold proteins. The most extensively studied MAGUK is PSD-95, SAP-90 and AKAP150. AKAP150 is a scaffolding protein known to organize signaling complexes in neurons. AKAP150 interacts with PKA, PKC, protein phosphatase 2B (PP2B), as well as with membrane receptors, ion channels and postsynaptic proteins PSD95 and SAP97 In the nervous system, the function of AKAP79/150 is to bring PKC, PKA and PP2B into close proximity to a variety of membrane receptors including excitatory NMDA and AMPA glutamate receptors, mGluR5 metabotropic glutamate receptor and inhibitory GABAA receptors (Colledge et al., 2000). Changes in the levels of AKAP150 influence synaptic AMPAR content. We consequently evaluated the effects of NMDA and Aβo on AKAP150 levels, as shown in Figure 7F and Figure 8F, 60 min NMDA stimulations significantly ($P < 0.05$) reduced the levels of AKAP150. On the other

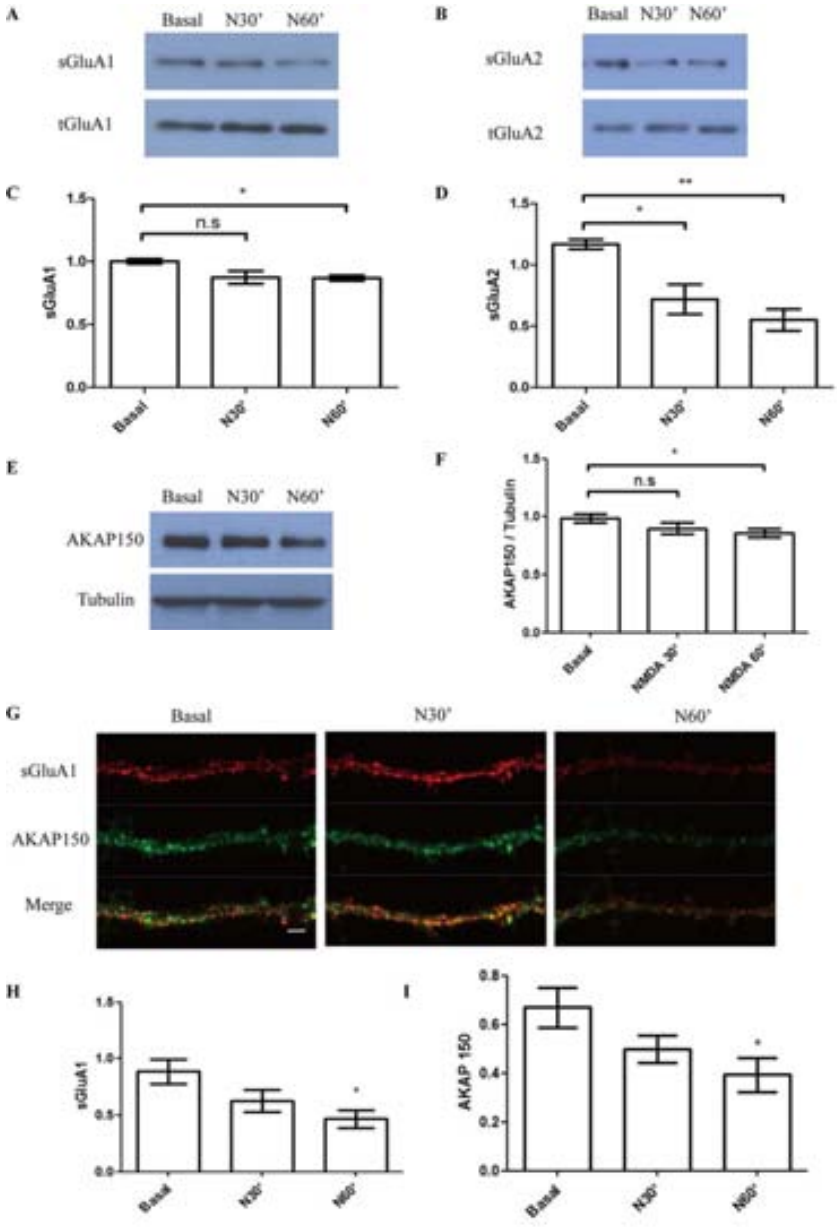

FIGURE 7. The reduction of AKAP150 and the levels of surface GluA1 induced by NMDA. Neurons were treated with 50 μM NMDA for 30 or 60 min. **A**, Sample blots showing levels of surface GluA1 (upper blot) and total GluA1 (lower blot). The graph (**C**) represents quantified changes in surface GluA1 in response to NMDA stimulations compared with baseline. **B**, Sample blots showing levels of surface GluA2 (upper blot) and total GluA2 (lower blot). The graph (**D**) represents quantified changes in surface GluA2 in response to NMDA stimulations compared with baseline. **E**, Sample blots showing levels of AKAP150 (upper blot) and GAPDH (lower blot). **F**, The graph represents quantified changes in AKAP150 in response to NMDA stimulations compared with baseline. G, Examples of dendritic staining for surface GluA1 (red) and AKAP150 (green) after NMDA treatment. **H**, Quantitation of the amount of NMDAR-triggered AMPAR endocytosis occurring, which normalized to original surface levels in the dendrites. **I**, Quantitation of the AKAP150 staining in cells treated with NMDA for 30 or 60 min, which normalized to the basal levels in the dendrites. Scale bars represent 100 μm. ** P< 0.01; * P< 0.05; n.s., P> 0.05. Error bars represent s.e.m.

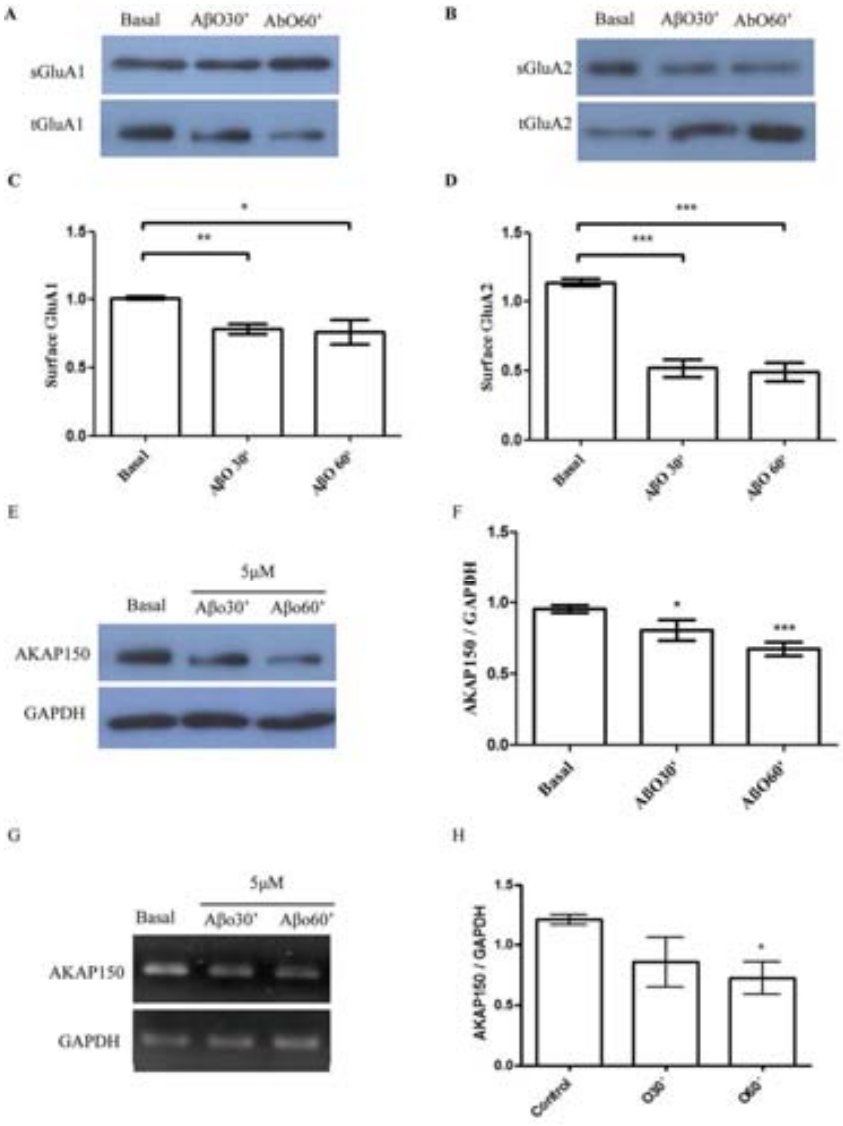

FIGURE 8. The reduction of AKAP150 and the levels of surface GluA1 induced by AβO. Neurons were treated with 5 μM AβO for 30 or 60 min. **A**, Sample blots showing levels of surface GluA1 (upper blot) and total GluA1 (lower blot). The graph (**C**) represents quantified changes in surface GluA1 in response to AβO stimulations compared with baseline. **B**, Sample blots showing levels of surface GluA2 (upper blot) and total GluA2 (lower blot). The graph (**D**) represents quantified changes in surface GluA2 in response to AβO stimulations compared with baseline. **E**, Sample blots showing levels of AKAP150 (upper blot) and GAPDH (lower blot). **F**, The graph represents quantified changes in AKAP150 in response to AβO stimulations compared with baseline. **G**, Sample blots showing levels of mRNA of AKAP150 (upper blot) and GAPDH (lower blot). **H**, The graph represents quantified changes in AKAP150 in response to AβO stimulations compared with baseline. *** P< 0.001; ** P< 0.01; * P< 0.05; n.s., P> 0.05. Error bars represent s.e.m.

hand, both 30 min ($P < 0.05$) and 60 min ($P < 0.001$) treatment with Aβo cause the decrease of AKAP150 as shown in Figure 8F. We also investigated the messenger RNA levels of AKAP150 and we found that 60 min of Aβo treatment stimulation could significantly ($P < 0.05$) induce the decrease of mRNA levels of AKAP150 as shown in Figure 8H.

2. NMDA AND Aβo-INDUCED DOWN-REGULATION OF AKAP150 DEPENDS ON NMDAR, PP2B AND PROTEASOME ACTIVITIES, WHILE Aβo-INDUCED DOWN-REGULATION OF AKAP150 DEPENDS ON NMDAR ACTIVITY

To test the role of NMDARs in the effects of NMDA and AβO on AKAP150 levels, cortical neurons were pretreated (30 min) with NMDAR antagonist MK-801 (10 μM) before being exposed to NMDA. As shown in Figures 9B, D and 11B. Western blot analysis of cell lysates revealed that MK-801 inhibited both NMDA and AβO-induced down-regulation of AKAP150 levels indicating that NMDAR activation is required for manifestation of the NMDA and AβO effects. However, blocking AMPAR with CNQX failed to affect AβO-induced down-regulation of AKAP150 levels.

FK506, called cyclosporine (CsA), binds to its immunophilin, cyclophylin (CpN), forming a complex between cyclosporine and CpN. The CsA –CpN complex binds and blocks the function of the enzyme calcineurin (CaN), which has a serine/threonine phosphatase activity. When neurons were pre-treated with FK-506 (10 μM) followed by treatment with NMDA (50 μM) or AβO (5 μM) for 60 min. Applying FK506 significantly partially rescued the reductions of AKAP150 induced by NMDA and Aβo as shown in Figure 10B, and Figure 11F.

MG132 is a specific, potent and reversible proteasome inhibitor that was able to rescue the decrease in AKAP150 mediated by either NMDA or Aβo as shown in Figure 12B and Figure 13 B, E.

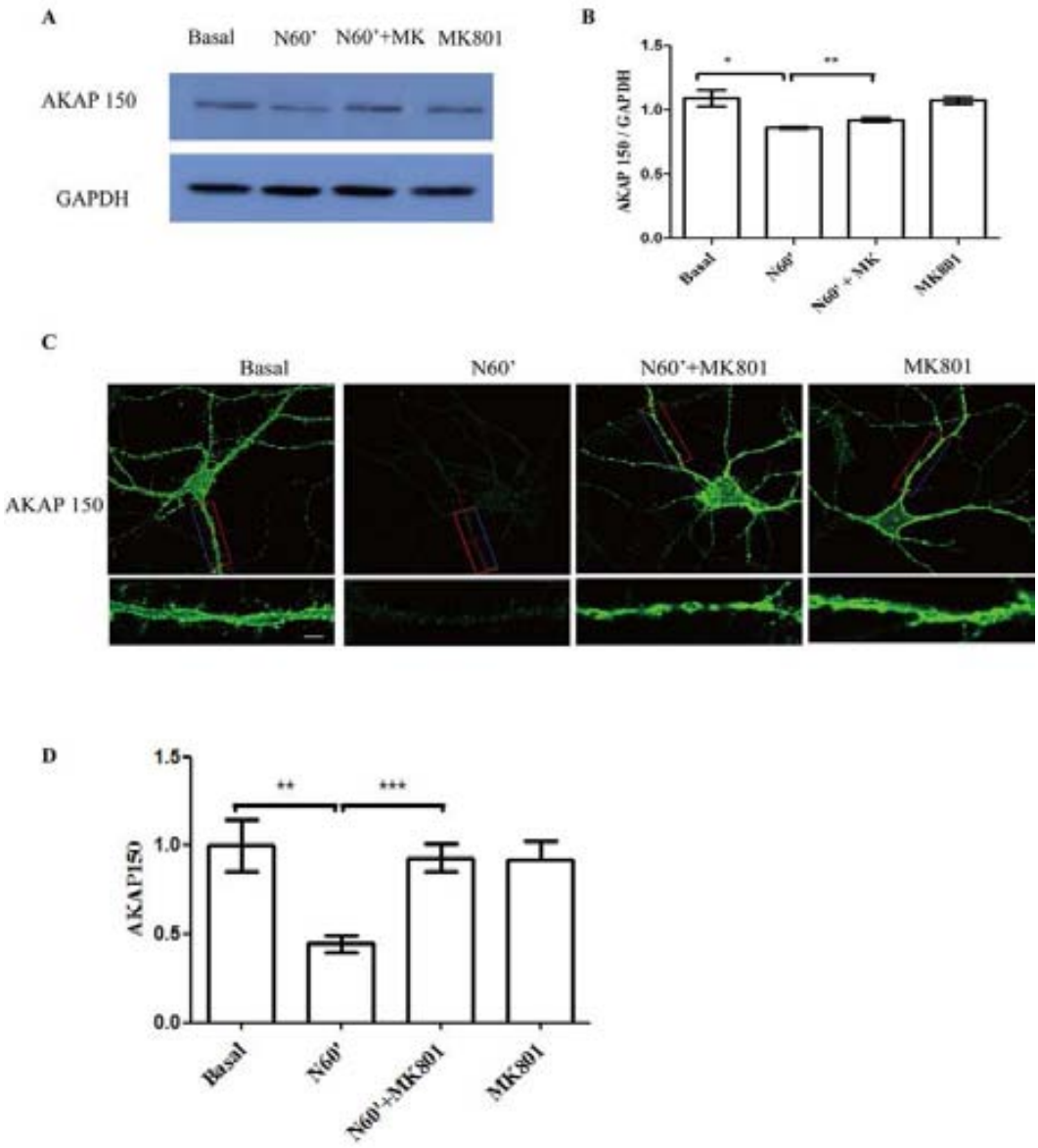

FIGURE 9. NMDA induced AKAP150 down-regulation requires NMDAR activity. Neurons were treated with 50 μM NMDA for 60 min without or with inhibitors. **A**, Sample blots showing levels of AKAP150 (upper blot) and GAPDH (lower blot). Treatment (60 min) of cells with MK-801 (10 μM) prevented the NMDA-induced decrease in AKAP150 levels. **B**, The graph represents quantified changes in AKAP150 in response to NMDA stimulations without or with MK-801 compared with baseline. **C**, Examples of whole cell and dendrite staining for AKAP150 after NMDA treatment without or with MK-801. **D**, The graph represents quantified changes in AKAP150 in response to NMDA stimulations without or with MK-801 compared with baseline. Scale bar represents 100 μm. *** P< 0.001; ** P< 0.01; * P< 0.05; Error bars represent s.e.m.

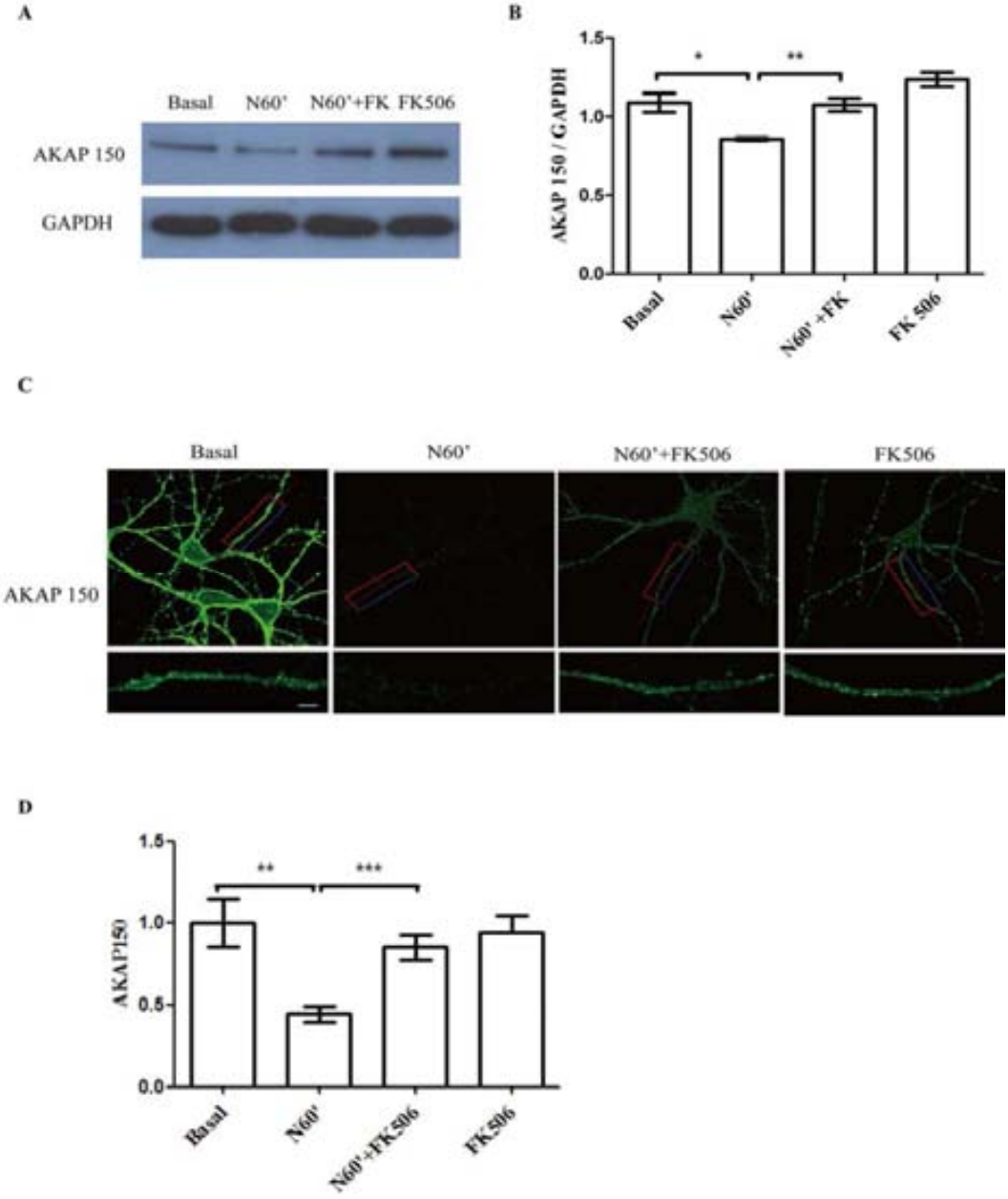

FIGURE 10. NMDA induced AKAP150 down-regulation requires calcineurin. Neurons were treated with 50 μM NMDA for 60 min without or with inhibitors. **A**, Sample blots showing levels of AKAP150 (upper blot) and GAPDH (lower blot). Treatment (60 min) of cells with FK506 (10 μM) prevented the NMDA-induced decrease in AKAP150 levels. **B**, The graph represents quantified changes in AKAP150 in response to NMDA stimulations without or with FK506 compared with baseline. **C**, Examples of whole cell and dendrite staining for AKAP150 after NMDA treatment without or with FK506. **D**, The graph represents quantified changes in AKAP150 in response to NMDA stimulations without or with FK506 compared with baseline. Scale bar represents 100 μm. *** P< 0.001; ** P< 0.01; * P< 0.05; Error bars represent s.e.m.

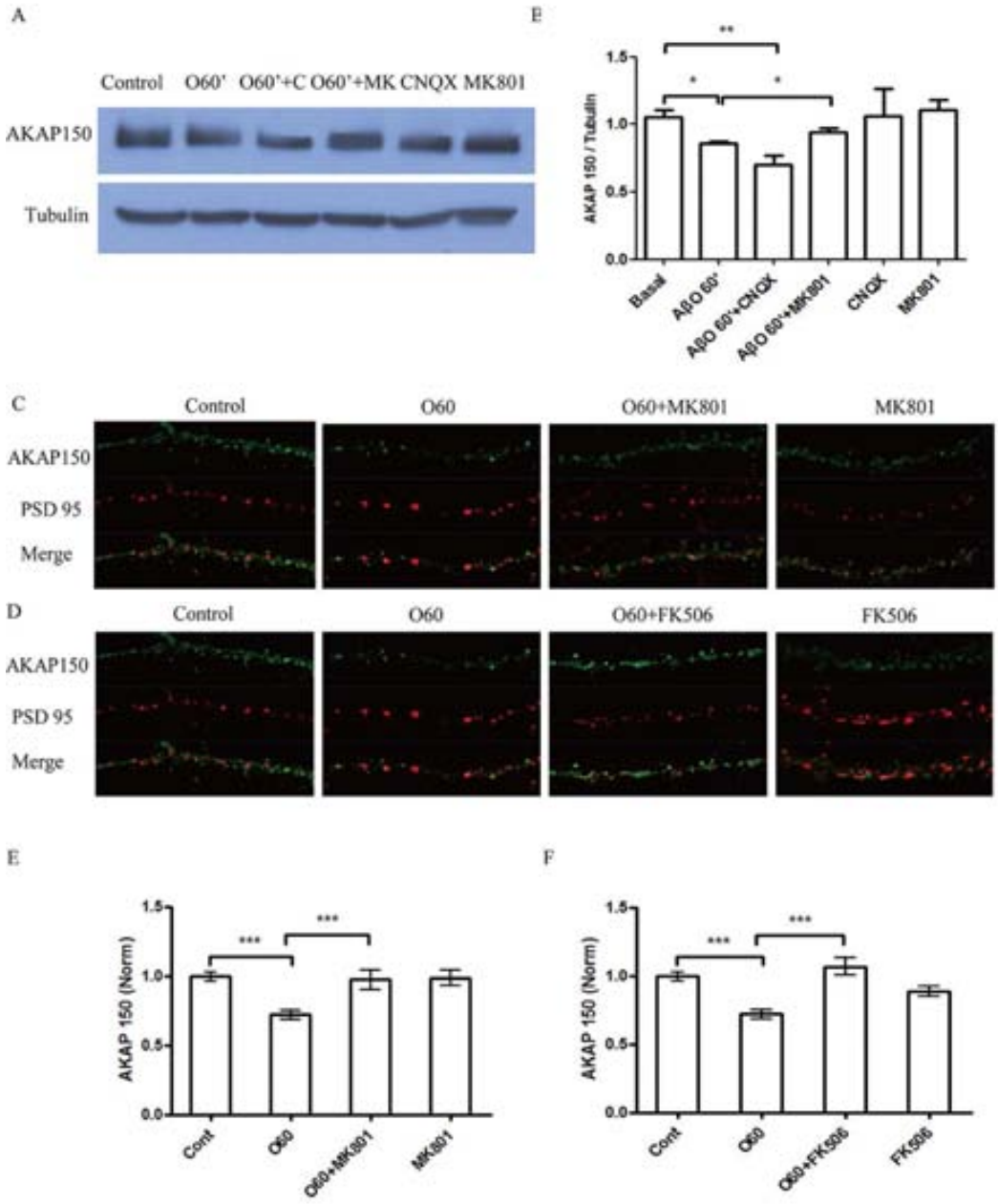

FIGURE 11. AβO induced AKAP150 down-regulation requires NMDAR activity and calcineurin, but not AMPAR activity. Neurons were treated with 5 μM AβO for 60 min without or with inhibitors. **A**, Sample blots showing levels of AKAP150 (upper blot) and GAPDH (lower blot). Treatment (60 min) of cells with MK-801 (10 μM), but not CNQX (50 μM) prevented the Aβo -induced decrease in AKAP150 levels. **B**, The graph represents quantified changes in AKAP150 in response to Aβo stimulations without or with MK-801 and CNQX compared with baseline. **C**, Examples of dendrite staining for PSD95 (red) and AKAP150 (green) after AβO treatment without or with MK-801. **D**, Examples of dendrite staining for PSD95 (red) and AKAP150 (green) after AβO treatment without or with FK506. **E**, The graph represents quantified changes in AKAP150 in response to AβO stimulations without or with MK-801 compared with baseline. **F**, The graph represents quantified changes in AKAP150 in response to AβO stimulations without or with FK-506 compared with baseline. Scale bar represents 100 μm. *** P< 0.001; ** P< 0.01; * P< 0.05; Error bars represent s.e.m.

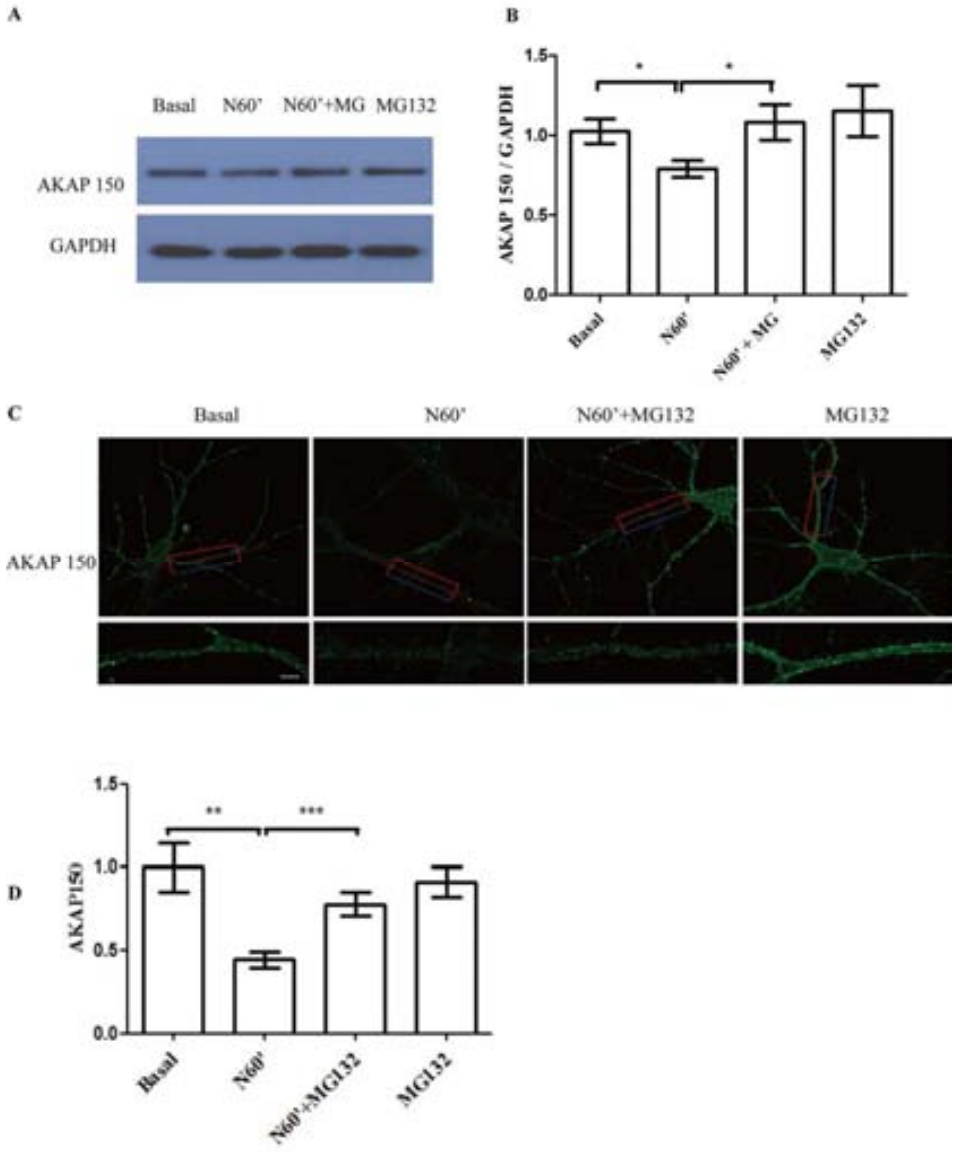

FIGURE 12. NMDA induced AKAP150 down-regulation requires proteasome. Neurons were treated with 50 μM NMDA for 60 min without or with inhibitors. **A**, Sample blots showing levels of AKAP150 (upper blot) and GAPDH (lower blot). Treatment (60 min) of cells with MG132 (0, 1 μM) prevented the NMDA-induced decrease in AKAP150 levels. **B**, The graph represents quantified changes in AKAP150 in response to NMDA stimulations without or with MG132 compared with baseline. **C**, Examples of whole cell and dendrite staining for AKAP150 after NMDA treatment without or with FK506. **D**, The graph represents quantified changes in AKAP150 in response to NMDA stimulations without or with MG132 compared with baseline. Scale bar represents 100 μm. *** P< 0.001; ** P< 0.01; * P< 0.05; Error bars represent s.e.m.

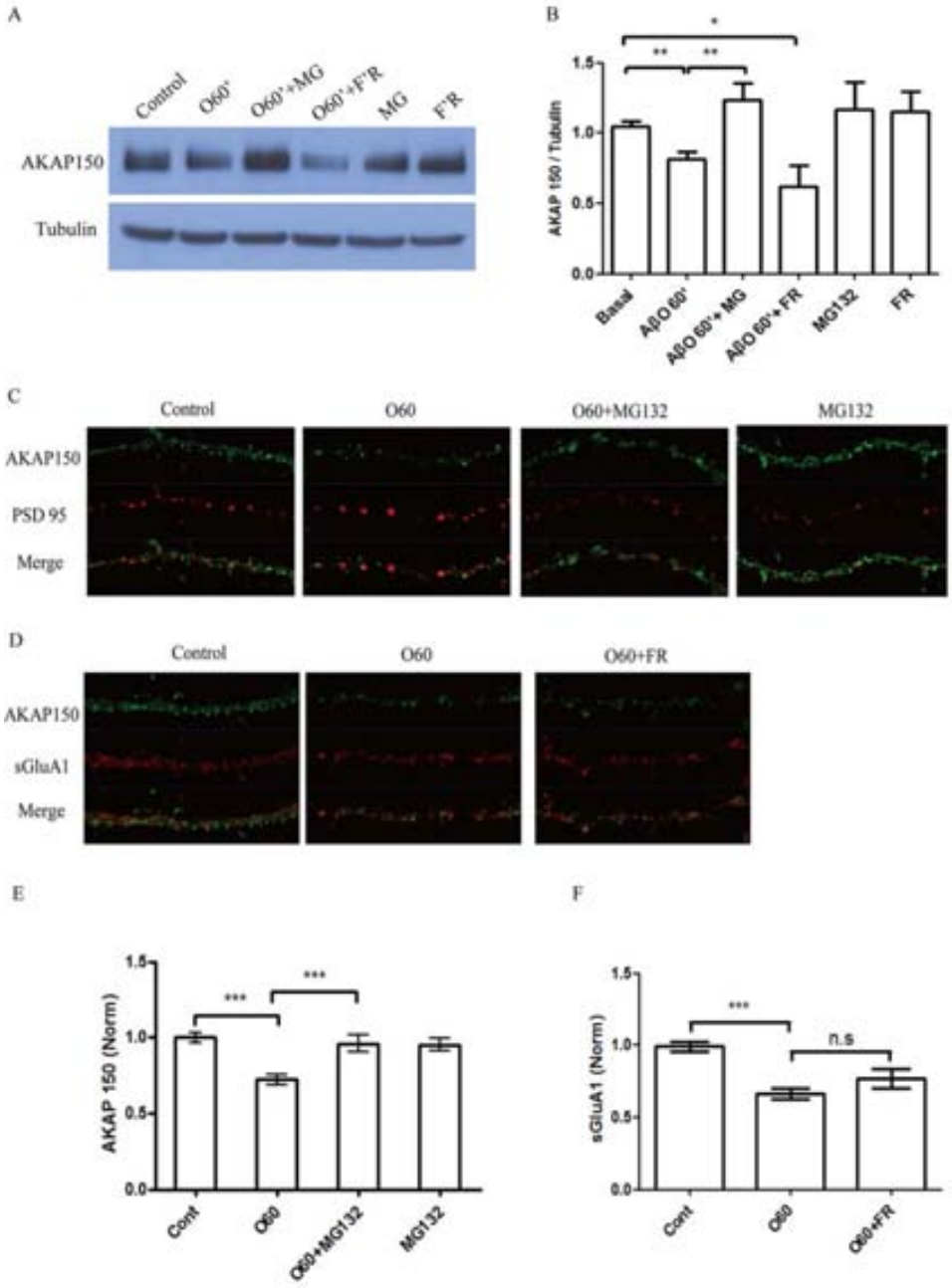

FIGURE 13. AβO induced AKAP150 down-regulation requires proteasome activity, while chemical LTP could not rescue the down-regulation of AKAP150. Neurons were treated with 5 μM AβO for 60 min without or with inhibitors, or neurons (pre-treated or not with 5 μM AβO during 60 min) were stimulated with forskolin/rolipram (F'R; 50 μM/0.1 μM) for 60 min. **A**, Sample blots showing levels of AKAP150 (upper blot) and GAPDH (lower blot). Treatment (60 min) of cells with MG132 (0,1 μM), prevented the AβO -induced decrease in AKAP150 levels, while the AKAP150 down-regulation induced by 60 min AβO could not be rescued by F'R stimulation for 60 min. **B**, The graph represents quantified changes in AKAP150 in response to AβO stimulations without or with MG-132 and F'R compared with baseline. **C**, Examples of dendrite staining for PSD95 (red) and AKAP150 (green) after AβO treatment without or with Mg-132. **D**, Examples of dendrite staining for surface GluA1 (red) and AKAP150 (green) after AβO treatment without or with another 60min of F'R stimulation. **E**, The graph represents quantified changes in AKAP150 in response to AβO stimulations without or with MG-132 compared with baseline. **F**, The graph represents quantified changes in AKAP150 in response to AβO stimulations without or with another 60min of F'R stimulation compared with baseline. Scale bar represents 100 μm. *** P< 0.001; ** P< 0.01; * P< 0.05; n.s P> 0.5; Error bars represent s.e.m.

3. CHEMICAL LTP WAS UNABLE TO RESCUE THE REDUCTION OF AKAP150 INDUCED BY NMDA (cLTD) OR Aβo

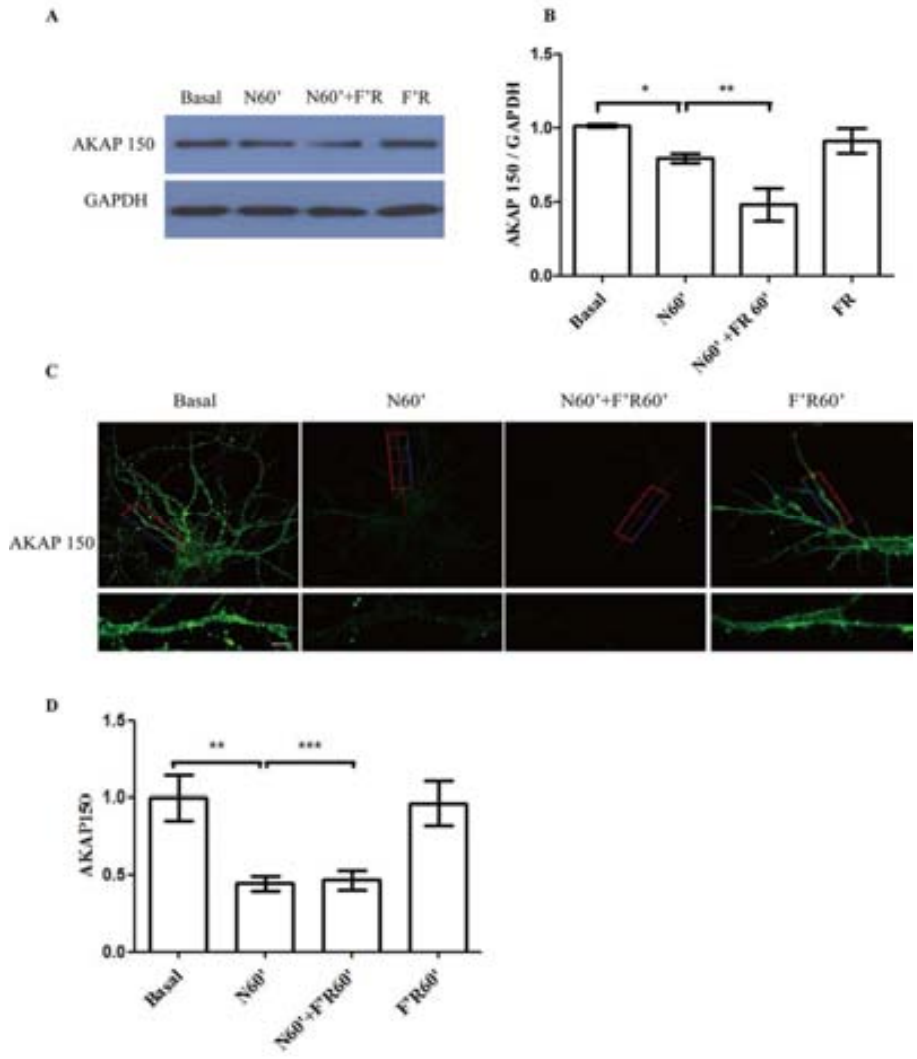

FIGURE 14. NMDA induced AKAP150 down-regulation could not be rescued by chemical LTP. Neurons (pre-treated or not with 50 µM NMDA during 60 min) were stimulated with forskolin/rolipram (F'R; 50 µM/0.1 µM) for 60 min. **A**, Sample blots showing levels of AKAP150 (upper blot) and GAPDH (lower blot). Treatment (60 min) of cells with another 60 min of F'R could not prevent the NMDA-induced decrease in AKAP150 levels. **B**, The graph represents quantified changes in AKAP150 in response to NMDA stimulations without or with another 60 min of F'R compared with baseline. **C**, Examples of whole cell and dendrite staining for AKAP150 after NMDA treatment without or with extra 60 min of F'R stimulation. **D**, The graph represents quantified changes in AKAP150 in response to NMDA stimulations without or with extra 60 min of F'R stimulation compared with baseline. Scale bar represents 100 µm. *** P< 0.001; ** P< 0.01; * P< 0.05; Error bars represent s.e.m.

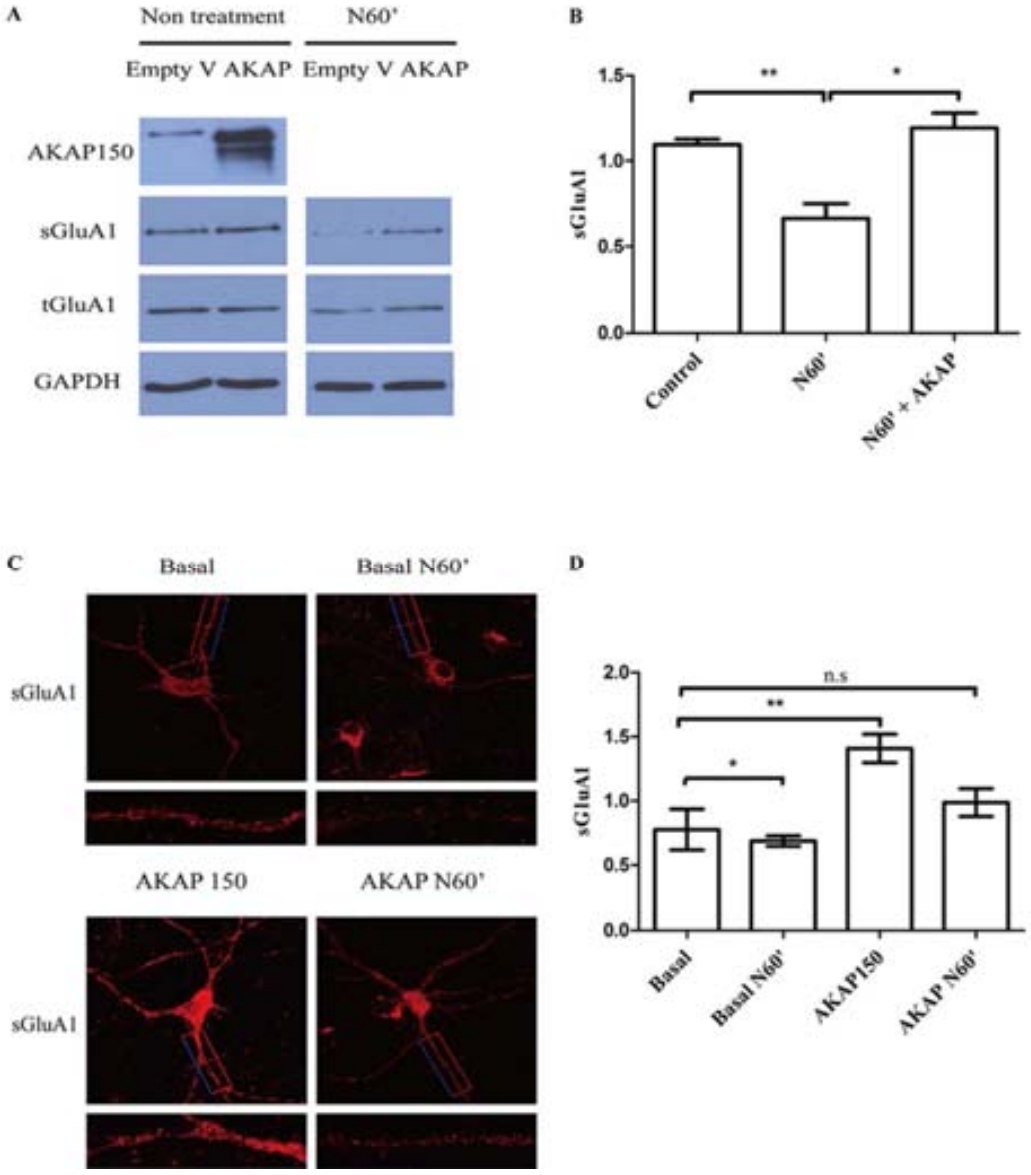

FIGURE 15. Overexpression of AKAK150 block the NMDA induced GluA1 endocytosis. Neurons (Basal or overexpression of AKAP150) treated with 50 µM NMDA during 60 min. A, Sample blots showing levels of surface GluA1 (upper blot), total GluA1 (middle blot) and GAPDH (lower blot). B, The graph represents quantified changes in surface GluA1 in response to NMDA stimulations without or with overexpression of AKAP150 compared with baseline. C, Examples of whole cell or dendrite staining for GluA1 after NMDA treatment without or with overexpression of AKAP150. D, The graph represents quantified changes in surface GluA1 in response to NMDA stimulations without or with overexpression of AKAP150 compared with baseline. Scale bar represents 100 µm. ** P< 0.01; * P< 0.05; n.s., P> 0.05. Empty V: control empty vector of overexpression of AKAP150. AKAP150: overexpression of AKAP150. Error bars represent s.e.m.

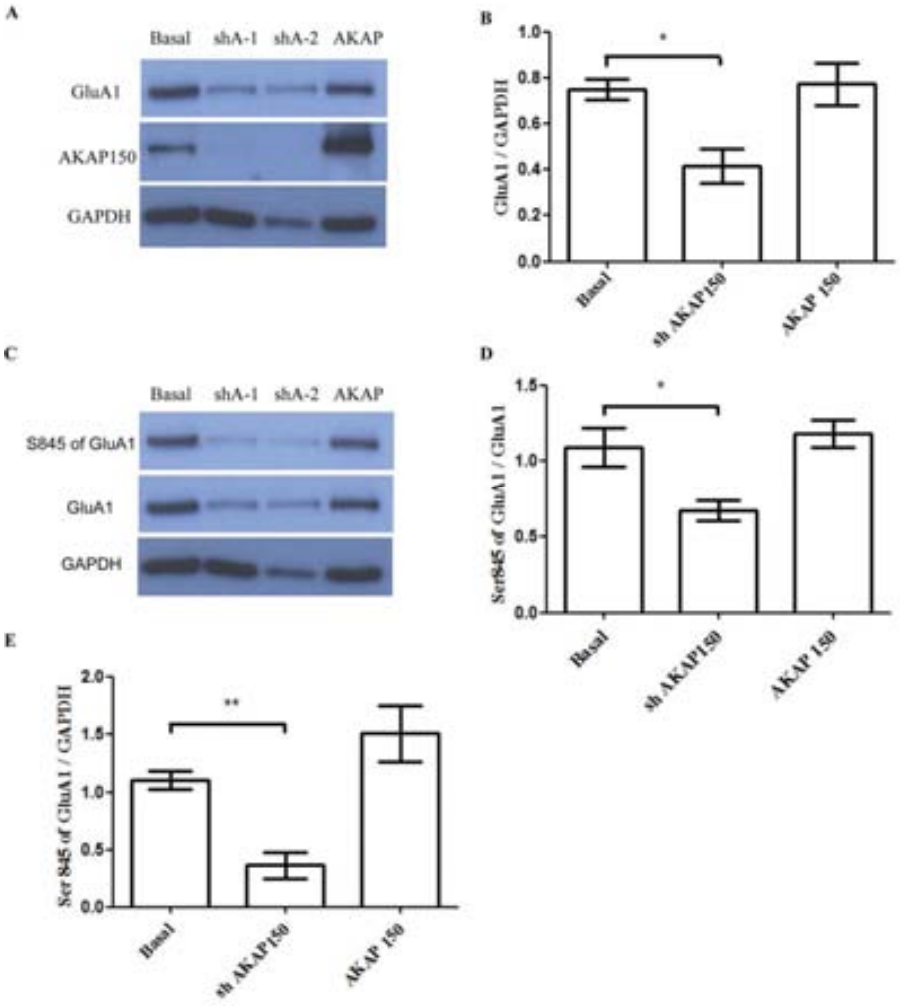

FIGURE 16. Knock-down of AKAK150 induced the reduction of GluA1. Neurons for basal, knock-down and overexpression of AKAP150 conditions. A, Sample blots showing levels of GluA1 (upper blot), AKAP150 (middle blot) and GAPDH (lower blot). **B**, The graph represents quantified changes in GluA1 in response to knock-down or overexpression of AKAP150 compared with baseline. **C**, Sample blots showing levels of ser845 of GluA1 (upper blot), GluA1 (middle blot) and GAPDH (lower blot). **D**, The graph represents quantified changes in ser845 of GluA1 in response to total GluA1. E, The graph represents quantified changes in ser845 of GluA1 in response to GAPDH. ** P< 0.01; * P< 0.05. Error bars represent s.e.m.

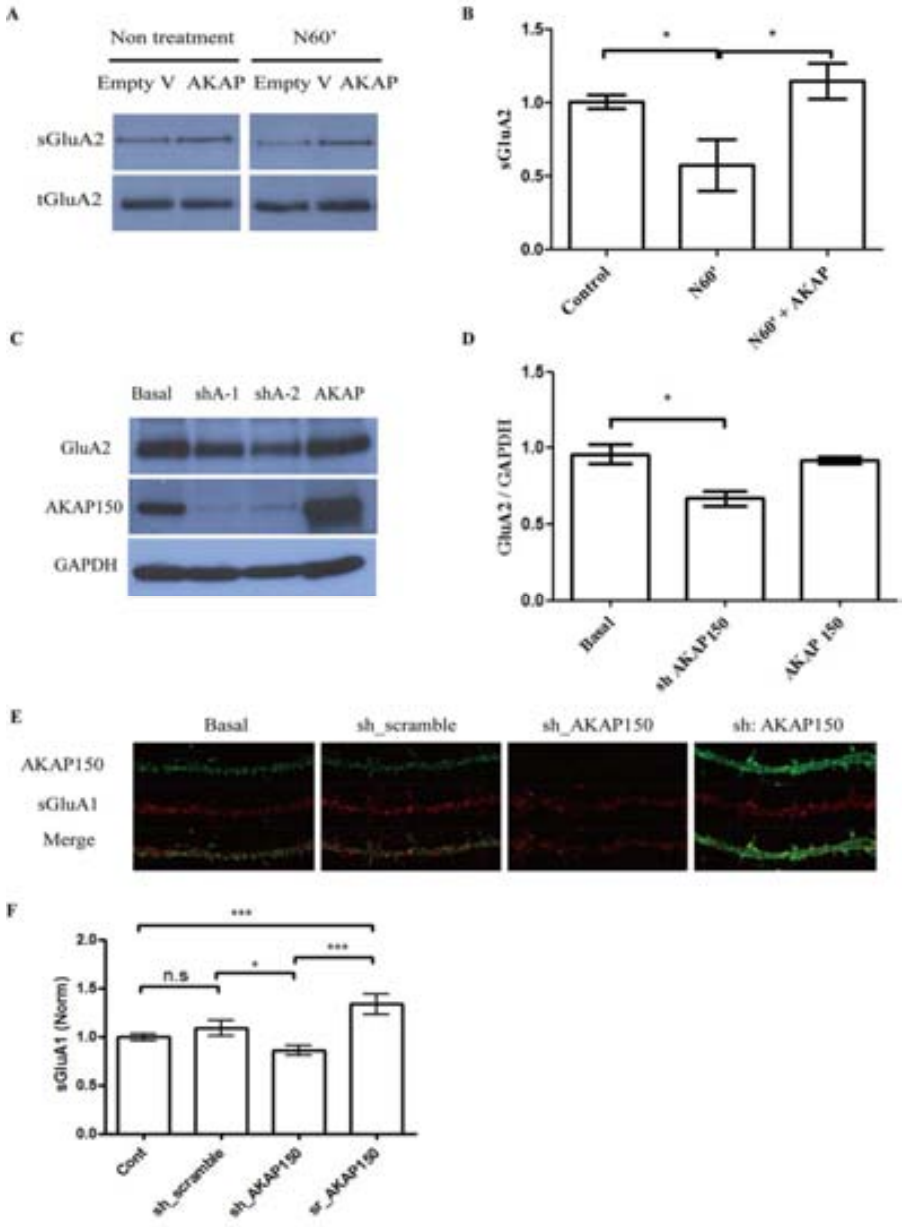

FIGURE 17. Overexpression of AKAK150 block the NMDA induced GluA2 endocytosis while Knock-down of AKAK150 induced the reduction of GluA2. A. Overexpression of AKAK150 blocked the NMDA induced GluA2 endocytosis. Neurons (Basal or overexpression of AKAP150) treated with 50 μM NMDA during 60 min. **B**, The graph represents quantified changes in surface GluA2 in response to NMDA stimulations without or with overexpression of AKAP150 compared with baseline. **C**. Neurons for basal, knock-down and overexpression of AKAP150 conditions. Sample blots showing levels of GluA2 (upper blot), AKAP150 (middle blot) and GAPDH (lower blot). **D**, The graph represents quantified changes in GluA2 in response to knock-down or overexpression of AKAP150 compared with baseline. E, Examples of dendrite staining for surface GluA1 (red) and AKAP150 (green) for Basal, control empty vector of silence AKAP150, silence AKAP150, silence and rescuing AKAP150 conditions. F, The graph represents quantified changes in surface GluA1 in response to Basal, control empty vector of silence AKAP150, silence AKAP150, silence and rescuing AKAP150 conditions. ***P< 0.001; * P< 0.05; n.s., P> 0.05. Scale bar represents 100 μm. Empty V: control empty vector of overexpression of AKAP150. AKAP150: overexpression of AKAP150. Error bars represent s.e.m.

I next confirmed that the induction of cLTP by F/R, produced an increase in surface GluA1 as expected (Figure. 19 C). Consequently, the cLTP was applied after the reduction of AKAP150 induced by NMDA or Aβo treatments expecting to study whether the cLTP could induce the recovery of downregulation of AKAP150. However, as shown in in Figure 13B, 13F, the NMDA and Aβo-mediated reduction in AKAP150 was not rescued by the application of cLTP, as it is shown in Figure. 14B and Figure. 14D.

4. OVEREXPRESSION OF AKAP150 BLOCKED BOTH THE NMDA AND AβO INDUCED GLUA1 ENDOCYTOSIS

I next overexpressed full-length, wild-type AKAP150 in primary cortical neurons. We first tested and confirmed by western blotting that overexpression of AKAP150 was successful as shown in Figure. 20 A, D, F. I then checked which was the effect of overexpression of AKAP150 on surface GluA1 and what I found was that the level of surface GluA1 was significantly increased (** $P< 0.01$) compared to the empty vector of AKAP150 infection (control) as showing in Figure. 19 C, D. In order to determine the impact of overexpressing AKAP150 on the impairment of surface AMPARs induced by NMDA or Aβo, the cells were either basal condition (control) or overexpressing AKAP150 condition were treated by NMDA or Aβo for 1 hour. Interestingly, compared with control groups, application of NMDA to the overexpression groups showing a significant resistance of surface GluA1 levels (Figure. 15 A, B, C, D) and the GluA2 levels (Figure. 17 A, B). In the meanwhile, compared with control groups, application of Aβo to the overexpression groups showing a significant resistance of surface GluA1 levels (Figure. 18A, B, E, F), and the GluA2 levels (Figure. 18 C, D)

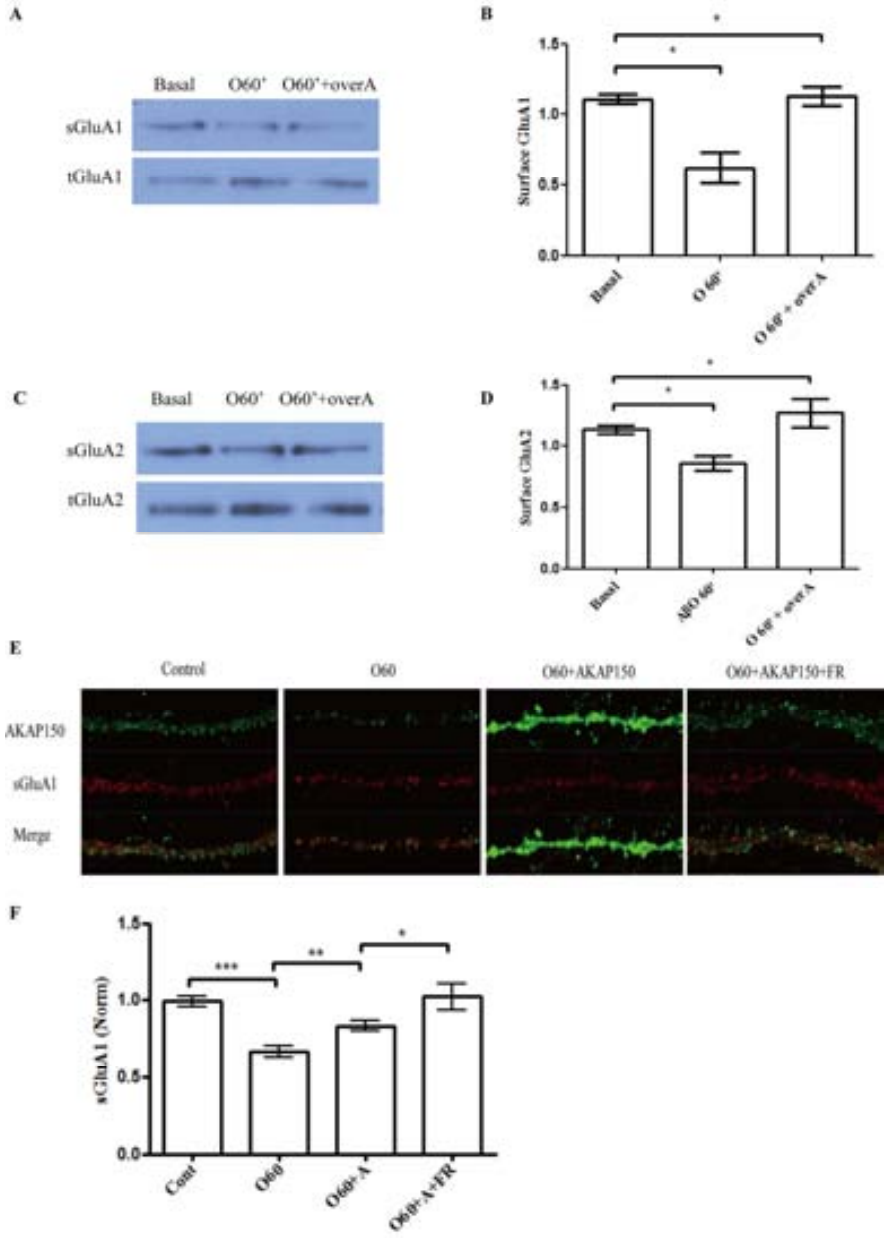

FIGURE 18. Overexpression of AKAK150 blocked surface GluA1/2 endocytosis induced by Aβo, while the chemical LTP could increase the levels of GluA1. A. Overexpression of AKAK150 blocked the Aβo induced GluA1 endocytosis. Neurons (Basal or overexpression of AKAP150) treated with 5 μM Aβo during 60 min. **B**, The graph represents quantified changes in surface GluA1 in response to Aβo stimulations without or with overexpression of AKAP150 compared with baseline. **C.** Overexpression of AKAK150 blocked the Aβo induced GluA2 endocytosis. Neurons (Basal or overexpression of AKAP150) treated with 50 μM Aβo during 60 min. **D**, The graph represents quantified changes in surface GluA2 in response to AβO stimulations without or with overexpression of AKAP150 compared with baseline. **E**. Examples of dendrite staining for surface GluA1 (red) and AKAP150 (green) showing overexpression of AKAK150 blocked the Aβo induced GluA1 endocytosis, while F'R increased the surface GluA1 levels. F. The graph represents quantified changes in surface GluA1 in response to Aβo stimulations without or with overexpression of AKAP150 compared with baseline, and the chemical LTP induced the increase of the surface levels of GluA1 with the Aβo stimulations for overexpression of AKAP150. *** P< 0.001; ** P< 0.01; * P< 0.05; Scale bar represents 100 μm. Error bars represent s.e.m.

5. ROLE OF AKAP150 IN NMDAR-TRIGGERED AMPAR ENDOCYTOSIS. KNOCK-DOWN OF AKAP150 INDUCED CHANGES OF AMPARS LEVELS.

Using a lentivirus-mediated molecular replacement strategy targeting AKAP150, it was shown that an AKAP150 induced reduction of total AMPARs. We found that expression of a highly effective short-hairpin RNA specific to Akap5 in mice cortical slice cultures produced a modest decrease in the levels of subunits of AMPARs-GluA1/2 as shown in Figure. 16 A, B and Figure.17 C, D. It is well established that PKA-dependent phosphorylation of GluA1 at Ser-845 increases cell surface expression of AMPARs, whereas NMDA-induced AMPAR dephosphorylation triggers its internalization. We then examined the phosphorylation levels of Ser-845 in GluA1 and Ser-880 in GluA2 and we found that both protein levels were reduced. In addition, there were no significant changes in the total amount of GluA1 mRNA (Figure. 20E, G, H). We also examined the consequence of knocking down AKAP150 on two other proteins: PSD95 and SAP97, but no significant changes were found as showing in Figure. 20 A, B, C.

As it is shown in Figure. 13D, 14B, 14D, we found that the down-regulation of AKAP150 induced by both NMDA and Aβo could not be rescued by the cLTP. Meanwhile, cLTP was applied to overexpressing AKAP150 cells, which pretreated with Aβo for 60 min, we found the surface GluA1 could be significantly increased (Figure. 18E, F). It has been shown previously that AMPARs interact with stargazin and related TARPs (Almeida et al., 2005), which are important in the synaptic clustering of AMPARs via their interactions with MAGUKs such as PSD-95. Furthermore, phosphorylation of stargazin can be dynamically regulated by NMDAR activity in a manner that influences LTP and LTD and AMPARs can dissociate from TARPS on binding glutamate. Thus, the interactions between PSD-95 and AMPARs via TARPS may be another important site of modulation for regulating AMPAR surface expression and NMDAR triggered endocytosis of AMPARs. Because loss of PSD-95 and AKAP79/150 from synapses has been suggested to be important for endocytosis of synaptic AMPARs, we examined whether such trafficking was directly correlated with NMDAR-triggered AMPAR endocytosis.

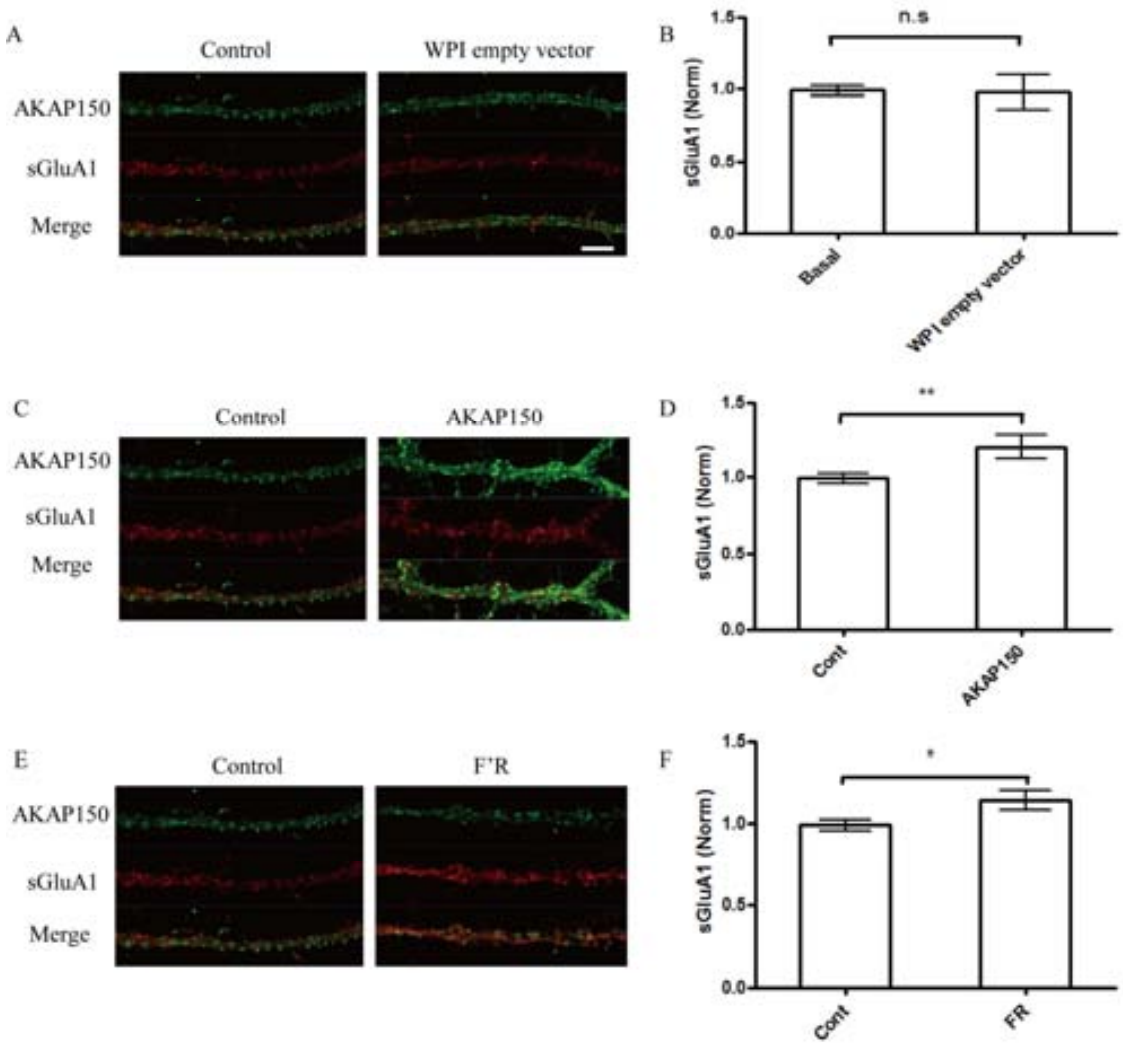

FIGURE 19. Both overexpression of AKAK150 and cLTP could induce the increase of surface GluA1, while empty vector of overexpression of AKAP150 has no impaction on the suface GluA1 level. A. Examples of dendrite staining for surface GluA1 (red) and AKAP150 (green) showing the effects of empty vector of overexpression of AKAP150 on the level of surface GluA1. B. The graph represents quantified changes in surface GluA1 in response to empty vector of overexpression of AKAP150 compared with basal cells. **C.** Examples of dendrite staining for surface GluA1 (red) and AKAP150 (green) showing the effects of overexpression of AKAP150 on the level of surface GluA1. D. The graph represents quantified changes in surface GluA1 in response to overexpression of AKAP150 compared with empty vector infection cells (Cont). **E.** Examples of dendrite staining for surface GluA1 (red) and AKAP150 (green) showing the effects of cLTP (F'R) on the level of surface GluA1. F. The graph represents quantified changes in surface GluA1 in response to cLTP compared with basal cells (Cont). ** P< 0.01; * P< 0.05; n.s, P> 0.05. Error bars represent s.e.m. Scale bar represents 100 μm.

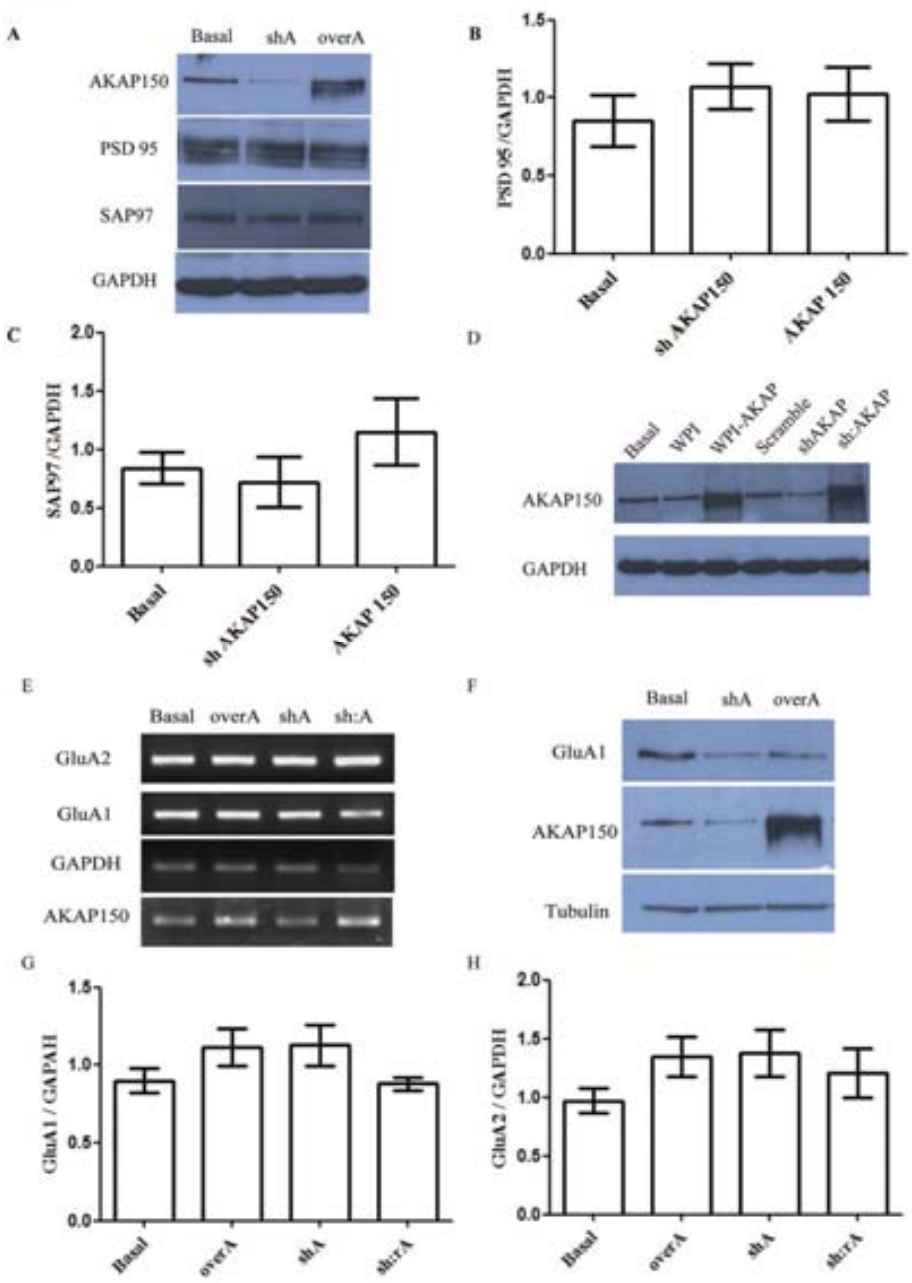

FIGURE 20. Knock down AKAK150 impair the total AMPAR protein levels via a post transcription manner. Neurons infected by lenti-virus to down regulate AKAP150. **A**, Sample blots showing levels of AKAP150 (upper blot), PSD95, SAP97 and GAPDH, corresponding graphs represent quantified changes in PSD95 and SAP97. B-C, The graph represents quantified changes in PSD95 (**B**) and SPA97 (**C**) compared with baseline. **D**, Sample blots showing levels of AKAP150 (upper blot), GAPDH (lower blot) for Basal, empty vecor of overexpression AKAP150 (WPI), overexpression of AKAP150 (WPI-AKAP) , control vector of silence AKAP150 (Scramble), silence AKAP150 (shAKAP), silence AKAP150 and rescuing (sh:AKAP) conditions. **E**. Sample blots showing mRNA levels of GluA2 (uppest blot), GluA1 (upper blot), GAPDH (lower blot) and AKAP150 (lowest blot). **F**, Sample blots showing levels of total GluA1 (upper blot), AKAP150 (middle blot) and GAPDH (lower blot). **G-H**, The graphs represent quantified changes mRNA of GluA1 and GluA2 compared with baseline. *** P< 0.001; * P< 0.05; n.s., P> 0.05. Error bars represent s.e.m.

6. LONG TERM EXPOSURE OF NMDA OR Aβo INDUCED A REDUCTION OF AMPARs AND miRNAS

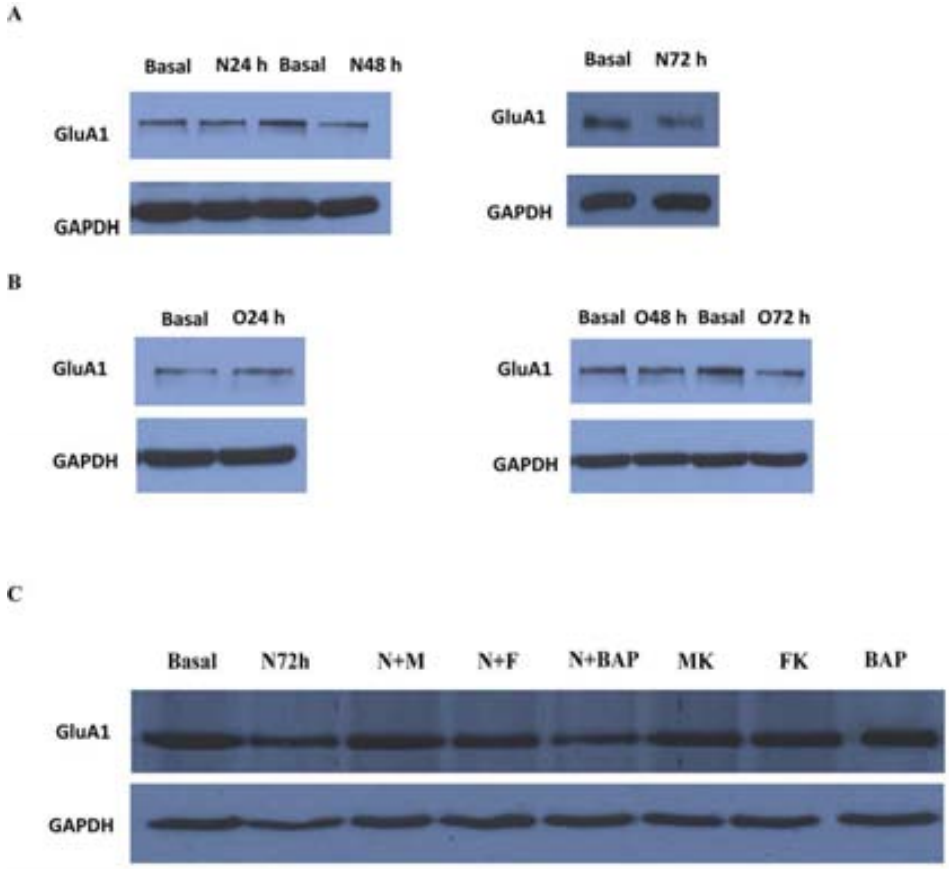

FIGURE 21. Long term exposure of NMDA and Aβo affections on AMPARs. A. Examples of 24 h, 48h, 72h of 50 μM NMDA stimulations on the levels of total GluA1. **B**. Examples of 24 h, 48h, 72h of 50 μM NMDA stimulations on the levels of total GluA2. **C**. Examples of 50 μM NMDA stimulations on the levels of total GluA1 for 72h with MK801 (M), FK506 (F) and BAPTA (BAP).

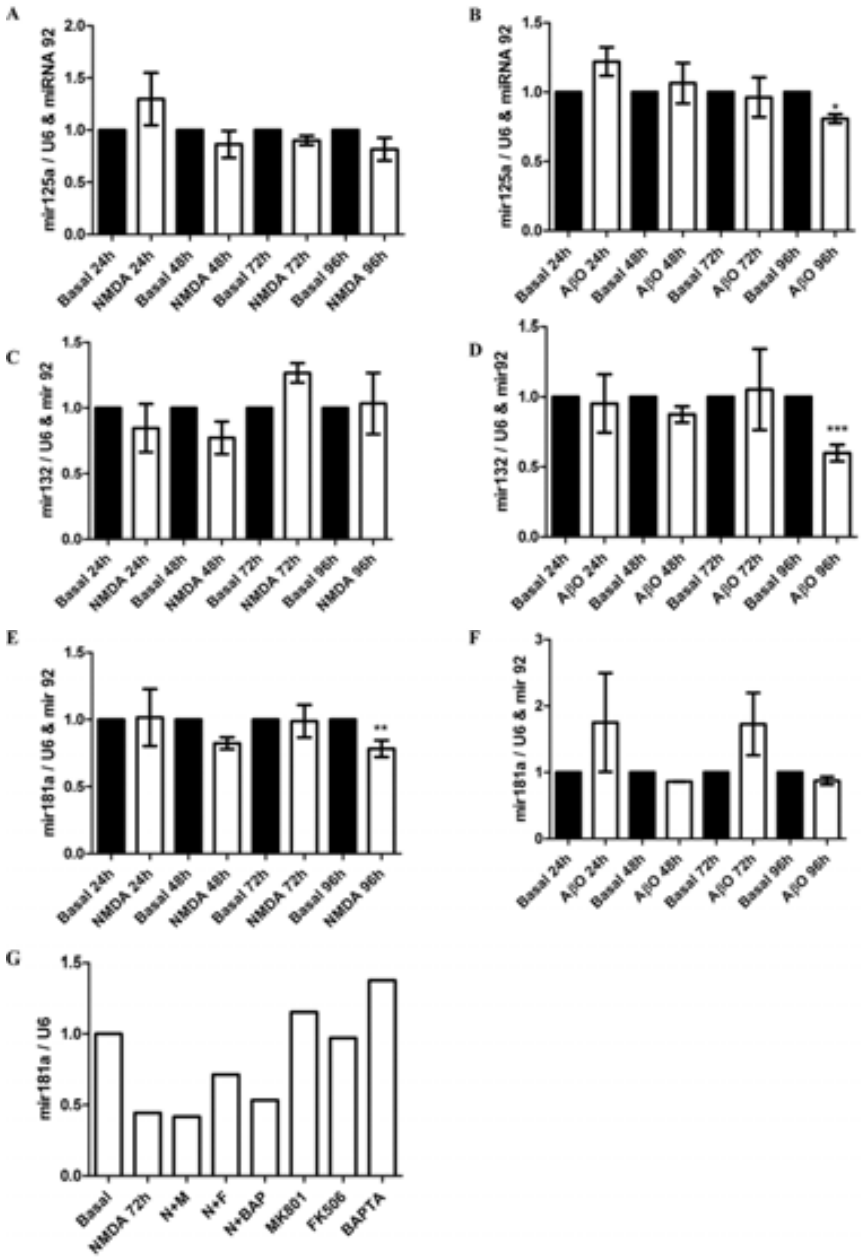

FIGURE 22. Long term exposure of NMDA and AβO affections on miRNAs. A. The graphs represent quantified changes in levels of mir125a with 50 μM NMDA stimulations for 24h, 48h and 72h compared with baseline. **B.** The graphs represent quantified changes in levels of mir125a with 5 μM AβO stimulations for 24h, 48h and 72h compared with baseline. **C.** The graphs represent quantified changes in levels of mir132 with 50 μM NMDA stimulations for 24h, 48h and 72h compared with baseline. **D.** The graphs represent quantified changes in levels of mir mir132 with 5 μM AβO stimulations for 24h, 48h and 72h compared with baseline. **E.** The graphs represent quantified changes in levels of mir181a with 50 μM NMDA stimulations for 24h, 48h and 72h compared with baseline. **F.** The graphs represent quantified changes in levels of mir125a with 5 μM Aβo stimulations for 24h, 48h and 72h compared with baseline. **G.** The graphs represent quantified changes in levels of mir181a with 50 μM NMDA stimulations for 72h compared with the inhibitors of MK801, FK506 and BAPTA. *** P< 0.001; ** P< 0.01; * P< 0.05. Error bars represent s.e.m.

Finally, we have studied the effects of long term exposure of NMDA or related to synaptic function. After applications of either NMDA or Aβo for 24 h, 48 h and 72h, I we checked the level of GluA1and we found that NMDA could induce the decrease of GluA1 after 48 h and 72 h as shown in Figure 21A. On the other hand we also checked the miR125a, miR132 and miR181a levels, after application of NMDA for 24, 48, 72 and 96 hours. We found that 96 hours of NMDA treatment leads to a significant reduction of miR181a (** $P < 0.01$) as it is shown in Figure 22E. On the other hand, it seemed 72 hour of Aβo treatment could induce the reduction of GluA1 as shown in Figure 21B, we also found a significant decrease of miR125a and miR132 after 96 hour NMDA treatments (Figure 22B, D). Consequently, MK801, FK506 and BAPTA were applied to investigate the signal pathways for long term exposure of NMDA, the results showed that MK801 and FK506, but not BAPTA could likely partially rescue the reduction of GluA1, we next tested the same inhibitors for investigation of NMDA treatment impaction on miR181 level, we found that it seemed only the FK506 could partially block the reduction (Figure 21C and Figure 22G).

DISCUSSION

The present study has explored the importance of the AKAP150 protein involved in the neurodegeneration induced by Aβo and cLTD (NMDA). The findings derived from the work in this thesis suggest that the AKAP150 might be essential for the trafficking of AMPARs and the impairment of synaptic function in AD or cLTD (NMDA). Accordingly, the observations described in this study support the concept of exposure of Aβo leads to synaptic alterations associated with multiple neurotransmitter deficiencies and cognitive failure. In addition to that, the findings from this work shed light on the link connecting the AKAP150 signals to the mediators of neuronal plasticity. Specific discussions focusing on the different implications depicted in this thesis are described below in their respective sections.

1. AβO INDUCED ABERRATIONS IN SYNAPSE COMPOSITION PROVIDES A MOLECULAR BASIS FOR LOSS OF CONNECTIVITY IN ALZHEIMER'S DISEASE

1.1. MEMORY LOSS IS A DISRUPTION OF SYNAPTIC PLASTICITY: THE OLIGOMER HYPOTHESIS

Investigation into the action of clusterin by Lambert, Klein and colleagues established that, concomitant with inhibition of amyloid formation, clusterin promotes accumulation of soluble Ab oligomers (Lambert et al., 1998). Small oligomers were evident by gel electrophoresis in the presence of SDS, with larger SDS-unstable species also present in aqueous buffer. Imaging the oligomers by atomic force microscopy showed globular proteins a few nanometers in diameter, about the dimensions of average-sized globular proteins. Oligomers were not in complexes with clusterin, and they also formed in the absence of clusterin when solutions contained very low levels of Ab. The oligomers were relatively long-lived, not converting into amyloid over periods of several days. Most importantly, these amyloid-free Ab oligomers were potent CNS neurotoxins. In a discovery providing the first molecular-level insight into AD memory loss, oligomers were found to inhibit functional synaptic plasticity (Lambert et al., 1998). LTP was inhibited within minutes. This rapid loss of LTP, measured in rat brain slices and *in situ* in mice, occurred without impact on baseline excitability, indicating impairment of signaling rather than degeneration. With chronic exposure, neurons ultimately were killed. Death was

selective for subpopulations of vulnerable neurons and was prevented by knockout of Fyn, a protein tyrosine kinase linked to NMDA receptor signaling. Consistent with dependence on signal transduction, toxicity required maturation of the hippocampus and association of oligomers with protease sensitive cell surface toxin receptors. These findings led to a new hypothesis for the role of Ab in Alzheimer's disease, the ''oligomer hypothesis.'' Memory loss, beginning early in the disease, was attributed to oligomer-induced disruption of synaptic plasticity, with later stages of dementia attributed to oligomer-induced cellular degeneration and death. Based on a central role for impaired signaling, the oligomer hypothesis predicted that early memory loss should be reversible. This prediction was confirmed in the transgenic mouse experiments mentioned above (Kotilinek et al., 2002). The impact of oligomers is in harmony with recent findings that clusterin, which prevents amyloid formation and promotes oligomer formation, is an AD risk factor (Thambisetty et al., 2010). The conclusion that Ab oligomers can be neurologically significant toxins, possibly the most important ones for AD, is now supported by more than a decade of further investigation, with over 1000 papers addressing the oligomer hypothesis.

1.2. OLIGOMERS ACCUMULATION

Metabolic effects of mutations promote increased levels of total Aβ, or increased Aβ42-Aβ40 ratio (Citron et al., 1992), conditions that favor oligomerization. Relative levels of Ab42–Ab40 appear to influence the mechanism of oligomerization, with higher levels of Ab40 in normal individuals likely impeding formation of stable toxic oligomers (Giuffrida et al., 2009). It is not known why toxic oligomers accumulate in sporadic AD. Most likely, accumulation is a consequence of various factors. Those affecting Aβ clearance may be especially germane, as the Aβ monomer is a metabolite with rapid turnover, determined by extracellular microdialysis in animal models and human subjects (Cirrito et al., 2005; Kang et al., 2009); Recent findings by Bateman and colleagues show that clearance of Aβ in AD patients is reduced by 30% (Mawuenyega et al., 2010). The mechanisms underlying reduced clearance are not known, but expression of the ApoE4 allele, a major risk factor for sporadic AD (Strittmatter et al., 1993), may be involved. Individuals homozygous for ApoE4 show an 8-fold elevated risk for AD compared to those with the more common ApoE3 allele. Biochemically, ApoE3 helps clear extracellular Aβ, whereas ApoE4 does not

(Yang et al., 1999), but whether this underlies elevated risk has not been determined. Co-morbidity factors also are important. For example, individuals with type 2 diabetes have an elevated AD risk (Luchsinger, 2008). At the cellular level, deficient insulin signaling results in impaired removal of Ab (Plum, et al., 2005) and Ab oligomers from the extracellular milieu (Zhao et al., 2009). Somewhat surprisingly, acutely elevated oligomer levels have been noted after exposure to general anesthetics (Eckenhoff et al., 2004). Traumatic brain injury also is associated with acutely elevated levels in CSF, with a positive correlation between oligomer levels and severity of sequelae. This is in harmony with rapid plaque formation seen in about 30% of brain injury patients (Johnson et al., 2009). Association with injury is consistent with APP, a trauma-induced protein that is upregulated in the optic nerve in shaken baby syndrome (Gleckman, et al., 2000), being the link etween mechanical trauma and AD. uggestions also have been made that AD could be transmissible, like a prion disease (Soto, et al., 2006), and it is possible that regulation of APP translation may be stimulated by oligomers themselves, producing a pathogenic spiral.

2. THE RELATIONSHIP BETWEEN AβO AND LONG TERM DEPRESSION OR LONG TERM POTENTIATION

It has been previously reported that, in hippocampal slices, synthetic oligomers caused rapid LTP inhibition (Jurgensen et al., 2011; Rammes, et al., 2011). Inhibition also has been observed in a number of experiments using uncharacterized Aβ preparations (Cullen et al., 1997). The glutamate receptor family of proteins appears to be centrally involved in neuronal targeting by Aβ oligomers. Co-immunoprecipitation and photoactivated amino acid cross-linking studies indicated that Aβ oligomers interact with complexes containing the GluR2 subunit of AMPA receptors, a conclusion that was corroborated by the observation that pharmacological inhibition or removal of surface AMPA receptors reduced oligomer binding to neurons (Zhao et al., 2010). Moreover, single particle tracking of quantum dot-labeled Aβ oligomers has demonstrated the participation of metabotropic glutamate receptors (mGluR5) in oligomer binding and clustering at synapses (Renner et al., 2010). Additionally, NMDARs co-immunoprecipitate with Aβ oligomers from detergent-extracted oligomer-treated rat synaptosomal membranes, and an N-terminal anti-NR1 antibody markedly reduced oligomer binding to dendrites (De Felice et al., 2007).

Consistent with those findings, oligomer binding is virtually abolished in dendrites of NMDAR knock-down neurons (Decker, et al., 2010). As predicted, NMDAR knock-down also abrogates neuronal oxidative stress induced by Ab oligomers, which is mediated by aberrant activation of NMDARs (De Felice et al., 2007).

Previous studies have shown that Aβo can facilitate the removal of AMPAR from the cell surface depending on the subunit composition of the receptors. Thus alteration in the functionality of these receptors could be involved in the early cognitive dysfunction observed in experimental models of AD. Although, the mechanisms involved in Aβo-mediated effect on AMPAR have not been fully elucidated yet. AMPARs are essential for excitatory synaptic transmission and play key roles in LTP and LTD, cellular mechanisms of plasticity that are believe to underlie learning and memory. Early evidence for this was provided when it was shown that LTP involves the rapid 'unsilencing' of 'silent' synapses (Malinow et al., 2002) - synapses that show NMDAR- but not AMPAR-mediated responses. Further work showed that LTD can involve the 're-silencing' of synapses (Luthi et al., 1999). Both the surface GluA1 and GluA2 were all reduced by application of NMDA, in this case, the NMDA receptors were actived by NMDA, thus the AMPARs have been triggered by NMDA receptors, but the mechanisms of this procedure are still unclear.

Among the different subunits present in AMPARs, GluA1 is the one whose trafficking depends on neuronal activity, whereas GluA2 is more prone to undergo constitutive, activity independent recycling (Bredt et al., 2003). Membrane insertion of GluA1 is regulated by two phosphorylation sites in the intracellular C-terminal tail: Ser-845 and Ser-831, which are phosphorylated by PKA and CaMKII, respectively (Song et al., 2002). Phosphorylation at Ser-845 contributes specifically to the recruitment of new AMPARs to extrasynaptic sites, a critical event for the establishment of LTP (Lee et al. 2003; Oh et al., 2006), whereas its dephosphorylation is essential for NMDA receptor-dependent LTD (Lee et al., 2010). Previously in our lab, the decrease in phosphorylation levels of GluA1 Ser-845 and cell surface GluA1 was observed by treatment of Aβo (Miñano-Molina et al., 2011), which induced GluA1dephosphorylation and reduced receptor surface levels are mediated by an increase in calcium influx into neurons through ionotropic glutamate receptors and activation of the calcium-dependent phosphatase calcineurin, Aβo blocked the

extrasynaptic delivery of AMPARs induced by chemical synaptic potentiation. Consistent with previous reports and our previous work, in the current studies, the endocytosis of AMPARs induced by Aβo was mimicked by NMDA in a protocol that induces cLTD indicating that somehow similar mechanisms are involved in Aβo and cLTD-mediated synaptic effects. A common key feature seems to be the reduction of membrane AMPAR.

3. THE ROLE OF AMPARS AND THEIR RELATIONSHIPS WITH AKAP150 IN AβO OR NMDA-TRIGGERED AMPARS ENDOCYTOSIS

A role for AKAP proteins in regulating AMPAR-mediated currents, AMPAR trafficking, and synaptic plasticity has been well established. LTP and LTD triggered by the activation of NMDARs and are extensively studied models for such synaptic modifications and compelling evidence suggests that they result, at least in part, from activity-dependent regulated trafficking of AMPARs to and away from synapses (Shepherd et al., 2007).. AMPARs are heteromeric complexes clustered in the postsynaptic density PSD of synapses via the binding of closely associated accessory proteins known as TARPS (transmembrane AMPAR regulatory proteins) to members of the membrane- MAGUK family of PDZ domain–containing scaffold proteins (Nicoll et al., 2006).

We have evaluated the effects of NMDA and Aβo on AKAP150 levels, as showing in Figure. 7F and Figure. 8F, both Aβo and NMDA could reduce the levels of AKAP150, on the other hand, Aβo and NMDA (cLTD) exert similar impairment of AMPARs trafficking. It was interesting to understand the relationship between AKAP150 and AMPARs during the long term depression induced by Aβo or NMDA (cLTD). It was also predicted that oligomers would initiate synapse loss (Wang et al., 2004). This prediction has indeed been confirmed (Lacor et al., 2007), as have the related predictions that oligomers cause dysfunctional trafficking of ionotropic glutamate receptors and metabotropic glutamate receptors (Gong et al., 2003; Miñano-Molina et al., 2011). These results are consistent with reports showing that Aβo facilitates LTD (Jurgensen et al., 2011). The Aβo -mediated decrease in GluA1 in the cell surface may be part of the primary stages of the mechanism by which Aβo facilitates/induces LTD, inhibits LTP, and causes synapse failure. A recent study has

suggested that induction of LTP needs transient incorporation of GluA1 homomers at perisynaptic sites (Yang et al., 2008). This incorporation is associated with phosphorylation of GluA1 Ser-845, which prevents endocytosis (Man et al., 2007) and lysosomal degradation of GluA1 (Ehlers et al., 2000).

In these previous studies an LTD like stimulation of NMDAR produces a decrease in phospho-Ser-845 and surface expression of GluA1, whereas stimulation with forskolin and rolipram recovered phosphor-Ser-845 and GluA1 surface expression. Actually, our previous results show that Aβo prevents forskolin/rolipram-mediated increase of phosphor-Ser-845 and cell surface GluA1 levels, which supports evidence showing that Aβo is able to block LTP (Wang et al., 2004). So, in theory, the inhibition of LTP induced by Aβo possibly impairs the trafficking of AMPARs and the level of AKAP150 on the synapse.

It is now clear that another consequence of NMDA receptor activation is clathrin-mediated endocytosis of AMPA receptors (Man et al., 2000). Although these data strongly suggest that AMPA receptor internalization also contributes to the expression of LTD, several questions remain. First, it is surprising to note that NMDA receptor activation has not yet been shown to cause a stable long-term reduction in surface-expressed AMPA receptors. In fact, the work from Ehlers (Ehlers et al., 2000) shows that NMDA receptor activation causes only a transient internalization of AMPA receptors. For LTD to be expressed by a reduction in the number of AMPA receptors, it must be possible for NMDA receptor activation to trigger a persistent change. Second, it is not clear what role plays dephosphorylation of PKA substrates in this process. Several findings suggest that the state of phosphorylation of Ser845 of GluR1 may regulate its surface expression. AMPA receptors internalized in response to Aβo have been shown to be dephosphorylated at GluR1 Ser845 in our previous work (Miñano-Molina et al. 2011). In addition, transgenic mice with targeted serine to alanine mutations at Ser845 and Ser831 of GluR1 are deficient in AMPA receptor endocytosis (Lee et al., 2003). However, it remains to be determined whether dephosphorylation of PKA substrates is sufficient for decreased AMPA receptor surface expression (as it is for LTD), and if so, what mechanisms account for such dephosphorylation.

Our results clearly showed that AKAP150 was down-regulated by Aβo or NMDA. The mechanisms beneath the reduction of AKAP150 were consequently investigated by applying inhibitors as MK 801, FK506, CNQX or MG132. Our results suggested that calcineurin is required for the reduction of AKAP150. It has been shown that Aβo alters homeostasis of [Ca^{2+}] (Alberdi et al., 2010). In our previous work (Miñano-Molina et al., 2011), we have described that calcium influx together with calcineurin activation is involved in the reduction of synaptic GluA1 by Aβo. In the present work we have extended these results showing that calcineurin is also needed to cLTD-mediated internalization of AMPAR from the synaptic surface. It is known that CaN may act to regulate Ca^{2+}-signaling processes indirectly through the action of other signaling proteins, such as protein phosphatases and protein kinases, or through adaptor or CaN binding proteins which might act to localize PP2B activity and facilitate the specificity of CaN action, so Aβo could be activating NMDARs (which was proved by application of MK801) first, then altering the Ca^{2+}-signaling processes for down-regulating AKAP150 (which happened by proteasome, confirmed by application of MG132), resulting in the endocytosis of AMPARs. AKAP79/150 is a protein that has been proposed to function as a scaffold for protein kinase A (PKA), protein kinase C and the Ca^{2+}/calmodulin-dependent protein phosphatase calcineurin (also known as PP2B) in a range of cell types, positioning these enzymes adjacent to key protein substrates (Klauck et al., 1996). The notion that AKAP79/150 is important in LTD is particularly attractive, as PKA and calcineurin have been implicated in the regulation of AMPAR trafficking during this form of synaptic plasticity (Snyder et al., 2005). Specificity in PKA signaling arises in part from the association of the enzyme with AKAPs which function to target PKA to specific substrates at precise subcellular locations. At the postsynaptic density, PKA is tethered to the neuronal anchoring protein, AKAP79/150 (human/rodent) (Colledge et al., 2000). Through association with the synaptic scaffolding MAGUK proteins, AKAP79/150 and its associated enzymes (PKA, protein kinase C, and PP2B) are directed to both NMDA- and AMPA-type glutamate receptors. Furthermore, AKAP79/150 has been shown to regulate AMPA receptor phosphorylation and function (Oliveria et al., 2003). Recent experiments have shown that the synaptic localization of AKAP79/150 itself can be altered by NMDA receptor activation and PP2B signaling cascades, suggesting that AKAP79/150 may play an important role in synaptic plasticity (Gomez et al., 2002).

To test the relevance of Aβo modulation of GluA1 phosphorylation and turnover on synaptic plasticity events, we took advantage of a recent described protocol of cLTP in cultured neurons (Otmakhov et al., 2004). What we found was that cLTP could not rescue the down regulation of AKAP150. In these previous studies an LTD like stimulation of NMDAR produces a decrease in phospho-Ser-845 and surface expression of GluA1, whereas stimulation with forskolin and rolipram recovered phosphor-Ser-845 and GluA1 surface expression (Miñano-Molina et al., 2011). Actually, our previous data show that Aβo prevents forskolin/rolipram-mediated increase of phosphor-Ser-845 and cell surface GluA1 levels, which supports evidence showing that Aβo is able to block LTP (Wang et al., 2004; Miñano-Molina et al., 2011).

So, the inhibition of LTP induced by Aβo possibly impairs the trafficking of AMPARs and reduces the level of AKAP150 on the synapse. The failure of recovering reduction of AKAP150 from applications of Aβo or NMDA by induction of cLTP indicates the loss of AKAP150 from the synapse might be related to the AMPARs trafficking, since previously we found that the loss of surface GluA1 induced by Aβo could not be rescued by applying cLTP either (Miñano-Molina et al., 2011). Moreover, we found that acute knockdown of AKAP150 markedly reduced synaptic AMPARs. These results are consistent with a model in which the binding of AKAP150 to PSD-95 is required to position calcineurin at the appropriate subsynaptic location so that it can be activated by Ca^{2+} influx through NMDARs and contribute to the endocytosis of AMPARs that underlies one major form of LTD (Bhattacharyya et al., 2009).

Next we wanted to examine the role of AKAP150 in cLTD by overexpressing AKAP150 or by a silencing-based treatment using shRNA-mediated knockdown of AKAP150.Overexpression of AKAP150 significantly increases the surface AMPARs level in the presence of Aβo or NMDA, thus demonstrating a reversion of the cLTP and Aβo-mediated reduction in AKAP150 levels. On the other hand, AKAP150 silencing produces a reduction in AMPARs comparable to the observed in cLTP conditions or after Aβo treatment. These results were further confirmed by knocking-down endogenous AKAP150 while at the same time we overexpressed AKAP150.

Under these conditions we are able to restore normal AKAP150 levels in neuronal cultures.

Changes in AKAP150 levels have a direct effect on AMPARs levels. Our results show that after knock-down of AKAP150, we got not only a strong reduction of AMPARs but also in the phosphorylated state of GluA1 at S845. Altogether, these results indicatethat AKAP150 silencing results in the down-regulation of surface AMPARs and a decrease recruitment of new AMPARs to extrasynaptic sites. Also, in our lab, Miñano-Molina et al. 2011 reported that Aβo reduces phosphorylation of GluA1 Ser-845 levels leading to a decrease of surface AMPAR, which consistent with the silence of AKAP150. The present results confirm that AKAP150 levels control surface presence of AMPAR.

Our work shows that phosphorylation of GluR1 at Ser845 is decreased for synaptic delivery of AMPA receptors which induced by silence of AKAP150, whereas AMPA receptors internalized in response to Aβo have been shown to be dephosphorylated at GluR1 Ser845 in our previous work (Miñano-Molina, 2011). In addition, transgenic mice with targeted serine to alanine mutations at Ser845 and Ser831 of GluR1 are deficient in AMPA receptor endocytosis (Lee et al., 2003). However, it remains to be determined whether dephosphorylation of PKA substrates is sufficient for decreased AMPA receptor surface expression (as it is for LTD), and if so, what mechanisms account for such dephosphorylation. Specificity in PKA signaling arises in part from the association of the enzyme with AKAPs, which function to target PKA to specific substrates at precise subcellular locations (Bauman et al., 2002).

Our data suggest a hypothesis that appropriate activation of NMDA receptors induced by Aβo may degrade AKAP150, thereby causing dephosphorylation of postsynaptic PKA substrates including AMPA receptors and depression of AMPA receptor-mediated transmission. Displacement of PKA from synapses in NMDA-treated cultures could account for the only partial recovery of AMPA receptor surface expression following treatment with PKA activators. Our results complement the finding that activation of NMDA receptors on hippocampal neurons can also lead to a redistribution of the AKAP79/150-PKA complex away from synaptic sites (Gomez et al., 2002). Ultimately, however, testing this hypothesis will require high resolution

molecular imaging and electrophysiology of individual synapses. An alternative and not mutually exclusive possibility is that PKA activity may be required for constitutive exocytosis of AMPA receptors to the membrane. In the latter case, PKA inhibition could reduce surface expression of AMPA receptors by preventing delivery of new receptors to the membrane and the replacement of constitutively endocytosed synaptic receptors.

4. THE ROLE OF MICRORNAS IN NEUROGENESIS AND NEUROPLASTICITY MECHANISMS

Evidence suggested the involvement of miRNAs in synaptic plasticity mechanisms. Schratt et al. (2006) showed that miR-134 regulates rat protein synthesis as well as the size of postsynaptic sites in dendritic spines of the synaptodendrites located in hippocampal neurons. Dendritic spine growth is regulated by miR-134 suppression mediated by the translation of mRNA encoding a specific protein kinase, Limdomain-containing protein kinase 1 (Limk1). Within dendrites miR-138 seems to down-regulate the size of dendritic spines in rat hippocampal neurons affecting the expression of acyl protein thioesterase 1 involved in the palmitoylation status of proteins having synaptic functions (Siegel et al., 2009). Spine growth determined by suppression of miR-138 may be inhibited by interference-mediated knockdown of acyl protein thioesterase 1 and expression of membrane-localized Ga13. Lugli et al. 2008 suggested that mature miRNAs are partially processed near synapses and play a relevant role in local protein synthesis. Research about long term exposure of Aβo or NMDA impact on the miRNA are inadequate in previous studies, we chose to apply 5μM Aβo or 50 μM NMDA to primary cultured cortical neurons for 1 day to 4 days aiming at the affection on postsynaptic proteins and the changes of miRNA levels, one of our goals was to investigate how the miRNAs behave during LTD. We were specifically checking miR-125a, which targeting PSD-95 mRNA allows reversible inhibition of translation and regulation by gp1 mGluR signaling, on the other hand, inhibition of miR125a increased PSD-95 levels in dendrites and altered dendritic spine morphology. In our studies, Aβo exposure for 96 hour could be remarkably decreasing the miR125a level, in the meanwhile, the level of GluA1 was checked after 96 hours as well, a corresponding reduction was observed. So, we next would

like to examine the levels of PSD95 and AKAP150 as to steadily uncover the role of miRNAs on the loss of synaptic plasticity.

miR132 was also checked after 1 to 4 days treatments of Aβo or NMDA, a significant reduction of miR132 was found after 4 days exposure of 5μM Aβo to primary cultured cortical neurons, as we know, intriguingly, the CREB-dependent miR-132 has been shown to control the development of dendrites and spines, and synaptic integration in cultured hippocampal neurons and newborn hippocampal neurons (Magill et al., 2010). More specifically, it was reported that knockout of the miR-212/132 locus using conditional transgenic mice or knockdown of miR-132 using viral vectors led to reduced dendritic complexity and spine density, respectively, in newborn neurons of the adult hippocampal neurogenic zone The dendritic effect were shown to be preferentially due to miR-132 loss, (Magill et al., 2010). On the other hand, evidence suggests that the acquisition of recognition memory depends upon CREB-dependent long-lasting changes in synaptic plasticity in the perirhinal cortex. The CREB-responsive microRNA miR-132 has been shown to regulate synaptic transmission, it has recently been reported that a transgenic mouse overexpressing miR-132 throughout the forebrain showed impairments in recognition memory (Hansen et al., 2010). More details needed to investigate about the role of miR132 in regulating GluA1 reduction.

miR181a, which was checked following the treatments of Aβo or NMDA for 1 to 4 days as well, interestingly, 4 days treatment with NMDA, a reduction ($p<0.01$) of miR181a level was found. Among the computationally predicted targets for miR-181a, there was an apparent bias toward genes involved in various brain functions. One of the target genes that we specifically focused on was the transcript encoding the GluA2 subunit of AMPA-Rs. A potential interaction between miR-181 family member miR-181b and GluA2 was previously investigated within the context of schizophrenia, where miR-181b showed elevated levels in the gray matter of the superior temporal gyrus (Beveridge et al., 2008). However, previous study used a glioblastoma cell culture model and did not address the functional consequences with regard to synapse morphology and physiology. Saba et al. 2012 observed a specific reduction in GluA2 surface expression and mEPSC frequency upon miR-181a expression, demonstrating for the first time an important functional role for miR-181a

at the synapse. Compared with our work, probably the GluA2 protein level would be a great interest of assessment.

5. MIRNAS AND PATHOLOGICALLY STRESS INDUCED CHANGES

Our long term stimulations of NMDA and Aβ induced ~~the~~ a reduction in ~~of~~ miR181a, mir132 and miR125a levels, suggesting that this miRNAs may have something to do with the trafficking of GluA1 or GluA2 since both stimulis were able to change total levels of GluA1 and GluA2. So we next tried to uncover the mechanisms of down regulation of miRNA, such as miR181a, which is critical for controlling of synaptic plasticity (Saba et al., 2012), by using MK801, FK506 and BAPTA-AM, inhibitors of NMDARs, PP2B, calcium, respectively. In particular, BAPTA-AM is a cell-permeant chelator, which is ~~a~~ highly selective for Ca^{2+} over Mg^{2+}, and it can be used to control the level of intracellular Ca^{2+}. We found the MK 801 and FK506, but not BAPTA could partially block the reduction miR181a by application of NMDA for 96 hour. Our results suggested the long term LTD induced by NMDA modulate miR181 needs calcineurin activity.

However, rare research have been looking into the role of miR181a playing with Calcineurin during the LTD, our result indicated the PP2B could be an opening of the investigation of miR181a for the neurodegeneration. NMDARs, on the other hand, involved in the regulation of miR181a proved by using MK801, suggesting NMDARs are required for the modulation of mirR181a during the LTD. Previous analysis (Pai et al., 2014) of LTP in the dentate gyrus of anesthetized rats demonstrates differential regulation of mature miRNA expression in whole lysates and the Ago2 immunoprecipitated fraction. Both quantitatively and qualitatively, miRNA expression in tissue lysates does not accurately reflect changes in the miRNA content of the Ago2-RISC. The ratio of Ago2/total miRNA expression was regulated bidirectionally in a miRNA-specific manner and was largely dependent on NMDA receptor activation during LTP induction. Their results identify miRNA association with Ago2 as a potential control point in activity-dependent synaptic plasticity in the adult brain. Consequently, interaction of miR181a with certain NMDARs could be an opening for the failure of synaptic plasticity.

Our results indicate mir181a might be involved in the long term application of cLTD (NMDA) while mir125a and mir132 might be involved in the long term treatment of Aβo. miR125a showed decreases in the treatment of Aβo in our study, it is known that the localization of miR-125a to dendrites, its abundance in synaptoneurosomes, and its involvement in an mGluR pathway functions to regulate local protein synthesis affecting dendritic spine-synapse morphology. Ravi et al., 2011 demonstrated that blocking miR-125a by transfecting antimiR-125a had a marked effect on the spine morphology of cultured hippocampal neurons. Inhibition of endogenous miR-125a function resulted in a marked increase in spine density and branching. It is also demonstrated that the spine phenotype observed by miR-125a inhibition is due to excess PSD-95 mRNA translation and could be rescued by PSD-95 knockdown. Inhibition of PSD-95 mRNA by miR-125a was shown to have bidirectional control of endogenous PSD-95 expression in dendrites and at synapses, on the other hand, It has been showed that exposure of cultured cortical neurons to Aβo reduces PSD-95 protein levels in a dose- and time-dependent manner and that the Aβo -dependent decrease in PSD-95 requires NMDAR activity. It is also showed that the decrease in PSD-95 requires cyclin-dependent kinase 5 activity and involves the proteasome pathway (Roselli et al., 2005). So, the role of PSD95 involved in the downregulating miR125a by long term exposure of NMDA (cLTD) might be interesting and crucial, thus the application of Aβo could be important as well. miR181a reduces AMPARs surface clusters, spine volume, and mEPSC frequency in cultured hippocampal neurons. To address whether miR-181a-directed regulation of GluA2 has any consequence on AMPARs function, saba et al., 2011 and colleagues decided to monitor AMPARs surface expression at synapses in primary hippocampal neurons. It has been identified that GluA2 mRNA as a genuine target gene of miR-181a in primary rat neurons. Moreover, it has been further raised the possibility that miR-181a-mediated modulation of GluA2 expression could be involved in synaptic function. It was shown that the number of surface AMPARs clusters correlates with the number of functional synapses, and the size of individual AMPARs surface clusters is a good measure for postsynaptic strength (Malenka and Nicoll 1999), however, in the current studies, we only checked the GluA1 levels with the application of long term exposure of Aβo, the role of GluA2 in this modulation of miR181a could be interesting.

CONCLUSIONS

1- It is shown that both AMPARs and AKAP150 levels were reduced by Aβo and cLTD.

2- The reduction of AKAP150 partially rescued by FK506 or MG132 suggested the PP2B and proteasome might be playing an important role of regulation of AMPARs trafficking.

3- Besides cLTP could recruit AMPARs to the surface of synapse, ~~h~~ it fails to restore AKAP150 levels decreased by Aβo or cLTP. We believe that the loss of AKAP150 from the synapse might not share identical molecular mechanisms than–AMPARs trafficking.

4- Overexpression of AKAP150 strongly up-regulated the surface AMPARs even in the presence of Aβo or after cLTD induction.

5- Down-regulation of endogenous AKAP150 induced a reduction of total AMPARs (GluA1 and GluA2), which could be restore by simultaneous overexpression of human AKAP.

6- cLTD produces a reduction of mir181a levels whereas Aβo produce a decrease in mir125a and mir132.

7- The regulation of 181a induced by cLTD requires NMDARs activation and the modulation of Calcineurin.

REFERENCE LIST

Ahmadian, G. et al. (2004) Tyrosine phosphorylation of GluR2 is required for insulin-stimulated AMPA receptor endocytosis and LTD. EMBO J. 23, 1040–1050.

Alberdi, E., Sa´nchez-Go´mez, M. V., Cavaliere F. et al., (2010) Amyloid beta oligomers induce Ca^{2+} dysregulation and neuronal death through activation of ionotropic glutamate receptors. Cell Calcium, 47, 264–272

Almeida, C.G., Tampellini, D., Takahashi, R.H., Greengard, P., Lin, M.T., Snyder, E.M., and Gouras, G.K. (2005) Beta-amyloid accumulation in APP mutant neurons reduces PSD-95 and GluR1 in synapses.Neurobiol. Dis. 20, 187–198.

Alzheimer, A. (1907) Über eine eigenartige Erkrankung der Hirnrinde. Allg. Z. Psychiatrie Psychisch-Gerichtl. Med. 64, 146–148.

Ashby, M. C. et al. (2004) Removal of AMPA receptors (AMPARs) from synapses is preceded by transient endocytosis of extrasynaptic AMPARs. J. Neurosci. 24, 5172–5176.

Ashraf, S.I., McLoon, A.L., Sclarsic, S.M., Kunes, S., (2006) Synaptic protein synthesis associated with memory is regulated by the RISC pathway in Drosophila. Cell 124, 191–205.

Asztély F, Gustafsson B., (1996) Ionotropic glutamate receptors. Their possible role in the expression of hippocampal synaptic plasticity. Mol. Neurobiol, 12, 1–11.

Bartel, D. P. (2009) MicroRNAs: target recognition and regulatory functions. Cell 136, 215–233.

Bartel, D. P. & Chen, C. Z. (2004) Micromanagers of gene expression: the potentially widespread influence of metazoan microRNAs. Nature Rev. Genet. 5, 396–400.

Barbado M, Fablet K, Ronjat M, De Waard M. (2009) Gene regulation by voltage-dependent calcium channels. Biochim. Biophys. Acta 1793 (6): 1096–104.

Barry, M.F., and Ziff, E.B. (2002) Receptor trafficking and the plasticity of excitatory synapses. Curr. Opin. Neurobiol. 12, 279–286.

Beattie, E.C., Carroll, R.C., Yu, X., et al., (2000) Regulation of AMPA receptor endocytosis by a signaling mechanism shared with LTD. Nat. Neurosci. 3, 1291–1300.

Benke, T. A., Luthi, A., Isaac, J. T. & Collingridge, G. L. (1998) Modulation of AMPA receptor unitary conductance by synaptic activity. Nature 393, 793–797.

Beveridge NJ, et al. (2008) Dysregulation of miRNA 181b in the temporal cortex in schizophrenia. Hum. Mol. Genet. 17:1156 –1168

Bhattacharyya, S., Biou, V., Xu, W., Schluter, O. et al., (2009) A critical role for PSD-95/AKAP interactions in endocytosis of synaptic AMPA receptors. Nature Neurosci. 12, 172–181.

Bliss, T.V. and Collingridge, G.L. (1993) A synaptic model of memory: long-term potentiation in the hippocampus. Nature 361, 31–39

Blackshaw LA, Page AJ, Young RL. (2011) Metabotropic glutamate receptors as novel therapeutic targets on visceral sensory pathways. Front. Neurosci. 24. 1-7.

Brown, T. C., Tran, I. C., Backos, D. S. et al., (2005) NMDA receptor-dependent activation of the small GTPase Rab5 drives the removal of synaptic AMPA Neuron. 45, 81-94.

Brandon, E. P. et al. (1995) Hippocampal long-term depression and depotentiation are defective in mice carrying a targeted disruption of the gene encoding the RIβ subunit of cAMP-dependent protein kinase. Proc. Natl Acad. Sci. USA 92, 8851–8855.

Bredt, D. S. & Nicoll, R. A. (2003) AMPA receptor trafficking at excitatory synapses. Neuron 40, 361–379.

Bredt, D.S., and Nicoll, R.A. (2003) AMPA receptor trafficking at excitatorysynapses. Neuron 40, 361–379.

Busciglio, J., Gabuzda, D. H., Matsudaira, P. et al., (1993) Generation of β-amyloid in the secretory pathway in neuronal and nonneuronal cells. Proc. Natl Acad. Sci. USA 90, 2092–2096.

Carroll, R. C., Beattie, E. C., von Zastrow, M. et al., (2001) Role of AMPA receptor endocytosis in synaptic plasticity. Nature Rev. Neurosci. 2, 315–324.

Chartier-Harlin, M. C. et al. (1991) Early-onset Alzheimer's disease caused by mutations at codon 717 of the β-amyloid precursor protein gene. Nature 353, 844–846.

Cirrito, J. R., Yamada, K. A., Finn, M. B., et al. (2005) Synaptic activity regulates interstitial fluid amyloid-beta levels in vivo. Neuron, 48, 913–922.

Citron, M., Oltersdorf, T., Haass, C., et al., (1992) Mutation of the beta-amyloid precursor protein in familial Alzheimer's disease increases beta-protein production. Nature, 360, 672–674.

Ciesla, M. et al., (2011) MicroRNAs as biomarkers of disease onset. Anal Bioanal Chem, 40, 2051-2061

Cleary, J. P. et al. (2005) Natural oligomers of the amyloid-β protein specifically disrupt cognitive function. Nature Neurosci, 8, 79–84.

Collingridge, G. L., Isaac, J. T. & Wang, Y. T. Receptor trafficking and synaptic

Colledge, M., Dean, R.A., Scott, G.K., et al., (2000) Targeting of PKA to glutamate receptors through a MAGUK-AKAP complex. Neuron 27, 107–119.

Crowder JM, Croucher MJ, Bradford HF, et al., (1987). Excitatory amino acid receptors and depolarization-induced Ca^{2+} influx into hippocampal slices. J. Neurochem. 48 (6): 1917–24.

Cull C S, Brickley S, Farrant M (2001). NMDA receptor subunits: diversity, development and disease. Curr. Opin. Neurobiol. 11 (3): 327–35.

Cullen, W. K., Suh, Y. H., Anwyl, R., et al., (1997) Block of LTP in rat hippocampus in vivo by beta-amyloid precursor protein fragments. NeuroReport, 8, 3213–3217.

Cummings, C. J. et al. (1999) Mutation of the E6-AP ubiquitin ligase reduces nuclear inclusion frequency while accelerating polyglutamine-induced pathology in SCA1 mice. Neuron 24, 879–892.

Davidson, H. T., Xiao, J., Dai, R. et al., (2009) Calcyon is necessary for activity-dependent AMPA receptor internalization and LTD in CA1 neurons of hippocampus. Eur. J. Neurosci. 29, 42–54.

Dacher, M. et al. (2013) A-kinase anchoring protein–calcineurin signaling in long-term depression of GABAergic synapses. J. Neurosci. 33, 2650–2660

De Felice, F. G., Velasco, P. T., Lambert, M. P., et al. (2007) Abeta oligomers induce neuronal oxidative stress through an Nmethyl-D-aspartate receptor-dependent mechanism that is blocked by the Alzheimer drug memantine. Journal of Biological Chemistry, 282, 11590–11601.

Decker, H., Jurgensen, S., Adrover, M. F., et al. (2010) N-methyl-D-aspartate receptors are required for synaptic targeting of Alzheimer's toxic amyloid-beta peptide oligomers. Journal of Neurochemistry, 115, 1520–1529.

Derkach VA, Oh MC, Guire ES, et al., (2007) Regulatory mechanisms of AMPA receptors in synaptic plasticity. Nat Rev Neurosci, 8,101–113.

Dickson, D. W. (1997) The pathogenesis of senile plaques. J. Neuropathol. Exp. Neurol. 56, 321–339.

Dingledine R, Borges K, Bowie D, et al., (1999). The glutamate receptor ion channels. Pharmacol. Rev. 51 (1): 7–61.

Dodge-Kafka, K.L. et al. (2005) The protein kinase A anchoring protein mAKAP coordinates two integrated cAMP effector pathways. Nature 437, 574–578

Donevan S. D., Rogawski M. A. (1995) Intracellular polyamines mediate inward rectification of Ca^{2+}-permeable alpha-amino-3-hydroxy-5-methyl-4-isoxazolepropio nic acid receptors. Proc. Natl. Acad. Sci. U.S.A., 92, 9298–9302

Eckenhoff, R. G., Johansson, J. S., Wei, H., et al., (2004) Inhaled anesthetic enhancement of amyloid-beta oligomerization and cytotoxicity. Anesthesiology, 101, 703–709.

Ehlers MD. (2000) Reinsertion or degradation of AMPA receptors determined by activity-dependent endocytic sorting. Neuron 28:511–525.

El-Husseini, A.E., Schnell, E., Chetkovich, et al., (2000) PSD-95 involvement in maturation of excitatory synapses. Science 290, 1364–1368.

Emond, M. R. et al. (2010) AMPA receptor subunits define properties of state-dependent synaptic plasticity. J. Physiol. 588, 1929–1946.

Esteban, J. A. et al. (2003) PKA phosphorylation of AMPA receptor subunits controls synaptic trafficking underlying plasticity. Nature Neurosci. 6, 136–143.

Filipowicz, W., Bhattacharyya, S. N. & Sonenberg, N. (2008) Mechanisms of post-transcriptional regulation by microRNAs: are the answers in sight? Nature Rev. Genet. 9, 102–114.

Fiore, R. et al. (2009) Mef2-mediated transcription of the miR379–410 cluster regulates activity-dependent dendritogenesis by fine-tuning Pumilio2 protein levels. EMBO J. 28, 697–710.

Flavell, S. W. & Greenberg, M. E. (2008) Signaling mechanisms linking neuronal activity to gene expression and plasticity of the nervous system. Annu. Rev. Neurosci. 31, 563–590.

Gerhard, S. (2011) microRNAs at the synapse. Nature. reviews 10, 842-849.

Giuffrida, M. L., Caraci, F., Pignataro, B., Cataldo, S., De Bona, P., Bruno, V., et al. (2009) Beta-amyloid monomers are neuroprotective. Journal of Neuroscience, 29, 10582–10587.

Gover TD, Moreira TH, Weinreich D (2009). Role of calcium in regulating primary sensory neuronal excitability. Handb Exp Pharmacol 194 (194): 563–87.

Gong, Y., Chang, L., Viola, K. L., et al., (2003). Alzheimer's disease-affected brain: Presence of oligomeric A beta ligands (ADDLs) suggests a molecular basis for reversible memory loss. Proceedings of the National Academy of Sciences of the United States of America, 100, 10417–10422.

Gomez, L.L. et al. (2002) Regulation of A-kinase anchoring protein 79/ 150-cAMP-dependent protein kinase postsynaptic targeting by NMDA receptor activation of calcineurin and remodeling of dendritic actin. J. Neurosci. 22, 7027–7044

Goate, A. et al. (1991) Segregation of a missense mutation in the amyloid precursor protein gene with familial Alzheimer's disease. Nature 349, 704–706.

Goto H, Watanabe K, Araragi N, et al. (2009) The identification and functional implications of human-specific "fixed" amino acid substitutions in the glutamate receptor family. BMC Evol. Biol, 9, 224.

Gleckman, A. M., Evans, R. J., Bell, M. D., et al., (2000) Optic nerve damage in shaken baby syndrome: Detection by beta-amyloid precursor protein immunohistochemistry. Archives of Pathology and Laboratory Medicine, 124, 251–256.

Groc L, Choquet D, Stephenson FA, et al., (2007). NMDA receptor surface trafficking and synaptic subunit composition are developmentally regulated by the extracellular matrix protein Reelin. J. Neurosci. 27, 10165–75.

Grundke-Iqbal, I. et al. (1986) Abnormal phosphorylation of the microtubule-associated protein τ (tau) in Alzheimer cytoskeletal pathology. Proc. Natl Acad. Sci. USA 83, 4913–4917.

Haass, C. (2004) Take five-BACE and the γ-secretase quartet conduct Alzheimer's amyloid β-peptide generation. EMBO J. 23, 483–488.

Hansen, K.F., Sakamoto, K., Wayman, G.A., et al. (2010) Transgenic miR132 alters neuronal spine density and impairs novel object recognition memory. PLoS ONE, 5, e15497

Hardy, J. A. & Higgins, G. A. (1992) Alzheimer's disease: the amyloid cascade hypothesis. Science 256, 184–185.

Hayashi, Y. et al. (2000) Driving AMPA receptors into synapses by LTP and CaMKII: requirement for GluR1 and PDZ domain interaction. Science 287, 2262–2267.

Hardy, J. & Selkoe, D. J. (2002) The amyloid hypothesis of Alzheimer's disease: progress and problems on the road to therapeutics. Science 297, 353–356.

Helen H., Jannic B., Chihiro S., Takeshi I., Taisuke T., Sangram S., and Roberto M. (2006) AMPAR Removal Underlies Aβ-Induced Synaptic Depression and Dendritic Spine Loss. Neuron 52, 831–843

Hirling H (2009) Endosomal trafficking of AMPA-type glutamate receptors. Neuroscience 158:36–44.

Hoogenraad, C. C., Akhmanova, A., Galjart, N. & De Zeeuw, C. I. (2004) LIMK1 and CLIP-115: linking cytoskeletal defects to Williams syndrome. Bioessays 26, 141–150.

Hollmann, M., and Heinemann, S. (1994) Cloned glutamate receptors. Annu. Rev. Neurosci. 17, 31–108.

Hébert S.S., De Strooper B. (2009) Alterations of the microRNA network cause neurodegenerative disease. Trends Neurosci, 32, 199-206

Johnson JW, Ascher P (1990). Voltage-dependent block by intracellular Mg2+ of N-methyl-D-aspartate-activated channels. Biophys. J. 57 (5): 1085–90.

Johnson, V. E., Stewart, W., Graham, D. I., Stewart, J. E., Praestgaard, A. H., & Smith, D. H. (2009) A neprilysin polymorphism and amyloid-beta plaques after traumatic brain injury. Journal of Neurotrauma, 26, 1197–1202.

Jurgensen, S., Antonio, L. L., Mussi, G. E., Brito-Moreira, J., Bomfim, T. R., De Felice, F. G., et al. (2011) Activation of D1/D5 dopamine receptors protects neurons from synapse dysfunction induced by amyloid-{beta} oligomers. Journal of Biological Chemistry, 286, 3270–3276.

Jurado, S. et al. (2010) A calcineurin/AKAP complex is required for NMDA receptor-dependent long-term depression. Nat. Neurosci. 13, 1053–1055

Kamenetz, F. et al. (2003) APP processing and synaptic function. Neuron 37, 925–937, 3044-3051.

Kameyama, K., Lee, H.K., Bear, M.F., Huganir, R.L., (1998) Involvement of a postsynaptic protein kinase A substrate in the expression of homosynaptic long-term depression. Neuron 21, 1163–1175.

Kandel, E. R. (2001) The molecular biology of memory storage: a dialogue between genes and synapses. Science 294, 1030–1038.

Kang, J. et al. (1987) The precursor of Alzheimer's disease amyloid A4 protein resembles a cell-surface receptor. Nature 325, 733–736.

Kang, J. E., Lim, M. M., Bateman, R. J., et al. (2009) Amyloid-beta dynamics are regulated by orexin and the sleep-wake cycle. Science, 326, 1005–1007

Karres, J. S., Hilgers, V., Carrera, I., et al., (2007) The conserved microRNA miR-8 tunes atrophin levels to prevent neurodegeneration in Drosophila. Cell 131, 136–145.

Kemp, A. & Manahan-Vaughan, D. (2007) Hippocampal longterm depression: master or minion in declarative memory processes? Trends Neurosci. 30, 111–118.

Kessels HW, Kopec CD, Klein ME, Malinow R (2009) Roles of stargazin and phosphorylation in the control of AMPA receptor subcellular distribution. Nat Neurosci 12:888–896.

Kim, M. J. et al. (2007) Synaptic accumulation of PSD-95 and synaptic function regulated by phosphorylation of serine-295 of PSD-95. Neuron 56, 488–502.

Kim, J. et al. (2004) Identification of many microRNAs that copurify with polyribosomes in mammalian neurons. Proc. Natl Acad. Sci. USA 101, 360–365.

Klein, W. L. (2002) Neurochem. Int. 41, 345–352

Klein, M. E. et al. (2007) Homeostatic regulation of MeCP2 expression by a CREB-induced microRNA. Nature Neurosci. 10, 1513–1514.

Kleckner NW, Dingledine R (1988). "Requirement for glycine in activation of NMDA-receptors expressed in Xenopus oocytes". Science 241, 835–7.

Kotilinek, L. A., Bacskai, B., Westerman, M., Kawarabayashi, T., Younkin, L., Hyman, B. T., et al. (2002). Reversible memory loss in a mouse transgenic model of Alzheimer's disease. Journal of Neuroscience, 22, 6331–6335.

Klyubin, I. et al. (2005) Amyloid β protein immunotherapy neutralizes Aβ oligomers that disrupt synaptic plasticity in vivo. Nature Med. 11, 556–561.

Kocerha, J. et al. (2009) MicroRNA-219 modulates NMDA receptor-mediated neurobehavioral dysfunction. Proc. Natl Acad. Sci. USA 106, 3507–3512.

Kosik, K. S. The neuronal microRNA system. (2006) Nature Rev. Neurosci. 7, 911–920.

Kosik, K. S., Joachim, C. L. & Selkoe, D. J. (1986) Microtubule-associated protein τ (tau) is a major antigenic component of paired helical filaments in Alzheimer disease. Proc. Natl Acad. Sci. USA 83, 4044–4048.

Lacor, P. N., Buniel, M. C., Furlow, P. W., et al., (2007). Abeta oligomer-induced aberrations in synapse composition, shape, and density provide a molecular basis for loss of connectivity in Alzheimer's disease. Journal of Neuroscience, 27, 796–807.

Lambert, M. P., Barlow, A. K., Chromy, B. A., et al., (1998). Diffusible, nonfibrillar ligands derived from Abeta1-42 are potent central nervous system neurotoxins. Proceedings of the National Academy of Sciences of the United States of America, 95, 6448–6453.

Lee, H. K., Takamiya, K., He, K., Song, L., et al., (2010) J. Neurophysiol.103, 479–489

Lee, H.K., Barbarosie, M., Kameyama, K., et al., (2000). Regulation of distinct AMPA receptor phosphorylation sites during bidirectional synaptic plasticity. Nature neuroscience 12, 172-181.

Lee, S.H., Liu, L., Wang, Y.T., and Sheng, M. (2002). Clathrin adaptor AP2 and NSF interact with overlapping sites of GluR2 and play distinct roles in AMPA receptor trafficking and hippocampal LTD. Neuron 36, 661–674.

Lee HK, Takamiya K, Han JS, et al., (2003) Cell.112, 631–643.

Lee, ST. et al., (2012) miR-206 Regulates Brain-Derived Neurotrophic Factors in Alzheimer's Disease Model. Ann Neurol. 72, 269-277

Lee CH, Lü W, Michel JC., et al., (1990) NMDA receptor structures reveal subunit arrangment and pore architecture. 2014. Nature. 511,191-7.

Levy, E. et al. Mutation of the Alzheimer's disease amyloid gene in hereditary cerebral hemorrhage, Dutch type. Science 248, 1124–1126.

Liu Y, Zhang J (2000). Recent development in NMDA receptors.

Li, H. et al. (2011) Interaction of calcineurin with substrates and targeting proteins. Trends Cell Biol. 21, 91–103

Li, H. et al. (2012) Balanced interactions of calcineurin with AKAP79 regulate Ca^{2+}–calcineurin–NFAT signaling. Nat. Struct. Mol. Biol. 19, 337–345

Lin, D. T. & Huganir, R. L., (2007) PICK1 and phosphorylation of the glutamate receptor 2 (GluR2) AMPA receptor subunit regulates GluR2 recycling after NMDA receptor-induced internalization. J. Neurosci. 27, 13903–13908.

Liu XB, Murray KD, Jones EG (2004). Switching of NMDA receptor 2A and 2B subunits at thalamic and cortical synapses during early postnatal development. J. Neurosci. 24, 8885–95.

Liu Y, Wong TP, Aarts M, et al., (2007) NMDA receptor subunits have differential roles in mediating excitotoxic neuronal death both in vitro and in vivo. J. Neurosci. 27, 2846–57.

Li, Z. et al. (2010) Caspase-3 activation via mitochondria is required for long-term depression and AMPA receptor internalization. Cell 141, 859–871.

Lomeli H., Mosbacher J., Melcher T., et, al. (1994). Control of kinetic properties of AMPA receptor channels by nuclear RNA editing. Science 266 1709–1713

Luthi, A. et al. (1999) Hippocampal LTD expression involves a pool of AMPARs regulated by the NSF-GluR2 interaction. Neuron 24, 389–399.

Lu, W. et al. (2001) Activation of synaptic NMDA receptors induces membrane insertion of new AMPA receptors and LTP in cultured hippocampal neurons. Neuron 29, 243–254.

Lugli, G., Torvik, V.I., Larson, et al., (2008). Expression of microRNAs and their precursors in synaptic fractions of adult mouse forebrain. J. Neurochem.106, 650–661.

Luchsinger, J. A. (2008). Adiposity, hyperinsulinemia, diabetes and Alzheimer's disease: An epidemiological perspective. European Journal of Pharmacology, 585, 119–129.

Lugli, G., Larson, J., Martone, M. E., et al., (2005) Dicer and eIF2c are enriched at postsynaptic densities in adult mouse brain and are modified by neuronal activity in a calpain-dependent manner. J. Neurochem. 94, 896–905.

Luscher, C., Xia, H., Beattie, E.C., et al., (1999). Role of AMPA receptor cycling in synaptic transmission and plasticity. Neuron 24, 649–658.

Lukiw W.J. (2007) Micro-RNA speciation in fetal, adult and Alzheimer's disease hippocampus. Neuroreport.18, 297-300.

Man, H. Y. et al. (2003) Activation of PI3-kinase is required for AMPA receptor insertion during LTP of mEPSCs in cultured hippocampal neurons. Neuron 38, 611–624.

Malenka RC, Nicoll RA. (1999). Long-term potentiation—a decade of progress? Science 285:1870 –1874.

Magill ST, Cambronne XA, Luikart BW, et al. (2010) microRNA-132 regulates dendritic growth and arborization of newborn neurons in the adult hippocampus. Proc Natl Acad Sci U S A 107: 20382–20387.

Man, H. Y., Sekine-Aizawa, Y., and Huganir, R. L. (2007) Proc. Natl. Acad.Sci. U.S.A. 104, 3579–3584

Mawuenyega, K. G., Sigurdson, W., Ovod, V., et al., (2010). Decreased clearance of CNS beta-amyloid in Alzheimer's disease. Science, 330, 1774.

Masters, C. L. et al. (1985) Amyloid plaque core protein in Alzheimer disease and Down syndrome. Proc. Natl Acad. Sci. USA 82, 4245–4249.

Malinow, R., and Malenka, R.C. (2002). AMPA receptor trafficking and synaptic plasticity. Annu. Rev. Neurosci. 25, 103–126.

McAllister, A. K. (2007) Dynamic aspects of CNS synapse formation. Annu. Rev. Neurosci. 30, 425–450.

McLean, C. A. et al. (1999) Soluble pool of Aβ amyloid as a determinant of severity of neurodegeneration in Alzheimer's disease. Ann. Neurol. 46, 860–866.

Miñano-Molina AJ, España J, Martín E, et al., (2011) Soluble oligomers of amyloid-β peptide disrupt membrane trafficking of α-amino-3-hydroxy-5-methylisoxazole-4-propionic acid receptor contributing to early synapse dysfunction. J Biol Chem. 5, 27311-21

Mochida, S. and Hunt, T. (2012) Protein phosphatases and their regulation in the control of mitosis. EMBO Rep. 13, 197–203

Morishita, W. et al. (2007) Activation of NR2B-containing NMDA receptors is not required for NMDA receptordependent long-term depression. Neuropharmacology 52, 71–76.

Murphy et al., (2014) AKAP-Anchored PKA Maintains Neuronal L-type Calcium Channel Activity and NFAT Transcriptional Signaling, Cell Rep.12, 1577-88

Mulkey, R. M., Herron, C. E. & Malenka, R. C. (1993) An essential role for protein phosphatases in hippocampal long-term depression. Science 261, 1051–1055.

Muto T, Tsuchiya D, Morikawa K, Jingami H (007). Structures of the extracellular regions of the group II/III metabotropic glutamate receptors. Proc. Natl. Acad. Sci. U.S.A. 104, 3759–64.

Nicoll, R.A., Tomita, S. & Bredt, D.S. (2006) Auxiliary subunits assist AMPA-type glutamate receptors. Science 311, 1253–1256.

Nishiyama, M., Hong, K., Mikoshiba, K., et al., (2000) Calcium stores regulate the polarity and input specificity of synaptic modification. Nature 408, 584–588.

Nunez-Iglesias J., Liu C.C., Morgan T.E. et al., (2010) Joint genome-wide profiling of miRNA and mRNA expression in Alzheimer's disease cortex reveals altered miRNA regulation. PLoS One,.5(2):e8898

Otmakhov, N., Tao-Cheng, J. H., Carpenter. (2004) J. Neurosci. 24, 9324–9331

Oliveria SF, Gomez LL, Dell'Acqua ML. J. (2003) Cell Biol.; 160:101–112.

Oliveria, S.F. et al. (2012) Localized calcineurin confers Ca^{2+}- dependent inactivation on neuronal L-type Ca^{2+} channels. J. Neurosci. 32, 15328–15337

Olson, M. I. & Shaw, C. M. (1969) Presenile dementia and Alzheimer's disease in mongolism. Brain 92, 147–156.

Oh, M. C., Derkach, V. A., Guire, E. S., and Soderling, T. R. (2006) J. Biol.Chem. 281, 752–758

Ohshima, T. et al. (2005) Impairment of hippocampal longterm depression and defective spatial learning and memory in p35 mice. J. Neurochem. 94, 917–925.

Oliet, S. H., Malenka, R. C. & Nicoll, R. A. (1997) Two distinct forms of long-term depression coexist in CA1 hippocampal pyramidal cells. Neuron 18, 969–982.

Oliveria, S.F. et al. (2012) Localized calcineurin confers Ca^{2+} - dependent inactivation on neuronal L-type Ca^{2+} channels. J. Neurosci. 32, 15328–15337

Pai B, Siripornmongcolchai T, Berentsen B. (2014) NMDA receptor-dependent regulation of miRNA expression and association with Argonaute du ring LTP in vivo. Front Cell Neurosci. 13,7:285

Palmada M, Centelles J (1998). Excitatory amino acid neurotransmission. Pathways for metabolism, storage and reuptake of glutamate in brain. Front Biosci, 3, 701–18.

Palmer, M. J., Isaac, J. T. & Collingridge, G. L. (2004) Multiple developmentally regulated expression mechanisms of longterm potentiation at CA1 synapses. J. Neurosci. 24, 4903–4911.

Palmer, C. L. et al. (2005) Hippocalcin functions as a calcium sensor in hippocampal LTD. Neuron 47, 487–494.

Passafaro, M., Piech, V., and Sheng, M. (2001). Subunit-specific temporal and spatial patterns of AMPA receptor exocytosis in hippocampal neurons. Nat. Neurosci. 4, 917–926.

Paoletti P, Neyton J (2007). NMDA receptor subunits: function and pharmacology. Curr Opin Pharmacol 7 (1): 39–47.

Pickard, L. et al. (2001) Transient synaptic activation of NMDA receptors leads to the insertion of native AMPA receptors at hippocampal neuronal plasma membranes.Neuropharmacology 41, 700–713.

Peineau, S. et al. (2009) A systematic investigation of the protein kinases involved in NMDA receptor-dependent LTD: evidence for a role of GSK-3 but not other serine/ threonine kinases. Mol. Brain 2, 22.

Peineau, S. et al. (2007) LTP inhibits LTD in the hippocampus via regulation of GSK3β. Neuron 53, 703–717.

Petroff OA (2002). "GABA and glutamate in the human brain".Neuroscientist 8 (6): 562–573.

Pérez-Otaño I, Ehlers MD (2005). Homeostatic plasticity and NMDA receptor trafficking. Trends Neurosci. 28 (5): 229–38.

Pin JP, Acher F (2002). "The metabotropic glutamate receptors: structure, activation mechanism and pharmacology". Curr Drug Targets CNS Neurol Disord 1 (3): 297–317.

Platt SR (2007). "The role of glutamate in central nervous system health and disease--a review". Vet. J. 173 (2): 278–86.

Plum, L., Schubert, M., & Bruning, J. C. (2005). The role of insulin receptor signaling in the brain. Trends in Endocrinology and Metabolism, 16, 59–65.

Qinwen W., Dominic M. W., Michael J. R., et al., (2005) Block of Long-Term Potentiation by Naturally Secreted and Synthetic Amyloid β-Peptide in Hippocampal Slices Is Mediated via Activation of the Kinases c-Jun N Terminal Kinase, Cyclin-Dependent Kinase 5, and p38 Mitogen-Activated Protein Kinase as well as Metabotropic Glutamate Receptor Type 5. J. Neurosci. 24, 3370 -3378.

Querfurth HW, and LaFerla FM. (2010) Mechanisms of Disease: Alzheimer's Disease. N Engl J Med.362, 329-44.

Rammes, G., Hasenjager, A., Sroka-Saidi, K., Deussing, J. M., & Parsons, C. G. (2011). Therapeutic significance of NR2B-containing NMDA receptors and mGluR5 metabotropic glutamate receptors in mediating the synaptotoxic effects of beta-amyloid oligomers on long-term potentiation (LTP) in murine hippocampal slices. Neuropharmacology, 60, 982–990.

Ramocki, M. B. & Zoghbi, H. Y. (2008) Failure of neuronal homeostasis results in common neuropsychiatric phenotypes. Nature 455, 912–918.

Ravi S. M, Vijayalaxmi C. Nalavadi et al., (2011) Reversible Inhibition of PSD-95 mRNA Translation by miR-125a, FMRP Phosphorylation, and mGluR SignalingMolecular Cell, 42, 673–688

Renner, M., Lacor, P. N., Velasco, P. T., Xu, J., Contractor, A., Klein, W. L., et al. (2010). Deleterious effects of amyloid beta oligomers acting as an extracellular scaffold for mGluR5. Neuron, 66, 739–754.

Reinhart, B. J. et al. (2000) The 21-nucleotide let-7 RNA regulates developmental timing in Caenorhabditis elegans. Nature 403, 901–906

Richmond, S. A. et al. (1996) Localization of the glutamate receptor subunit GluR1 on the surface of living and within cultured hippocampal neurons. Neuroscience 75, 69–82.

Roselli F, Tirard M, Lu J. et al., (2005) Soluble beta-amyloid1-40 induces NMDA-dependent degradation of postsynaptic density-95 at glutamatergic synapses. J Neurosci. 30, 11061-70.

Rocca, D. L., Martin, S., Jenkins, E. L. & Hanley, J. G. (2008) Inhibition of Arp2/3-mediated actin polymerization by PICK1 regulates neuronal morphology and AMPA receptor endocytosis. Nat. Cell Biol. 10, 259–271.

Ryan, T. J. & Grant, S. G. N. (2009) The origin and evolution of synapses. Nat Rev Neurosci 10.

Saba R, Störchel PH, Aksoy-Aksel A et al., (2012) Dopamine-regulated microRNA MiR-181a controls GluA2 surface expression in hippocampal neurons. Mol Cell Biol. 32:619-32

Sanderson, J.L. et al. (2012) AKAP150-anchored calcineurin regulates synaptic plasticity by limiting synaptic incorporation of Ca2+- permeable AMPA receptors. J. Neurosci. 32, 15036–15052

Schratt, G.M., Tuebing, F., Nigh, E.A., Kane, C.G., Sabatini, M.E., Kiebler, M., Greenberg, M.E., 2006. A brain-specific microRNA regulates dendritic spine.

Schaffar, G. et al. (2004) Cellular toxicity of polyglutamine expansion proteins: mechanism of transcription factor deactivation. Mol. Cell 15, 95–105.

Scott, J.D. et al. (2013) Creating order from chaos: cellular regulation by kinase anchoring. Annu. Rev. Pharmacol. Toxicol. 53, 187–210

Siegel, G., Obernosterer, G., Fiore, R., et al., (2009) A functional screen implicates microRNA-138-dependent regulation of the depalmitoylation enzyme APT1 in dendritic spine morphogenesis. Nat Cell Biol.1:705-16.

Shepherd, J.D. & Huganir, R.L. (2007) The cell biology of synaptic plasticity: AMPA receptor trafficking. Annu. Rev. Cell Dev. Biol. 23, 613–643.

Shi, S. H. et al. (1999) Rapid spine delivery and redistribution of AMPA receptors after synaptic NMDA receptor activation. Science 284, 1811–1816.

Shi, S., Hayashi, Y., Esteban, J.A., and Malinow, R. (2001). Subunitspecific rules governing AMPA receptor trafficking to synapses in hippocampal pyramidal neurons. Cell 105, 331–343.

Soto, C., Estrada, L., & Castilla, J. (2006). Amyloids, prions and the inherent infectious nature of misfolded protein aggregates. Trends in Biochemical Sciences, 31, 150–155

Stark, K. L. et al. (2008) Altered brain microRNA biogenesis contributes to phenotypic deficits in a 22q11-deletion mouse model. Nature Genet. 40, 751–760.

Stein, V., House, D.R., Bredt, D.S. & Nicoll, R.A. (2003) Postsynaptic density-95 mimics and occludes hippocampal long-term potentiation and enhances long-term depression. J. Neurosci. 23, 5503–5506.

Snyder, E. M. Nong Y., Almeida C. G. et al. (2005) Regulation of NMDA receptor trafficking by amyloid-β. Nature Neurosci. 8, 1051–1058.

Sprengel R. et al. (1998). Importance of the intracellular domain of NR2 subunits for NMDA receptor function in vivo. Cell 92: 279–289.

Stephenson F.A. (November 2006). Structure and trafficking of NMDA and GABAA receptors. Biochem. Soc. Trans. 34 : 877–81.

Snyder, E. M. et al. (2001) Internalization of ionotropic glutamate receptors in response to mGluR activation. Nature Neurosci. 4, 1079–1085.

Steinhäuser C, Gallo V (1996). News on glutamate receptors in glial cells. Trends Neurosci. 19: 339–45.

Strittmatter, W. J., Saunders, A. M., Schmechel, et al., (1993). Apolipoprotein E: High-avidity binding to betaamyloid and increased frequency of type 4 allele in late-onset familial Alzheimer disease. Proceedings of the National Academy of Sciences of the United States of America, 90, 1977–1981.

Staubli, U. & Scafidi, J. (1997) Studies on long-term depression in area CA1 of the anesthetized and freely moving rat. J. Neurosci. 17, 4820–4828.

Song, I., and Huganir, R. L. (2002) Trends Neurosci. 25, 578–588

Sutton, M. A. & Schuman, E. M. (2006) Dendritic protein synthesis, synaptic plasticity, and memory. Cell 127, 49–58.

Tardin, C., Cognet, L., Bats, C., et al., (2003) Direct imaging of lateral movements of AMPA receptors inside synapses. EMBO J. 22, 4656–4665.

Tavalin, S.J., Colledge, M., Hell, J.W., et al., (2002). Regulation of GluR1 by the A-kinase anchoring protein 79 (AKAP79) signaling complex shares properties with long-term depression. J. Neurosci. 22, 3044-51.

Teichberg VI. (1991) Glial glutamate receptors: likely actors in brain signaling. FASEB J. 5: 3086–91.

Terashima, A. et al. (2008) An essential role for PICK1 in NMDA receptor-dependent bidirectional synaptic plasticity. Neuron 57, 872–882.

Thambisetty, M., Simmons, A., Velayudhan, et al. (2010) Association of plasma clusterin concentration with severity, pathology, and progression in Alzheimer disease. Archives of General Psychiatry, 67, 739–748.

Thomson, J. M. et al. (2006) Extensive post-transcriptional regulation of microRNAs and its implications for cancer. Genes Dev. 20, 2202–2207.

Thorsen, T. S. et al. (2010) Identification of a small-molecule inhibitor of the PICK1 PDZ domain that inhibits hippocampal LTP and LTD. Proc. Natl Acad. Sci. USA 107, 413–418.

Tsai, J., Grutzendler, J., Duff, K. & Gan, W. B. (2004) Fibrillar amyloid deposition leads to local synaptic abnormalities and breakage of neuronal branches. Nature Neurosci. 7, 1181–1183.

Tsang, J., Zhu, J. & van Oudenaarden, A. (2007) MicroRNA-mediated feedback and feedforward loops are recurrent network motifs in mammals. Mol. Cell 26, 753–767.

Tunquist, B.J. et al. (2008) Loss of AKAP150 perturbs distinct neuronal processes in mice. Proc. Natl. Acad. Sci. U.S.A. 105, 12557–12562

Turrigiano, G. (2007) Homeostatic signaling: the positive side of negative feedback. Curr. Opin. Neurobiol. 17, 318–324.

Vasudevan, S., Tong, Y. & Steitz, J. A. (2007) Switching from repression to activation: microRNAs can up-regulate translation. Science 318, 1931–1934.

Vasuta, C. et al. (2007) Effects of exercise on NMDA receptor subunit contributions to bidirectional synaptic plasticity in the mouse dentate gyrus. Hippocampus 17, 1201–1208.

Watanabe M, Maemura K, Kanbara K, et al., (2002). "GABA and GABA receptors in the central nervous system and other organs". Int. Rev. Cytol. International Review of Cytology, 213, 1–47.

Wang, Q., Walsh, D. M., Rowan, M. J. et al., (2004) Block of long-term potentiation by naturally secreted and synthetic Amyloid β-Peptide in hippocampal slices is mediated via Activation of the kinases c-Jun N-Terminal kinase, cyclin-dependent kinase 5, and p38 mitogen-activated protein kinase as well as metabotropic glutamate receptor type 5, J. Neurosci. 24, 3370–3378

Weisenhaus M, Allen ML, Yang L, et al., (2010) Mutations in AKAP5 disrupt dendritic signaling complexes and lead to electrophysiological and behavioral phenotypes in mice. PLoS One 5:e10325.

Walsh, D. M., Klyubin, I., Fadeeva, J. V., et al. (2002). Naturally secreted oligomers of amyloid beta protein potently inhibit hippocampal long-term potentiation in vivo. Nature, 416, 535–539.

Wang, D. O. et al. (2009) Synapse- and stimulus-specific local translation during long-term neuronal plasticity. Science 324, 1536–1540.

Weiler IJ, Greenough WT. (1993) Metabotropic glutamate receptors trigger postsynaptic protein synthesis. Proc. Natl. Acad. Sci. U.S.A. 15: 7168–71.

Woo, N. H. et al. (2005) Activation of p75NTR by proBDNF facilitates hippocampal long-term depression. Nature Neurosci. 8, 1069–1077.

Wong, T. P. et al. (2007) Hippocampal long-term depression mediates acute stress-induced spatial memory retrieval impairment. Proc. Natl Acad. Sci. USA 104, 11471–11476.

Wu, L. J. et al. (2010) DREAM (Downstream Regulatory Element Antagonist Modulator) contributes to synaptic depression and contextual fear memory. Mol. Brain 3, 3.

Xiao, M. Y., Zhou, Q. & Nicoll, R. A. (2001) Metabotropic glutamate receptor activation causes a rapid redistribution of AMPA receptors. Neuropharmacology 41, 664–671.

Yang, Y., Wang, X. B., Frerking, M., and Zhou, Q. (2008) Proc. Natl. Acad. Sci. U.S.A. 105, 11388–11393

Yang, D. S., Small, D. H., Seydel, U., Smith, J. D., Hallmayer, J., Gandy, S. E., et al. (1999). Apolipoprotein E promotes the binding and uptake of beta-amyloid into Chinese hamster ovary cells in an isoform-specific manner. Neuroscience, 90, 1217–1226.

Yang, C. H., Huang, C. C. & Hsu, K. S. (2005) Behavioral stress enhances hippocampal CA1 long-term depression through the blockade of the glutamate uptake. J. Neurosci. 25, 4288–4293.

Yashiro, K. & Philpot, B. D. (2008) Regulation of NMDA receptor subunit expression and its implications for LTD, LTP, and metaplasticity. Neuropharmacology 55, 1081–1094.

Zhang, M. at al., (2013) Regulation of STAT3 by miR-106a is linked to cognitive impairment in ovariectomized mice. Brain Research. 29;1503:43-52

Zhao, W. Q., Santini, F., Breese, R., Ross, D., Zhang, X. D., Stone, D. J., et al. (2010). Inhibition of calcineurin-mediated endocytosis and alpha-amino-3-hydroxy-5-methyl-4-isoxazolepropionic acid (AMPA) receptors prevents amyloid beta oligomer-induced synaptic disruption. Journal of Biological Chemistry, 285, 7619–7632.

Zhao, W. Q., Lacor, P. N., Chen, H., Lambert, M. P., Quon, M. J., Krafft, G. A., et al. (2009). Insulin receptor dysfunction impairs cellular clearance of neurotoxic oligomeric a{beta}. Journal of Biological Chemistry, 284, 18742–18753.

Zhang, J. and Shapiro, M.S. (2012) Activity-dependent transcriptional regulation of M-TypeKv7 K+ channels by AKAP79/150-mediated NFAT actions. Neuron 76, 1133–1146

Zhu, Y. et al. (2005) Rap2-JNK removes synaptic AMPA receptors during depotentiation. Neuron.46, 905-16.

Zhou M, Baudry M (2006) Developmental changes in NMDA neurotoxicity reflect developmental changes in subunit composition of NMDA receptors. J. Neurosci.26, 2956–63.

APPENDIX